DEPARTMENT OF WOMEN'S AND CHILDREN'S HEALTH
Karolinska Institutet, Stockholm, Sweden

NEPHROPROTECTIVE EFFECT OF THE CARDIOTONIC STEROID OUABAIN

Ievgeniia Burlaka

Karolinska Institutet

Stockholm 2014

Published by Karolinska Institutet. Printed by Åtta.45 Tryckeri AB.

ISBN 978-91-7549-574-3

DEPARTMENT OF WOMEN'S AND CHILDREN'S HEALTH
Karolinska Institutet, Stockholm, Sweden

NEPHROPROTECTIVE EFFECT OF THE CARDIOTONIC STEROID OUABAIN

THESIS FOR DOCTORAL DEGREE (Ph.D.)

Friday the 23rd of May, 13:30
Karolinska Universitetssjukhuset, Astrid Lindgren Children's Hospital, Skandiasalen

by

Ievgeniia Burlaka

Principal Supervisor:
Professor Anita Aperia
Karolinska Institutet
Science for Life Laboratory
Department of Women's and Children's Health
Division of Pediatric Cell and Molecular Biology

Co-supervisors:
Associated Professor Ulla Holtbäck
Karolinska Institutet
Department of Women's and Children's Health

MD, PhD Xiao Li Liu
Karolinska Institutet
Department of Medical Biochemistry and Biophysics

Professor Vitaliy Maidannyk
National O.O. Bogomolets Medical University (Kyiv, Ukraine)
Department of Pediatrics №4

Opponent:
Professor Raymond C. Harris
Vanderbilt University Medical Center
Department of Medicine
Nephrology Division

Examination Board:
Professor Bengt Rippe
Lund University
Department of Nephrology

Professor Jenny Nyström
University of Gothenburg
Department of Physiology

Docent Anna Nilsson
Karolinska Institutet
Department of Women's and Children's Health

Stockholm 2014

To my family and my country Ukraine

ABSTRACT

It has been shown that Na,K-ATPase (NKA) is a signal transducer. Our group described the anti-apoptotic effect of ouabain to the signaling function of NKA. Exposure of renal cells to low concentrations of the highly specific NKA ligand, ouabain, will trigger a signaling cascade that involves interaction between the catalytic subunit of NKA and the inositol 1,4,5 triphosphate receptor (IP3R), intracellular calcium oscillations and activation of the NF-κB p65 subunit. It has been demonstrated that in nM ouabain can provide protection against apoptosis in fetal rat kidneys exposed to malnutrition.

In this thesis we studied whether ouabain can prevent apoptosis in kidney tissue induced by Shiga toxin 2 (Stx2). We found that Stx2 at concentrations in the range of 3-4 ng/mL gave a reproducible level of apoptosis of rat proximal tubular cells (RPTC). In cells co-incubated with Stx and ouabain 5 nM the apoptotic effect was almost completely abolished. Stx2-induced apoptosis was due to stimulation Bax and the intrinsic apoptotic pathway activation. We show that the Stx2-induced down-regulation of the survival factor Bcl-xL in Stx2-treated renal epithelial cells was almost completely abolished by ouabain treatment. Treatment with ouabain protects kidneys from apoptosis by reversing an imbalance between Bcl-xL and Bax in mice inoculated with Stx2.

In this thesis we tested whether other cardiotonic steroids (CTS) beside ouabain can play role in NKA-triggered Ca^{2+} oscillations. We found that cardenolide digoxin and the bufadienolide marinobufagenin may also trigger Ca^{2+} oscillations of similar frequency as ouabain. Binding of cardiotonic steroids to NKA will also stimulate tyrosine phosphorylation (Kometiani et al., 1998; Haas et al., 2000). We show that Src phosphorylation but not extracellular-signal-regulated (Erk) kinase is required for the initiation of the CTS evoked Ca^{2+} signaling pathway.

Chronic kidney disease (CKD) is the 12th most common cause of death and the incidence is increasing worldwide. The albuminuria is a predictor of the progressive loss of kidney function, and is also considered a major cause of the progression of CKD (Anderson et al., 2009). In this thesis we tested whether ouabain can protect against albumin-induced apoptosis in vitro and on in vivo model of CKD. We found a time- and dose-dependent increase in apoptotic index in RPTC incubated with albumin. Observed apoptosis is an early sign of RPTC damage and precedes fibrosis. Co-incubation with ouabain resulted in substantial reduction of the apoptotic index and a fibroric marker TGF-beta 1 expression in cells incubated with albumin.

We found that albumin enters the RPTC. We documented almost immediate translocation of Bax to the mitochondria accompanied by a depolarization of the mitochondrial membrane. Here we present evidence that ouabain counteracts the translocation of apoptotic factor Bax to mitochondria and the change in mitochondrial membrane potential in albumin-exposed RPTC. Treatment with ouabain restored albumin-induced down-regulated expression of the anti-apoptotic factor Bcl-xL. To examine whether ouabain will also protect from loss of renal cells in proteinuric CKD, we have used a well known model of a proteinuric disease, Passive Heymann Nephritis (PHN). We found that chronic treatment with ouabain decreases the value of albuminuria, the apoptotic index (AI) in glomerular-tubular junction, glomerular-tubular disconnection, loss of podocytes as an indicators of permanent renal damage, expression of fibrotic markers. Serum creatinine, which was used as an end-point parameter in this study, was significantly lower in PHN rats treated with ouabain that in PHN rats treated with vehicle.

In conclusion we have described a new downstream effect of the ouabain-induced NKA signaling mechanism preventing apoptosis throught regulation of mitochondrial intrinsic apoptotic pathway in acute and chronic kidney diseases.

LIST OF PUBLICATIONS

I. **Ievgeniia Burlaka**, Xiao Li Liu, Johan Rebetz, Ida Arvidsson, Liping Yang, Hjalmar Brismar, Diana Karpman, and Anita Aperia.
Ouabain Protects against Shiga Toxin–Triggered Apoptosis by Reversing the Imbalance between Bax and Bcl-xL.
J Am Soc Nephrol 24: 1413–1423, 2013.

II. Jacopo M. Fontana, **Ievgeniia Burlaka**, Georgiy Khodus, Hjalmar Brismar, and Anita Aperia.
Calcium oscillations triggered by cardiotonic steroids.
FEBS Journal 280: 5450–5455, 2013.

III. **Ievgeniia Burlaka**, Ulla Holtbäck, Ann-Christine Eklöf, Agnes B. Fogo, Hjalmar Brismar, and Anita Aperia.
Ouabain halts progression of chronic kidney disease by inhibition of albumin-triggered apoptosis.
Manuscript.

CONTENTS

LIST OF ABBREVIATIONS

NKA	Sodium-potassium Na,K-ATPase
IP_3Rs	Inositol 1,4,5-trisphosphate receptors
ER	Endoplasmatic reticulum
PLC	Phospholipase C
MAPK	Mitogen-activated protein kinase
NF-κB	Nuclear factor kappa-light-chain-enhancer of activated B cells
RHD	Rel homology domain
TAD	Transactivation domains
TLR	TNF receptor
IL-1R	IL-1 receptor
TLR4	Toll-like receptor 4
DISC	Death-inducing signaling complex
MPT	Mitochondrial permeability transition
MOM	Mitochondrial outer membrane
PTP	Permeability transition pore
VDAC	Voltage-dependent anion channel
ANT	Adenine nucleotide translocase
PT	Permeability transition
ARPKD	Autosomal recessive polycystic kidney disease
SLE	Systemic lupus erythematosus
HUS	Hemolytic-uremic syndrome
STEC-HUS	Shiga-like toxin-producing E. coli HUS
GB3	Globotriaosylceramide
IL-1	Interleukin-1
CKD	Chronic kidney disease
ESRD	End-stage renal disease
ROS	Reactive oxygen species
PI 3-kinase	Phophatidylinositide 3-kinase
ERK	Extracellular-signal-regulated kinase
EMT	Epithelial to mesenchymal transformation
ECM	Extracellular matrix
RPTC	Rat proximal tubular cells
PHN	Passive Heymann Nephritis
MN	Membranous nephropathy
IHC	Immunohistochemistry
TUNEL	Terminal deoxynucleotidyl transferase dUTP nick end labeling
TdT	Terminal deoxynucleotidyl transferase
CICR	Ca^{2+}-induced Ca^{2+} release
PRR_S	Pattern recognition receptors
RESV	Resveratrol
CoQ_{10}	Coenzyme Q_{10}
Kd	Dissociation constant

1 BACKGROUND

1.1 . Na,K-ATPase.

1.1. 1. Na,K-ATPase structure.

The Na/K-ATPase (or sodium pump) was discovered by Skou in 1957 (Scou, 1989). The Na/K-ATPase is a member of the P-type ATPase family and the most important ion pump in cell physiology. Na/K-ATPase is capable of transporting sodium and potassium ions across the cell membrane against their concentration gradients. The Na/K-ATPase consists of two non-covalently linked α and β subunits.

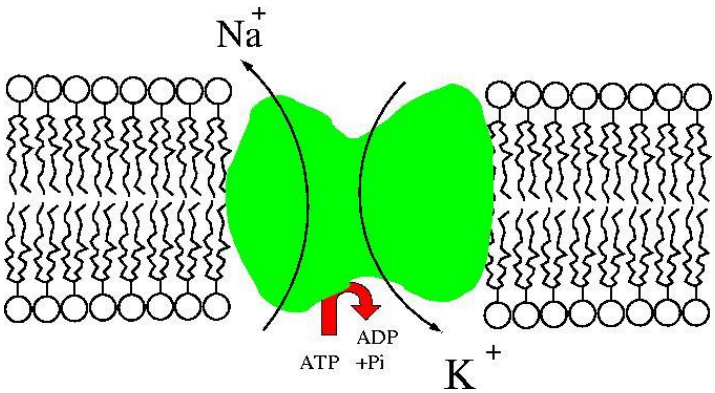

Figure 1.1. Structure of the Na,K-ATPase.

A γ subunit is associated with the Na/K-ATPase in a tissue-specific manner and regulates the functionality of the enzyme (Sweadner, 1989; Blanco and Mercer, 1998). The α subunit (about 112 kDa) contains the ATP and other ligand binding sites and couples ATP hydrolysis with ion movement. The β subunit is essential for the assembly of a fully functional enzyme. Four α isoforms are found in human tissues, and they are expressed in a tissue-specific manner. The α1 isoform is found in all cells. The α2 and α3 isoforms are mainly expressed in skeletal muscle, neuronal tissue, and cardiac myocytes. The α4 isoform is in testis and regulates sperm motility (Woo et al., 2000; Sanchez et al., 2006; Shull et al., 1985).

1.1.2. Na,K-ATPase pump function.

The sodium-potassium pump transports cations across the membrane using "alternative access" model, in which the protein alternates between two conformations, E1 and E2 (Horisberger, 2004) (Figure 1.2). The crystal structure of the E2 conformation in its phosphorylated state has been reported (Morth et al., 2007; Ogawa et al., 2009). In the E1 state, ATP is bound at the N domain and high affinity Na^+ binding sites are open to the cytosol. Binding of three Na^+ ions causes a conformational change that rotates the N domain so that the γ-phosphate of ATP is positioned near the phosphorylation site of the P domain. ATP is then cleaved and the γ-phosphate is transferred to D376. The A domain then rotates around a horizontal axis large translation and a kink in the first transmembrane helix. This action closes the cytosolic gate of the protein, leaving the three Na^+ molecules momentarily occluded in the transmembrane region of the protein (Horisberger, 2004). ADP is also released at this time. This state is known as E1-P (Horisberger, 2004; Tian, Xie, 2009). In the E2-P state, the affinity for Na^+ ions is reduced, allowing them to dissociate into the extracellular environment. Then extracellular K^+ ions bind at two high affinity sites (Tian, Xie, 2009).

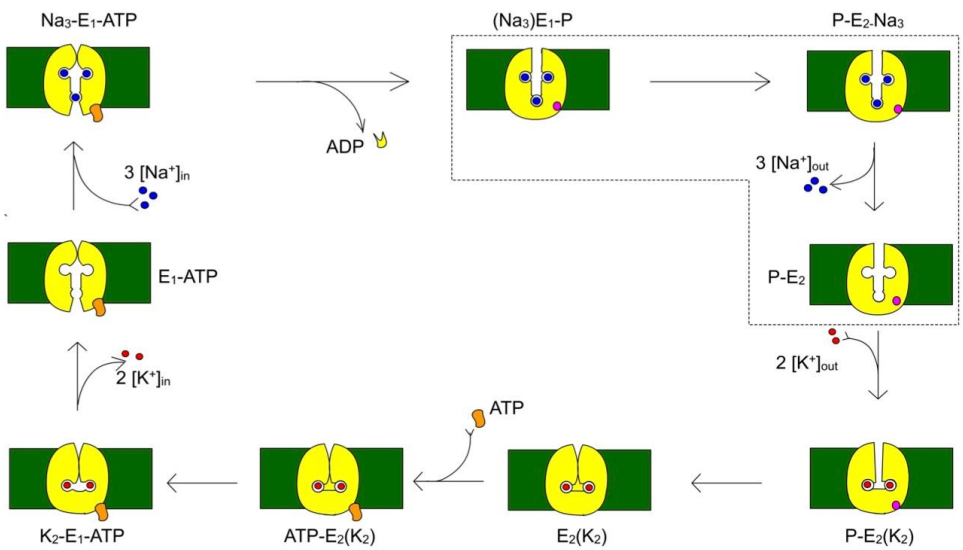

Figure 1.2. Na,K-ATPase pump function.

When both extracellular K^+ cations are bound, a conformational change occurs which closes the extracellular gate, occluding the potassium cations (Morth et al., 2007).

Binding of the cytoplasmic K^+ cation promotes helix-helix interactions between the A and P domains, triggering dephosphorylation (Tian, Xie, 2009). The dephosphorylated protein is now in the E2 state and has an open intracellular ATP binding site. When ATP binds at this site, the protein reverts to the E1 conformation, the cytosolic gate opens, and the K^+ cations dissociate from the binding sites which now have affinity for sodium cations (Horisberger, 2004).

1.1.3. Ligands of Na,K-ATPase.

For more than 200 years, digitalis, a cardiotonic steroid, has been used to treat congestive heart failure (Schoner, 2002). The endogenous cardiotonic steroids ouabain and marinobufagenin have been identified in humans. Cardiotonic steroids are considered to be important in the regulation of renal sodium transport and arterial pressure, control of cell growth, apoptosis and fibrosis, among other processes.

Almost all of the newly detected mammalian steroid hormones were previously isolated as cardiotonic constituents and toxins from plants and amphibians. Cardiotonic steroids or cardiac glycosides are specific ligands of the sodium pump (Na^+/K^+-ATPase) (Komiyama et al., 2001). Endogenous cardiotonic steroids (Figure 1.3) have been extracted from mammalian tissues such as hypothalamus (Mathews et al, 1991), heart (Komiyama, Nishimura et al, 1999) and adrenal gland (Doris et al., 1996; Laredo et al., 1994).

Ouabain (g-Strophanthin) was identified in human blood plasma (Goto et al., 1998), bovine adrenal glands (Inagami, Tamura, 1988) and hypothalamus (Mathews et al., 1991). Digoxin was isolated from the urine of healthy human subjects (Kitano et al., 1998). Moreover, a number of bufadienolides were identified in mammals: marinobufagenin was identified in the urine of patients with acute myocardial infarction (Greef and Wirth, 1981); telocinobufagin, the reduced form of marinobufagenin, was isolated from blood plasma of patients with terminal renal failure (Masugi et al, 1988), and 19-norbufalin was isolated from human cataractous lenses (Boulanger et al., 1993). The increased levels of proscillaridin A immunoreactivity were detected in patients with essential hypertension (Manunta et al., 1992).

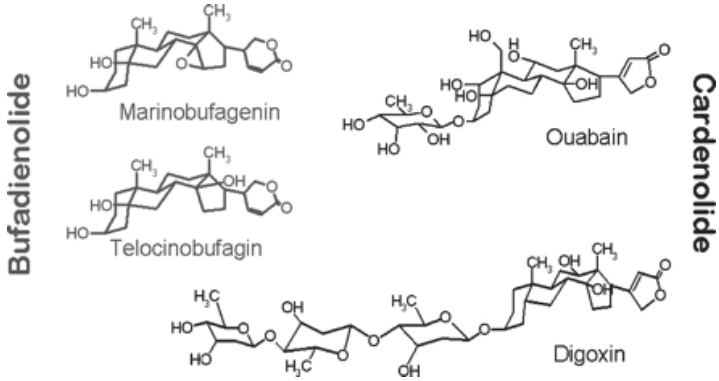

Figure 1.3. Cardiotonic steroids identified in mammalian tissues.

There is indication that cardenolides might be synthesized in the heart (Komiyama et al., 1999) and the hypothalamus (Laredo et al., 1994). Pregnenolone and progesterone are the precursors in the biosynthesis of endogenous ouabain and endogenous digoxin. Synthesis of bufadienolide-like marinobufagenin, marinobufotoxin and proscillaridine A also seems to occur in adrenocortical tumour cells (Paci et al., 2000).

The cardiotonic steroid-binding site of the Na,K-ATPase is often called the ouabain-binding site. The ouabain sensitivity of the Na,K-ATPase is determined by the α subunit. The Na,K-ATPase of almost all species is sensitive to the ouabain. Amino acids at various regions in the Na,K-ATPase influence ouabain sensitivity; however, of particular importance are two amino acids on the cell surface located on either side for the first extracellular domain (Lingrel, 2010). These amino acids (Price, Lingrel, 1988) are responsible for the differential ouabain sensitivity of the relatively ouabain-resistant α1 isoform of the Na,K-ATPase of rat and mouse compared to the ouabain-sensitive α2, α3, and α4 isoforms of these animals. As both the ouabain-sensitive and insensitive Na,K-ATPases are active ion transporters (Dostanic et al., 2004).

1.1.4. Na,K-ATPase as a signal transducer.

It has been shown that Na,K-ATPase is a signal transducer. This capacity appears to be independent from the ion transport function during its evolution because the specific binding motifs that transfer signals are located outside the conserved regions common to the different P-type ATPases.

Our group has shown that the low doses of ouabain triggering calcium oscillations cause only partial or no inhibition of pump-mediated transport. As it was well documented that intracellular calcium oscillations will require controlled release of calcium from the intracellular stores via the inositol 1,4,5-trisphosphate receptors (IP3R).

Calcium is stored in the endoplasmatic reticulum (ER) and can be released via the IP3R. G-protein coupled receptors will trigger calcium release from intracellular stores by activation of phospholipase C (PLC) and generation of 1,4,5-trisphosphate, which is a specific ligand and activator of the IP3R. A finding that ouabain triggers the release of calcium from the intracellular stores suggested that there are alternative ways to activate the IP3R. It was shown that the activation of the IP3R occurres via protein–protein interaction and does not require any soluble messenger. NKA and the IP3R were shown to form a signalling microdomain in the cell with the use of the fluorescent resonance energy transfer technique (Miyakawa-Naito et al., 2003).

Ouabain binds to the NKA and changes its conformation. This allosteric effect is transferred to the IP3R, and results in a rhythmic opening and closure of the channel. The periodicity of the calcium oscillations triggered by the NKA-IP3R interaction is in the range of 3–6 min. These slow oscillations have been reported to activate calcium dependent transcriptional factors (Hu et al., 1999). Ouabain-dependent calcium oscillations could be shown to specifically activate the calcium-dependent transcriptional factor NF-κB p65 subunit (Figure 1.4). This factor is a pleiotropic regulator of many genes that are involved in the regulation of cell growth, differentiation and apoptosis (Nakanishi, Toi, 2005).

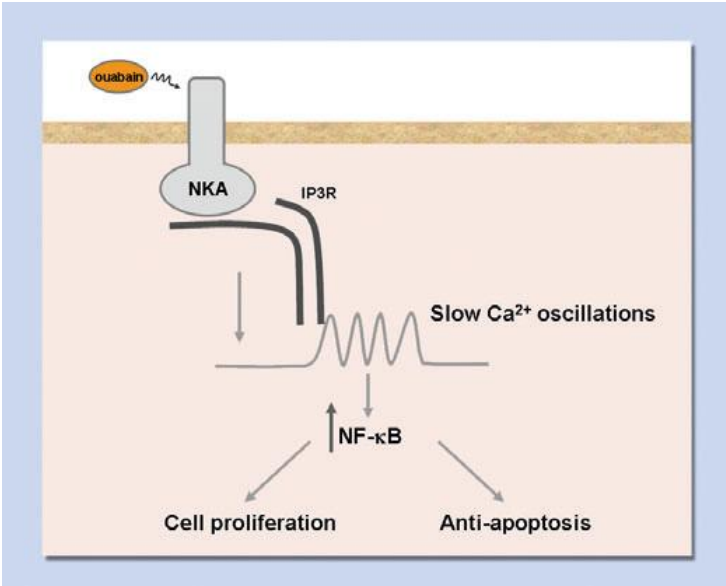

Figure 1.4. Signal function of the Na,K-ATPase.

Our group has shown that nanomolar concentrations of ouabain activate NF-κB and that 24 h exposure to nanomolar concentration of ouabain protect cells from starvation-triggered apoptosis (Li et al., 2006). We have demonstrated that in nM ouabain can provide protection against apoptosis in fetal rat kidneys exposed to malnutrition (Li et al., 2010) and in adult mouse kidneys exposed to Shiga toxin (Burlaka et al., 2013). It is also known that ouabain in very low doses can enhance cell growth (Trevisi et al., 2004).

Na,K-ATPase can also function as a cytokine receptor. It was demonstrated that ouabain can assemble with Src to form a receptor–tyrosine kinase complex. Ouabain binds to NKA resulting in Src phosphorylation. This activated protein complex will send signals to the cell, that have both growth promoting and antioxidant effects (Schoner et al., 2005; Ward et al., 2002). The NKA–Src signaling pathway has also been shown to play a role for the function of skeletal muscle. It was reported that ouabain can activate the NKA–Src signaling pathway in skeletal muscle and that this will result in increased glycogen synthesis, additively to insulin in skeletal muscle. By interacting with the sodium pump, ouabain regulates other signaling pathways such as the Ras-Raf–mitogen-activated protein kinase (MAPK) cascade through

transactivation of epidermal growth factor receptors (Counteras et al., 1999; Rajasekaran et al., 2005).

1.2. Inositol 1,4,5-trisphosphate receptors.

The inositol 1,4,5-trisphosphate (InsP3) receptors (InsP3Rs) are a family of Ca^{2+} release channels localized predominately in the endoplasmic reticulum of all cell types. They function to release Ca^{2+} into the cytoplasm in response to InsP3 produced by diverse stimuli, generating complex local and global Ca^{2+} signals that regulate many of cell physiological processes (Berridje, 1993; Bezprozvanny, 2005). The InsP3R is a calcium-selective cation channel whose gating is regulated not only by InsP3, but by other ligands as well, in particular cytoplasmic Ca^{2+}. Modulation of cytoplasmic free calcium concentration ($[Ca^{2+}]i$) is a signaling system involved in the regulation of numerous processes, - transepithelial transport, learning and memory, muscle contraction, membrane trafficking, synaptic transmission, secretion, motility, membrane excitability, gene expression, cell division, and apoptosis (Bezprozvanny, 2005).

The ER is the major Ca^{2+} storage organelle in most cells. ER membrane Ca^{2+}-ATPases accumulate Ca^{2+} in the ER lumen to quite high levels (Alvarez, Montero, 2002; Bassik et al., 2004; Bygrave, Benedetti, 1996; Montero, 1995). In contrast, the concentration of Ca^{2+} in the cytoplasm of unstimulated cells is between 50 and 100 nM, 3–4 orders of magnitude lower than in the ER lumen. This low concentration is maintained by Ca^{2+} pumps and other Ca^{2+} transporters located in the ER, as well as plasma, membranes. Upon binding InsP3, the InsP3R is gated open, providing a pathway for Ca^{2+} to diffuse down this electrochemical gradient from the ER lumen to cytoplasm. Ca^{2+} in the cytoplasm moves by passive diffusion, at a rate that is reduced by mobile and immobile Ca^{2+} binding proteins acting as buffers (Naraghi, Neher, 1997; Neher, 1998.).

Many studies have indicated that IP3R is involved in generating cytosolic Ca^{2+} oscillations (Berridge, Lipp, 2000; Fewtrell, 1993; Uhlen, Fritz, 2010). For instance, the FGF-induced Ca^{2+} oscillations in mice fibroblasts are inhibited by an IP3R antagonist (Uhlen, Burch et al., 2006). Ca^{2+} oscillations are thought to arise due to periodic release of Ca^{2+} from intracellular Ca^{2+} stores via IP3R (Berridge, Bootman, 2003). The IP3R is activated at low cytosolic Ca^{2+} concentrations, elevating the cytosolic Ca^{2+} concentration through a process often referred to as Ca^{2+}-induced Ca^{2+}

release (CICR). High cytosolic Ca^{2+} concentration can instead inhibit IP3R, leading to a decrease in intracellular Ca^{2+} release. In vivo, the binding of IP3 together with fluctuating cytosolic Ca^{2+} concentrations can trigger successive cycles of IP3R activation and inhibition, which result in cytosolic Ca^{2+} oscillations. These data, together with mathematical models (Falcke et al., 2000; Schuster et al., 2002), have confirmed that the cross-talk between Ca^{2+} and IP3 in regulating the IP3R is critical for generating Ca^{2+} oscillations.

1.3. Ca^{2+} oscillations.

Calcium plays an important role in control of many activities of cells. Cells draw on both intracellular and extracellular Ca^{2+} sources to generate signals that transduce exogenous stimulation into physiological output (Bootman et al., 2009). Prolonged elevations of Ca^{2+} cause cell damage or death (Hawrysh, Buck, 2013). Ca^{2+} oscillations regulate numerous physiological processes including cell maturation and differentiation (Kajiya, 2012), cell cycle progression (Chen et al., 2013), mitochondrial respiration (Mbaya et al., 2010).

The pattern of Ca^{2+} oscillation varies substantially between cell types, and even between cells of the same type, due to the expression of cell-specific Ca^{2+} signaling proteomes. Baseline Ca^{2+} oscillations are due to periodic release of Ca^{2+} from intracellular stores via intracellular Ca^{2+} channels (Berridge, Bootman, 2003). The generation of baseline Ca^{2+} oscillations is generally considered to be due to activation of two types of intracellular Ca^{2+} channels: inositol 1,4,5-trisphosphate receptors and ryanodine receptors. IP3Rs are large (1200 kDa) tetrameric proteins, with an amino-terminal domain projecting into the cytoplasm, and an integral Ca^{2+} channel formed by six membrane-spanning regions in the carboxy-terminal portion of each subunit (Taylor et al., 2004).

Ryanodine receptors are structurally and functionally homologous to IP3 receptors, except that they have approximately twice their mass. There are three cloned forms of the ryanodine receptor. Similar to IP3Rs, ryanodine receptor opening displays a `bell-shaped' dependence on cytosolic Ca^{2+} concentration, although they are generally activated and inhibited by slightly higher Ca^{2+} levels. Both IP3Rs and ryanodine receptors can operate as CICR channels; a property that is believed to lead to the

autocatalytic release of Ca^{2+} during the upstroke of a Ca^{2+} oscillation (Roderick et al., 2003; Sneyd et al., 2003).

Our group has shown that ligand-bound Na,K-ATPase assembles with $InsP_3R$ and that this assembly can give rise to intracellular Ca^{2+} oscillations with a constant periodicity in the minute range represents a novel principle for such a protein complex (Zhang et al., 2006). It was suggested that the ouabain-induced Ca^{2+}oscillation and signal-transducing function of Na,K-ATPase is made possible by the local organization of Na,K-ATPase and $InsP_3R$ into a spatially organized functional microdomain linking the plasma membrane to intracellular ER Ca^{2+}stores (Miyakawa-Naito et al., 2003). Using special molecular strategies i.e. $InsP_3$ sponge and pharmacological studies using the PLC inhibitor, U73122, it was found that the ouabain-induced Ca^{2+} oscillatory response is elicited via an $InsP_3$-independent mechanism of $InsP_3R$ activation. (Tian, Xie, 2008). Ouabain induces formation of the cell signaling microdomain containing Na,K-ATPase and $InsP_3R$ that acts as a signaling pathway for Ca^{2+} oscillations. The regular, low-frequency intracellular $[Ca^{2+}]_i$ oscillations induced by ouabain trigger the activation of the transcription factor NF-κB p65 subunit (Aizman et al., 2001; Li et al., 2006).

1.4. Transcriptional factor NF-κB.

NF-κB (nuclear factor kappa-light-chain-enhancer of activated B cells) is a protein complex that controls transcription of DNA. NF-κB is found in almost all animal cell types and is involved in cellular responses to stimuli such as stress, cytokines, free radicals, ultraviolet irradiation. NF-κB activation is governed by a number of positive and negative regulatory elements. In the "resting" state, NF-κB dimers are held inactive in the cytoplasm through association with IκB proteins. Specific stimuli trigger activation of the IκB kinase complex, leading to phosphorylation, ubiquitination, and degradation of IκB proteins. Released NF-κB dimers translocate to the nucleus, bind specific DNA sequences, and promote transcription of target genes. The core elements of the NF-κB pathway are the IKK complex, IκB proteins, and NF-κB dimers (Gilmore, 2006; Brasier, 2006).

There are five NF-κB family members in mammals: RelA/p65, RelB, c-Rel, p50 (NF-κB1), and p52 (NF-κB2) (Figure 1.5). NF-κB proteins bind to κB sites as dimers, either homodimers or heterodimers, and can exert both positive and negative effects

on target gene transcription. NF-κB proteins are characterized by the presence of an N-terminal Rel homology domain (RHD). Functional analyses and crystal structures of NF-κB dimers bound to κB sites have shown that it is the RHD that makes contact with DNA and supports subunit dimerization. Only p65, c-Rel, and RelB possess C-terminal transactivation domains (TADs) that confer the ability to initiate transcription. Although p52 and p50 lack TADs, they can positively regulate transcription through heterodimerization with TAD-containing NF-κB subunits or interaction with non-Rel proteins that have transactivating capability. Alternatively, p50 and p52 homodimers can negatively regulate transcription by competing with TAD-containing dimers for binding to κB sites. P50 and p52 dimers may also constitutively occupy some κB sites and thus enforce an activation threshold for certain NF-κB target genes. A hallmark of the NF-κB pathway is its regulation by IκB proteins (Tergaonkar et al., 2005). IκB proteins IκBα, IκBβ, IκBε, IκBζ, BCL-3 (B-cell lymphoma 3), and IκBns and the precursor proteins p100 (NF-κB2) and p105 (NF-κB1) are defined by the presence of multiple ankyrin repeat domains. Activation of NF-κB is achieved through phosphorylation of IκBs on conserved serine residues, so-called destruction box serine residues (Sun, Liu, 2011).

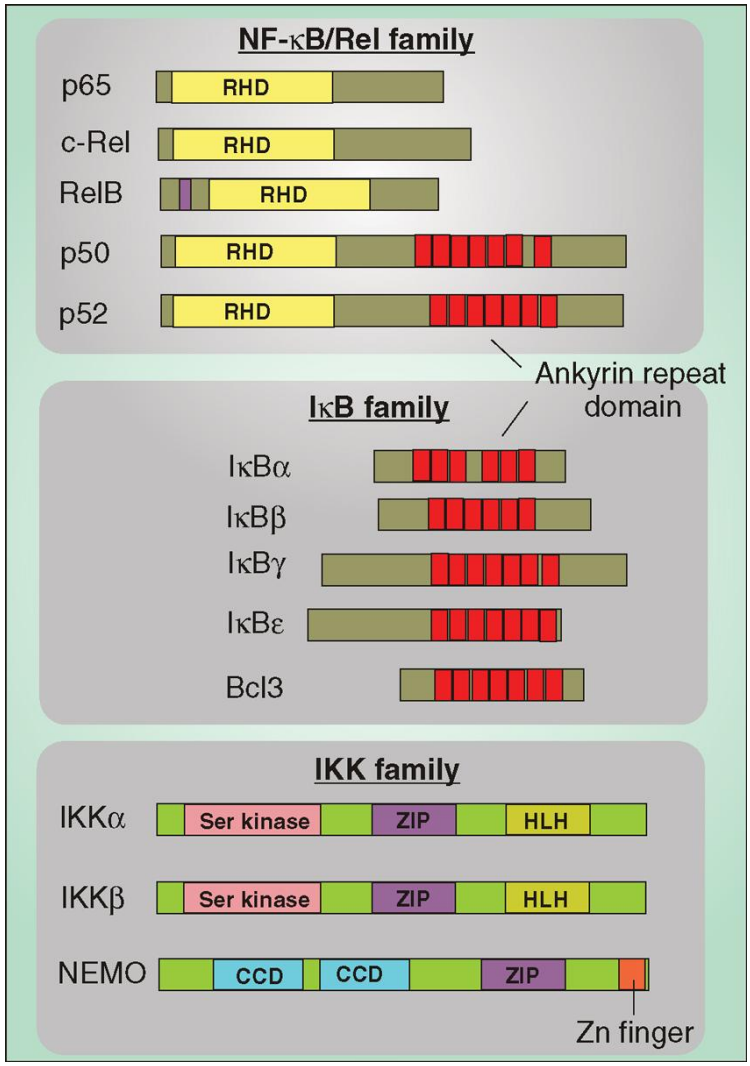

Figure 1.5. The NF-κB family.

The NF-κB signaling pathways have been classified into two types: canonical and noncanonical. The canonical, or classical, pathway is representative of the general scheme of how NF-κB is regulated. Upon recognition of ligand, cytokine receptors such as the TNF receptor (TNFR) and IL-1 receptor (IL-1R), pattern recognition receptors (PRRs) such as Toll-like receptor 4 (TLR4), and antigen receptors, among many other stimuli, trigger signalling cascades that culminate in the activation of IKKβ (also known as IKK2). IKKβ exists in a complex with the closely related kinase

IKKα (also known as IKK1) and the regulatory protein NEMO (also known as IKKγ). Activated IKKβ phosphorylates IκB proteins such as IκBα.

The noncanonical, or alternative, NF-κB pathway is induced by specific members of the TNF cytokine family, including the CD40 ligand and lymphotoxin-β (Sun, 2011). The noncanonical pathway depends on IKKα and is independent of NEMO. IKKα activation by these cytokines leads to phosphorylation of p100 and the generation of p52/RelB complexes. In addition to phosphorylation of IκB proteins, it is important to note that as the key enzymatic constituents of the NF-κB pathway, IKKα and IKKβ can mediate cross-talk with additional signalling pathways - including the p53, MAP kinase (MAPK) (Oeckinghaus et al., 2011).

Our group has shown that ouabain, the ligand of Na,K-ATPase, is a steroid derivative that binds specifically to an integral plasma membrane protein. We reported that binding of ouabain to Na,K-ATPase activates a $[Ca^{2+}]_i$ oscillatory signaling pathway that triggers the activation of NF-κB p65 subunit in renal epithelial cells. Ouabain, a highly specific Na,K-ATPase ligand, tethers the catalytic α-subunit of Na,K-ATPase with the IP3R, and triggers the release of a series of calcium waves (Aizman et al.,2001; Miyakawa-Naito et al., 2003; Zhang et al., 2006). Downstream effects of ouabain signalling include activation of the calcium-dependent transcription factor nuclear factor NF-κB and protection from apoptosis (Li et al., 2010; Burlaka et al., 2013).

1.5. Apoptosis.

Apoptosis is a form of cell death in which a programmed sequence of events leading to the elimination of cells without releasing harmful substances into the surrounding area. Apoptosis plays a crucial role in developing and maintaining the health of the body by eliminating old, unnecessary and sick cells. The human body replaces above one million cells per second. Apoptosis plays an important role in many diseases. When apoptosis does not work correctly, cells that should be eliminated may persist and become immortal. This takes place in cancer and leukemia. When apoptosis works overly well, it kills too many cells and leads to tissue damage. This is the case in as acute and chronic kidney diseases, neurogenerative disease etc. (Green, 2011).

1.5.1. Apoptotic pathways. Extrinsic pathway.

There are two main pathways of apoptosis - extrinsic and intrinsic (Figire 1.6). The extrinsic signaling pathways that initiate apoptosis involve transmembrane receptor-mediated interactions. These involve death receptors that are members of the TNF receptor gene superfamily. This death domain plays a critical role in transmitting the death signal from the cell surface to the intracellular signaling pathways. The best-characterized ligands and corresponding death receptors are FasL/FasR, TNF-α/TNFR1, Apo3L/DR3, Apo2L/DR4 and Apo2L/DR5 (Rubio-Moscardo et al., 2005).

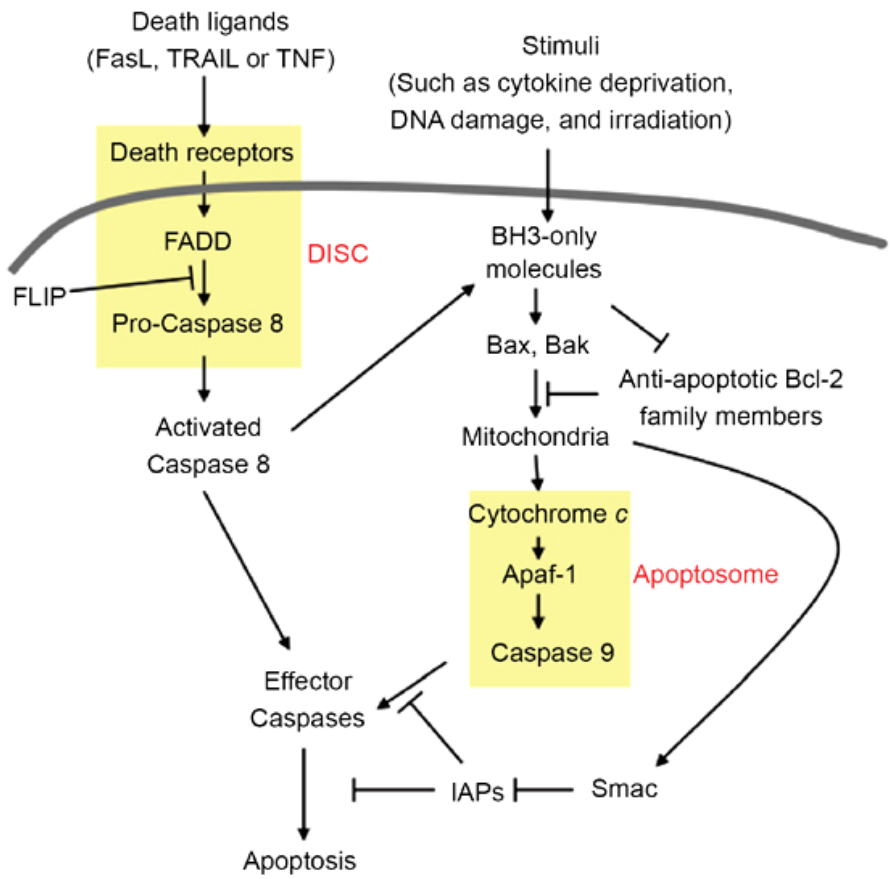

Figure 1.6. Apoptotic pathways.

TNF is a cytokine produced mainly by activated macrophages, and is the major extrinsic mediator of apoptosis. Most cells in the human body have two receptors for

TNF: TNF-R1 and TNF-R2. The binding of TNF to TNF-R1 has been shown to initiate the pathway that leads to caspase activation via the intermediate membrane proteins TNF receptor-associated death domain (TRADD) and Fas-associated death domain protein (FADD) (Wajant, 2002). FADD then associates with procaspase-8 via dimerization of the death effector domain. At this point, a death-inducing signaling complex (DISC) is formed, resulting in the auto-catalytic activation of procaspase-8. Once caspase-8 is activated, the execution phase of apoptosis is triggered. Death receptor-mediated apoptosis can be inhibited by a protein called c-FLIP which will bind to FADD and caspase-8, rendering them ineffective (Scaffidi, 1999).

1.5.2. Apoptotic pathways. Intrinsic pathway.

The intrinsic signaling pathways that initiate apoptosis involve a diverse array of non-receptor-mediated stimuli that produce intracellular signals that act directly on targets within the cell and are mitochondrial-initiated events. The stimuli that initiate the intrinsic pathway produce intracellular signals that may act in either a positive or negative fashion. All of these stimuli cause changes in the inner mitochondrial membrane that results in an opening of the mitochondrial permeability transition (MPT) pore, loss of the mitochondrial transmembrane potential and release of two main groups of normally sequestered pro-apoptotic proteins from the intermembrane space into the cytosol (Saelens et al., 2004).

The first group consists of cytochrome *c*, Smac/DIABLO, and the serine protease HtrA2/Omi (Garrido et al., 2005). These proteins activate the caspase-dependent mitochondrial pathway. Cytochrome *c* binds and activates Apaf-1 as well as procaspase-9, forming an "apoptosome". The clustering of procaspase-9 leads to caspase-9 activation (Schimmer, 2004). The second group of pro-apoptotic proteins, AIF, endonuclease G and CAD, are released from the mitochondria during apoptosis, but this is a late event that occurs after the cell has committed to die. AIF translocates to the nucleus and causes DNA fragmentation into ~50–300 kb pieces and condensation of peripheral nuclear chromatin (Joza et al., 2001). Endonuclease G also translocates to the nucleus where it cleaves nuclear chromatin to produce oligonucleosomal DNA fragments (Li, Luo et al., 2001). AIF and endonuclease G both function in a caspase-independent manner.

1.5.3. Bcl-2 system in apoptosis regulation.

The proteins of the Bcl-2 family are key regulators of the mitochondrial pathway of apoptosis. They control the permeabilization of the mitochondrial outer membrane (MOM) leading to the release of cytochrome *c* and other apoptotic factors into the cytosol. This results in downstream activation of the caspase cascade and is considered a point of no return in the cell commitment to die. The Bcl-2 family is involved in many diseases including kidney pathologies (Martinou, Youle, 2011).

Classically, three subgroups of the Bcl-2 members have been defined: the prosurvival Bcl-2 proteins, such as Bcl-2 itself, Bcl-xL, Bcl-w, Mcl-1 and A1, which inhibit cell death through direct interactions with the proapoptotic members; the proapoptotic proteins Bax and Bak, which are believed to participate directly in MOM permeabilization; and the BH3-only proteins, which share a common motif called the BH3 domain. BH3-only proteins are evolved to sense different stresses in the cell and to initiate apoptosis (Figure 1.7).

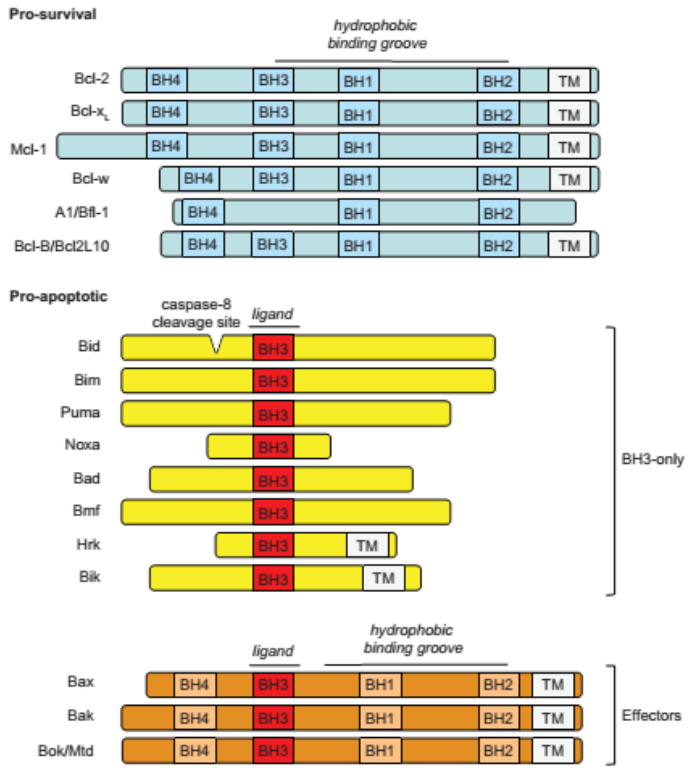

Figure 1.7. The Bcl-2 system.

Under normal conditions, the BH3-only proteins are inactive or exist at low levels in the cell. In the presence of apoptotic stimuli they are activated by post-translational modifications or their expression is increased to induce apoptosis (Shamas-Din et al., 2011).

1.5.3.1. Proapoptotic factors of the Bcl-2 system.

As a result of BH3-only stimulation, Bax and Bak become activated. It has been observed that upon activation during apoptosis, Bax and Bak translocate from the cytosol to the MOM. Once there, Bax and Bak, which is constitutively bound to the MOM, change conformation, insert into the membrane, oligomerize and induce the release of cytochrome *c* (Lovell et al., 2008). It was shown that also some antiapoptotic Bcl-2 members have ability to translocate and insert into the MOM upon apoptotic stimulation (Dludosz et al., 2006). In this scenario, the prosurvival

Bcl-2 proteins inhibit MOM permeabilization by direct interactions with the proapoptotic members. It is still unknown completely about how exactly Bax and Bak become activated in the cell and how they mediate MOM permeabilization. Hovewer, it was shown that upon their activation at the MOM during apoptosis, both Bax and Bak insert extensively into the membrane and oligomerize, which results in the release of cytochrome *c* into the cytosol. The most widely accepted model assumes that upon oligomerization, Bax and Bak form a large pore in the MOM that is responsible for the release of the apoptotic factors. This is mainly based on the structural similarities of Bcl-2 homologs with bacterial pore-forming toxins and on the observation that Bax and Bak exhibit pore activity in in vitro reconstituted systems with artificial lipid membranes (Landeta et al., 2011).

1.5.3.2. Antiapoptotic factors of the Bcl-2 system.

Several mechanisms have been proposed to explain the inhibition of apoptosis by the Bcl-2 proteins. It seems clear that the prosurvival members of the family can block apoptosis by direct binding both to the Bax and Bak, and to the BH3-only proteins. However, the hierarchy of the interactions that are responsible for apoptosis inhibition remains to be not well studied. It was reported that inhibition of MOM permeabilization by the prosurvival Bcl-2 members via sequestration of the BH3-only proteins is less efficient than via inhibition of Bax and Bak.

Moreover, Bcl-xL has been shown to inhibit Bax association with model membranes, but it is not clear whether this is via direct interactions in the cytosol or by sequestering cBid. There is an evidence refer to complexes of the prosurvival and the executioner Bcl-2 proteins being extensively inserted into the MOM. In line with this, Bcl-xL was described to inhibit Bax by binding to its membrane-inserted form and preventing its oligomerization and further autoactivation (Billen et al., 2008). It was reported recently (Edlich et al., 2011) that under normal conditions Bax is constitutively and constantly retro-translocating from mitochondria to the cytosol via a mechanism dependent on transient interactions with Bcl-xL.

1.5.4. Mitochondria in apoptosis.

Mitochondrial dysfunction has been shown to participate in the induction of apoptosis and has even been suggested to be central to the apoptotic pathway. Mitochondria have been described to play a key role in the apoptotic process due to the mitochondria being the "junction" of at least two distinct signaling pathways. Mitochondrial control of apoptosis has been described at several levels: (1) maintenance of ATP production; (2) mitochondrial membrane potential and mitochondrial membrane permeability for the release of certain apoptogenic factors from the intermembrane space into the cytosol (Desagher, Martinou, 2000).

The concept of mitochondrial permeability transition pore (PTP) the "megachannel" that results in the release of certain mitochondrial apoptogenic factors in some cell types during apoptosis has been emerged (Crompton, 2000). These include: cytochrome c, apoptosis-inducing factor AIF and Smac/Diablo (Halestrap et al., 2002).

The molecular nature of the PTP has not yet been fully defined. It is known that the PTP is thought to consist of the mitochondrial outer membrane voltage-dependent anion channel (VDAC), the inner membrane adenine nucleotide translocase (ANT) and the mitochondrial benzodiazepine receptor. These proteins cooperate to form a large conductance channel and are responsible for the "permeability transition" (PT) of mitochondria, which has been proposed to lead to apoptosis. PT is defined as a sudden increase in permeability of the mitochondrial membrane to solutes with a molecular mass less than 1.5 kDa, as a consequence of the charge difference (mitochondrial membrane potential, $\Delta\psi_m$) between the mitochondrial matrix and the cytosol (Figure 1.8). As the PTP opens, solutes (K^+, Mg^{2+} and Ca^{2+} ions) and water enter, leading to the swelling of the mitochondrial matrix, rupturing of the outer membrane and subsequent leakage of mitochondrial proteins as named above (De Giorgi et al., 2002; Halestrap et al., 2002).

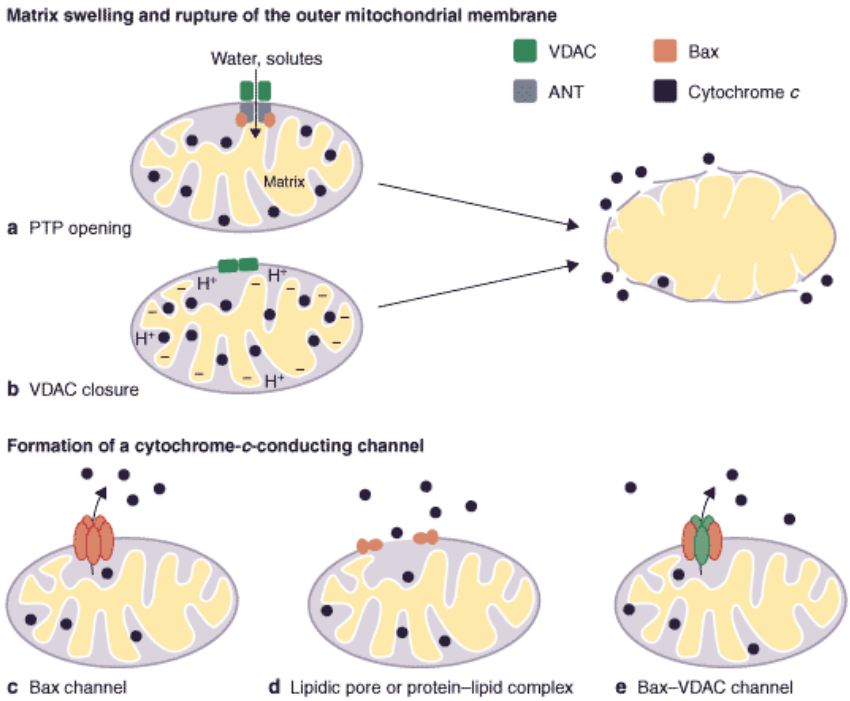

Figure 1.8. Mitochondria damage during apoptosis.

Changes in the $\Delta\psi_m$ have been orginally postulated to be early, obligate events in the apoptotic signaling pathway. Early loss of $\Delta\psi_m$ may occur independently of caspase activation. Dissipation of $\Delta\psi_m$ may also occur prior to caspase activation. The initial partial $\Delta\psi_m$ loss may be due to a yet unidentified non-caspase factor. At the same time the activation of caspase-9 would lead to further enhance $\Delta\psi_m$ dissipation. Caspase activation may provide a feedback amplification loop leading to dissipation of $\Delta\psi_m$ (Kaur, Sanyal, 2010).

1.6. Apoptosis in kidney diseases.

Normal function and development of the kidney has a great dependence on apoptosis. Apoptosis of cells within the kidney during organ development and during regeneration of tubules following renal damage insures proper nephron development and tubular repair (Schultz et al., 2003; Danial, Korsmeyer, 2004). Dysregulation of apoptosis during development is involved in the pathogenesis of congenital renal dysplasia and congenital polycystic kidney disease. In the pathogenesis of congenital renal dysplasia,

there is decreased branching of the uteric bud and failure of the renal mesenchyme to differentiate into nephrons. It is postulated that increased numbers of apoptotic cells in the mesenchyme surrounding dysplastic tubules may lead to spontaneous involution of the dysplastic kidney in congenital renal dysplasia. Deregulation of apoptosis in autosomal recessive polycystic kidney disease (ARPKD) appears to be associated with altered bcl-2 expression (Goliav et al., 2008).

Apoptosis is responsible for the progressive cell loss that occurs in the pathogenesis of glomerular sclerosis. Deletion of glomerular cells is accompanied by extracellular matrix accumulation in the rat kidney model of the disease. In contrast to glomerular sclerosis, during the chronic proliferative phase of systemic lupus erythematosus (SLE) there is a decrease in the number of apoptotic cells and an increase in the number of proliferating cells, causing an imbalance in tissue homeostasis (Kluz et al., 2009). Acute unilateral ureteral obstruction due to physical obstruction or congenital anomalies results in hydronephrosis and renal failure. In the neonatal and adult kidney, impairment of renal growth and tubular atrophy are associated with an increase in apoptosis, primarily in the distal tubular epithelium. The increase in apoptosis following obstruction is rapid; apoptotic cells appear after only 3 days of obstruction. Apoptosis-inhibiting pathways may be a key to the development of a rational treatment for obstructive nephropathy (Mao et al., 2008).

The regeneration process of the damaged kidney would not be successful without an increase in apoptosis. Acute ischemia followed by reperfusion induces acute tubular necrosis and apoptosis of the distal tubular epithelium. During the regeneration phase of tubular injury, there is an increase in cellular proliferation and a concomitant increase in apoptosis. In many cases, acute damage to proximal tubule epithelial cells appears to stimulate apoptosis within the distal tubules. Gentamicin-induced necrosis of proximal convoluted tubules was accompanied by a compensatory increase in apoptosis in the cortical and outer stripe of the medullary distal convoluted tubules (Oberbauer et al., 2001).

Apoptosis appears to contribute to the pathogenesis of both acute and chronic rejection of renal allografts. In an acute rejection, apoptosis occurs in the renal tubular epithelium, leading to tubular atrophy. Chronic transplant nephropathy is characterized by a sustained and irreversible loss of renal function accompanied clinically by

proteinuria and hypertension. Chronic renal allograft rejection is characterized by a gradual progression, suggesting persistent low grade injury. In support of this possibility, the mean number of apoptotic cells was higher in the proximal and distal tubules of rejected kidneys from patients with chronic renal allograft rejection (Porcheray et al., 2013).

1.6.1. Kidney damage in Hemolytic Uremic Syndrome.

Hemolytic-uremic syndrome (or haemolytic-uraemic syndrome), abbreviated HUS, is a disease characterized by hemolytic anemia (anemia caused by destruction of red blood cells), acute kidney failure (uremia), and a low platelet count (thrombocytopenia). It predominantly, but not exclusively, affects children. The more common form of the disease, Shiga-like toxin-producing E. coli HUS (STEC-HUS), is triggered by the infectious agent E. coli O157:H7 (Ruggenenti et al., 2001).

Shiga toxins (Stxs) are cytotoxic proteins expressed by the certain serotypes of STEC (Tarr et al., 2005). STEC may produce one or more genetic variants of Stxs, which are categorized based on their antigenic similarity to Stx. Stx type 1 (Stx1) is essentially identical to Stx, differing by a single amino acid residue in the A-subunit. Stx are ribosome-inactivating toxins, similar to Shiga toxin from Shigella dysenteriae serotype-1 and ricin from castor beans. The enzymatic A subunit and a cell binding B subunit that organizes into pentamers recognize a globotriaosylceramide (Gb3) membrane receptor on cells, particularly in glomerular endothelial cells. Internalized toxin-receptor complexes undergo retrograde transport to the endoplasmic reticulum via the Golgi apparatus where the A subunit N-glycosidase activity removes an adenine from 28S ribosomal RNA to inhibit protein synthesis (Melton-Celsa et al., 2012).

The most extensive tissue damage in HUS occurs in the kidneys (Figure 1.9). The injury is most prominent in the renal cortex, with pathological changes occurring in the glomerular endothelial cells and also in the tubular epithelial cells (Habib, 1992).

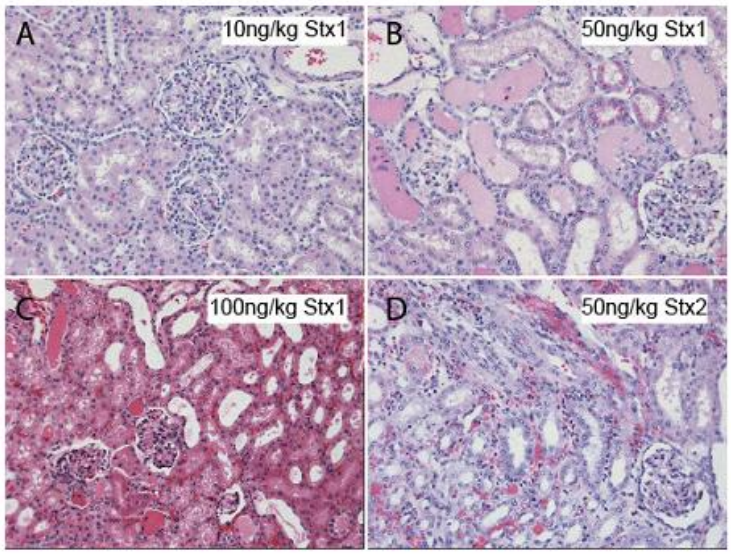

Figure 1.9. Histopathology of renal injury in nonhuman primates after challenge with Stx1 and Stx2.

Apoptosis is a primary injury induced by Stx. Apoptotic cells were detected in kidneys of mice with experimentally induced E. coli O157:H7 infection. Renal cortices from mice inoculated with Stx-2-positive E. coli O157:H7 exhibited high numbers of TUNEL-positive cells. Evidence for primary renal tubular cell damage in Stx HUS has been derived mainly from in vitro and in vivo studies in animals (Takeda et al., 1993; Shibolet et al., 1997; Karpman et al., 1998). Human renal tubular cells undergo apoptosis in vivo following D+ HUS and in an in vivo mouse model of E. coli-associated HUS (Shibolet et al., 1997). Apoptosis was also shown in human adenocarcinoma-derived renal tubular epithelial cells. It has been found that Stx1 binds to receptors and injures the proximal renal tubular cells. Incubation with interleukin-1 (IL-1) enhanced the cytotoxic effect of Stx1 and lipopolysaccharide increased cell sensitivity to Stx without altering Stx binding. A similar cascade of effects has been found in human renal endothelial cells (Hugles et al., 1998).

1.6.2. Kidney damage in Chronic Kidney Disease.

Worldwide, increasing numbers of patients are affected by Chronic Kidney Disease (CKD). Irrespective of the original cause, the degree of renal damage and loss of kidney function steadily progresses. A substantial part of the CKD patients ultimately progress to end-stage renal disease (ESRD) and therefore need renal replacement therapy, such as dialysis or renal transplantation (Meguid El Nahas, Bello, 2005).

1.6.2.1. Proteinuria in kidney damage.

In different clinical trials proteinuria is identified as an independent predictor of renal function decline and early reduction of proteinuria is associated with a slower progression of CKD. Proteinuria or albuminuria is a common feature of chronic kidney diseases, including diabetic nephropathy and nephrotic syndrome. Although proteinuria is a result of renal injury, it can also be a causative or aggravating factor for progressive renal damage. Excessive protein load can induce tubulointerstitial inflammation, fibrosis, tubular cell injury and death (Inker, 2014; Jafar et al., 2003).

1.6.2.2. Targets of proteinuria in CKD.

It is known that proximal tubular cells are targets of proteinuria in patients with CKD. Different theories exist on the potential mechanisms of proteinuria-induced tubular cell injury. The excessive reabsorption of ultrafiltered proteins by proximal tubular cells can lead to tubular damage and apoptosis/necrosis by exhaustion of the lysosomal degradation pathway and spillage of lysosomal enzymes into the cytoplasm or the production of reactive oxygen species (ROS) (Morigi et al., 2002; Shah et al., 2007). In addition, some compounds emerging from the catabolism of reabsorbed proteins have been considered to be harmful to the tubules, including ammonia and heme (Gonzalez-Michaca et al., 2004).

Proteinuria is not only a marker of renal damage, but ultrafiltered proteins are also toxic to the kidney, thereby contributing to tubulointerstitial damage. The urinary albumin level is an important prognostic indicator of renal diseases. In vitro exposure of tubular cells to high albumin concentrations activates a wide range of diverse intracellular signalling pathways (Zandi-Nejad et al., 2004). Also inflammatory and fibrogenic mediators are induced upon albumin exposure, including interleukin-8 (IL-8), tumor necrosis factor-α (TNF-α), endothelin, TGF-ß and collagen (Wohlfarth et al., 2003). Albumin can induce cell proliferation through phophatidylinositide 3-kinase (PI 3-

kinase) and extracellular-signal-regulated kinase (ERK, a member of mitogen-activated protein kinase)-dependent pathways (Dixon et al., 2000).

In vivo studies using overload proteinuria in rodents have confirmed many of these effects. For example, tubular IL-8, fractalkine, TGF-ß, osteopontin and MCP-1, and also interstitial collagens (Eddy, Giachelli, 1995; Donadelli et al., 2003) were upregulated after overloading rodents with albumin. It was shown that repeated intraperitoneal injections of albumin lead to increased transcapillary movement of albumin to the urinary space. This is accompanied with degenerative changes of glomerular epithelial cells characterized by swelling, vacuolization, increased reabsorption droplets, loss of foot processes, and lifting from the underlying glomerular basement membrane, ultimately resulting in defects in the glomerular sieving barrier (Moriwaki et al., 2007).

Podocytes are highly specialized epithelial cells with unique structure and function that are essential for maintenance of the glomerular filtration barrier. Because of their pivotal role in glomerular filtration, their delicate fimbriated structure, and their limited ability for regeneration and repair, podocytes have been considered critical and vulnerable targets of glomerular injury. Disruption of the anatomic relationships between adjacent foot processes and between foot processes and the glomerular basement membrane (GBM) are the earliest morphologic features of glomerular injury where proteinuria is a hallmark (Figure 1.10).

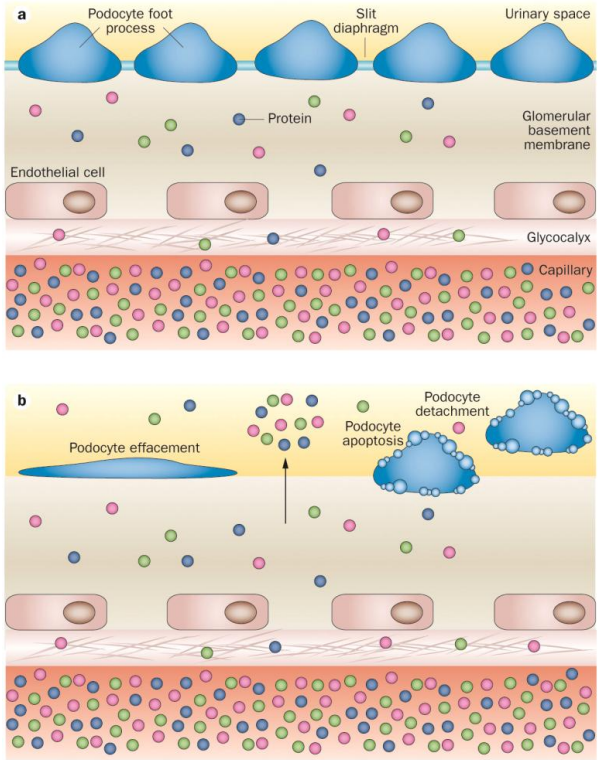

Figure 1.10. Podocytes in albumin filtration. A) – healthy kidney. B) – CKD.

Podocytes are generally regarded as passive targets of both immune and nonimmune injury. In experimental models, they are highly susceptible to a variety of injurious agents, including complement, ROS (Das et al., 2014), and toxins such as puromycin aminonucleoside. In Heymann nephritis, a rat model of human membranous nephritis, the combined insults of sublytic amounts of complement membrane attack complex and ROS induce podocyte injury and proteinuria (Wang et al., 2012). Glomerular epithelial cells produce the proinflammatory cytokines TNF-α and IL-6 after LPS stimulation in vitro. The ability of intrinsic renal cells to amplify inflammatory glomerular injury by their capacity to produce cytokines, particularly TNF-α, has been previously reported in murine anti-GBM nephritis, and in human membranous nephritis, podocytes are a prominent source of TNF-α (Müller et al., 2012).

1.6.2.3. Albuminuria-induced outcomes in CKD.

Proteinuria, which has been considered as a marker of glomerular injury, has also been implicated as an important factor involved in renal disease progression, especially causing tubulointerstitial fibrosis. Proteinuria is the result of altered permselectivity of the glomerular filtration barrier, caused by hemodynamic and nonhemodynamic factors. It is known that the result of detachment of glomerular endothelial cells and visceral epithelial cells from the glomerular basement membrane and appearance of protein reabsorption droplets seen as blebs in podocytes, observed on ultrastructural examination. Direct role for angiotensin II in modulating glomerular capillary permselectivity is thought to be mediated by nonhemodynamic effect on the cellular components of the glomerular filtration barrier, resulting in the opening of interendothelial junctions and epithelial cell disruption and through its hemodynamic effect, principally a reduction in renal perfusion and an increase in filtration fraction. Furthermore, angiotensin II and aldosterone have been shown to reduce nephrin expression in podocytes and may therefore directly affect glomerular permselectivity (Mundel, Shankland, 2002; Dvorak, 2006).

A causative association between excessive proteinuria and glomerular and interstitial inflammation was suggested by various in vitro studies. Cellular uptake by proximal tubular cells of the protein by endocytosis was observed to increase secretion of endothelin-1, interleukin-8 (IL-8), reactive oxygen species. The release of these molecules predominantly from the basolateral aspect of the cells contributes to the development of tubulointerstitial inflammation and fibrosis. The tubulointerstitial inflammation is also thought to be due to misdirection of protein rich glomerular filtrate into the interstitium due to formation of adhesion of tuft to the Bowman's capsule.

Tubulointerstitial damage is characterized by inflammatory cell infiltrates, loss of peritubular capillaries, tubular atrophy, and interstitial fibrosis. Proteins in the ultrafiltrate, such as albumin, but also lipids, glucose and growth factors, may injure/activate the tubular epithelial cells that consequently will produce various proinflammatory cytokines and chemokines and different interleukins. These in turn can attract inflammatory cells, such as monocytes and macrophages, to the renal interstitium. Macrophages can produce several factors contributing to ongoing renal damage and have an important role in the initiation and progression of interstitial

damage (Schlondorff, 2008). Activated tubular epithelium cells can undergo apoptosis leading to tubular atrophy.

Resident interstitial fibroblasts and myofibroblasts proliferate in response to macrophage-derived profibrotic cytokines. Also, under the influence of TGF-ß1 tubular epithelium cells can undergo epithelial to mesenchymal transformation (EMT), and migrate into the interstitium where they transform into myofibroblasts. Activated fibroblasts and myofibroblasts in the renal interstitium, which can be identified by α-smooth muscle cell expression, are a major source of extracellular matrix (ECM) proteins. An excessive production in parallel with reduced degradation of ECM proteins can lead to excessive ECM deposition and fibrosis (Schlondorff, 2008; López-Novoa, 2011). The final outcome of tubulointerstitial injury depends on the capacity of tubules to regenerate and inflammation to regress, and has been shown to be (to a certain extent) reversible.

1.6.3. Antiapoptotic drugs. Current state.

The apoptotic process is a physiological pathway that is essential for tissue homeostasis. In physiological conditions, the apoptotic route serves to remove cells that are no longer required. However, activation of apoptosis in kidneys is a hallmark of acute and chronic kidney diseases (Inker, 2014; Jafar et al., 2003). It is widely accepted that mitochondria are the main regulators of apoptosis and is a target for the anti-apoptotic treatment (Erkan, 2007). Mitochondrial-targeted substances (caspase inhibitors, resveratrol, melatonin etc.) are potent regulators of the mitochondrial apoptosis.

Caspases inhibitors inhibit cysteine-aspartic proteases or cysteine-dependent aspartate-directed proteases which are the family of cysteine proteases that play essential roles in apoptosis. Most of the inhibitors act like the peptidic caspase inhibitors. However, the animal toxicology studies showed liver abnormalities after a 9-month exposure to high doses (Lamkanfi et al., 2007).

Resveratrol (RESV) is a polyphenol that is an abundant component of red wine. Apart from its antioxidant properties, RESV may act as an activator of sirtuin 1 (SIRT1) (Robb et al., 2008). Once SIRT1 is activated, it exerts antiapoptotic effects by deacetylating transcription factors, such as the tumour suppressor p53, the FOXO

family of proteins (also called FKHR, a member of the Forkhead family of transcription factors), and NF-κB, thereby reducing their capacity to trigger cell death. Harmful properties of resveratrol may be pronounced in the human fetus, as it has diminished detoxification systems. Therefore, resveratrol as commonly sold combined with other "bioflavonoids", should not be used by pregnant women (Robb et al., 2008; Tomé-Carneiro et al., 2013).

Melatonin is a well-tolerated compound with multiple actions. Melatonin prevents mitochondrial calcium overload, mitochondrial depolarization, ROS formation, and the opening of the mitochondrial permeability transition pore that precedes Cyt c release (Paredes et al., 2009). Melatonin appears to cause very few side effects in the short term, up to three months. It was documented that healthy people taking it at low doses can develop a sleep disturbances. Recent studies have found results which suggested that it is toxic to photoreceptor cells in rats retinas when used in combination with exposure to sunlight. Melatonin also increases the incidence of tumours in white mice (Paredes et al., 2009; Rodriguez et al., 2010).

Coenzyme Q10 (CoQ10) and its short-chain analogue idebenone acting as a cofactor of the electron transport chain. Elevated levels of liver enzymes and insomnia in people taking doses of 300 mg per day for long periods of time were documented (Pravst et al., 2010).

Minocycline is a tetracycline derivative that has several differential features. This drug exerts antiapoptotic effects through a number of pathways. Several reports indicate that it decreases the activation of the intrinsic apoptotic pathway. It increases the expression of the antiapoptotic protein Bcl-2 and inhibits caspase 1 and -2 expressions. However, it was found that minocycline may cause a high range of side-effects: increased sensitivity to sunlight, sleep disorders, autoimmune disorders, thyroid cancer (Dean et al., 2012).

Rasagiline (N-propargyl-[1R]aminoindan) is a drug effective and useful for the antiapoptotic treatment since it inhibits apoptosis at multiple points. Rasagiline prevents mitochondrial depolarization, the release of pro-apoptotic proteins, and the activation of caspase 3. The main mechanism to explain the participation of rasagiline in mitochondrial membrane stabilization is unclear; however, it upregulates

antiapoptotic proteins such as Bcl-2 and Bcl-xL and decreases the expression of pro-apoptotic molecules, like Bax (Naoi et al., 2003). All these actions may contribute to the modulation of mitochondrial architecture (Oldfield et al., 2007; Naoi et al., 2003).

High doses of all described above compounds may be toxic, owing to prooxidative effects. These effects are particularly due to their potential to react with beneficial concentrations of ROS normally present at physiological conditions that are required for optimal cellular functioning. Due to this fact administration of these compounds have some limitations. More pre-clinical and clinical studies are necessary in order to evaluate the effectiveness and toxicity of mitochondrially-targeted antiapoptotic agents. In contrast, the results of our studies show that cardiotonic steroid hormone ouabain can be used in treatment of kidney diseases due to its capacity to prevent apoptosis via regulation of balance between pro- and anti-apoptotic effectors in mitochondrial intrinsic apoptotic pathway.

2 SPECIFIC AIMS

1. To evaluate whether ouabain-triggered Na,K-ATPase signaling may counteract the apoptotic action of Stx2 in kidney.
2. To study dose-dependent effect of different cartiotonic steroid hormones on Na,K-ATPase-triggered Ca^{2+} oscillations in kidney epithelial cells.
3. To evaluate whether ouabain-triggered Na,K-ATPase signaling may protect against albumin-induced kidney damage in Chronic Kidney Disease.

3 METHODOLOGICAL CONSIDERATIONS

3.1. Primary cell cultures of kidney cells.

Tissue culturing as a technique was first used almost 100 years ago to elucidate some of the most basic question in the developmental biology. Cell culture is a precious tool for investigators in numerous fields. It facilitates analysis of biological processes and properties which are not readily accessible at the level of the intact organism. To getting the cells for culture they must be isolated from a donor animal tissue or organ. The cell culture may be divided into three types according to their history: 1) primary, 2) secondary and 3) continuous cell culture. The primary and secondary cells are usually diploid cells. Primary cell lines derived directly from an intact tissue like animal's embryo or kidney. Secondary cells are derived from primary cultures. And the continuous cell lines are usually derived from malignant tissue.

Cells taken directly from the living tissue and established for the growth in vitro are primary cell culture. These cells undergo very few populations and are more representative of the major functional component of the tissue from which they are derived in comparison to continuous cell lines thus representing a more representative model to the in vivo studies. Primary cells from different species may be used allowing highlighting potential differences between humans and preclinical test species. Primary cultures are used to study the functional ability of cells, effect of external stimuli on cell functions, cell-cell interactions etc.

In this thesis we used rat proximal tubular cells (RPTC) and podocytes in primary culture in order to study the mechanism of protective effect of ouabain under the treatment with Stx2 and albumin. Advantage of the use of primary cultures is that cultured cells are used for reconstruction of damaged tissue or replacement of non-functional cells or tissues; ability to study the processes taking place in animal cells, e.g., metabolic regulations, cell physiology.

3.2. Experimental model of CKD. Passive Heymann Nephritis.

Passive Heymann Nephritis (PHN) is an experimental model of Membranous nephropathy (MN). PHN is a slowly progressive glomerular disease characterized by subepithelial immune complex deposits associated with increased protein excretion

without associated glomerular hypercellularity in acute injury. Subepithelial deposits, generalized thickening of the basement membrane, sclerosis and interstitial changes can occur depending on the severity and duration of the disease. Immunization of rats with a proximal tubular epithelial fraction (Fx1A) induces an immune complex "membranous" nephritis characterized by subepithelial immune deposits and proteinuria with striking resemblance to human disease. Fx1A contains a large glycoprotein gp330 (megalin) a nephritogenic antigen produced by glomerular epithelial cells. Passive administration of anti-Fx1A antibody produces a nephritis defined by two phases: 1) a heterologous phase representing an acute nephritis induced by exogenously administered antibody, and 2) a chronic autologous phase characterized by the production of the hosts own response to the exogenous (heterologous) sheep immunoglobulin planted within glomerular structures. All variants of the model produce subepithelial deposits and proteinuria.

3.3. Western blot.

A Western blot is a laboratory method used to detect specific protein molecules from among a mixture of proteins. This mixture can include all of the proteins associated with a particular tissue or cell type. Western blots can also be used to evaluate the size of a protein of interest, and to measure the amount of protein expression. This procedure was named for its similarity to the previously invented method known as the Southern blot.

The first step in a western blot is to prepare the protein sample by mixing it with a detergent called sodium dodecyl sulfate, which makes the proteins unfold into linear chains and coats then with a negative charge. Next, the protein molecules are separated according to their sizes using a method called gel electrophoresis. Following separation, the proteins are transferred from the gel onto a blotting membrane. Although this step is what gives the technique the name "western blotting," the term is typically used to describe the entire procedure.

Once the transfer is complete, the membrane carries all of the protein bands originally on the gel. Next, the membrane goes through a treatment called blocking, which prevents any nonspecific reactions from occurring. The membrane is then incubated with an antibody called the primary antibody, which specifically binds to the protein of interest. Following incubation, any unbound primary antibody is washed away, and the membrane is incubated yet again, but this time with a secondary antibody that

specifically recognizes and binds to the primary antibody. The secondary antibody is linked to a reporter enzyme that produces color or light, which allows it to be easily detected and imaged. These steps permit a specific protein to be detected from among a mixture of proteins. In this thesis Western blot has been used to determine the expression of apoptotic (Bax, caspase-3, caspase-8) and antiapoptotic (Bcl-xL) proteins in primary culture of RPTC subjected to influence of Stx2 and albumin with or without ouabain treatment.

3.4. Immunocytochemistry and immunohistochemistry.

Immunohistochemistry or IHC staining of tissue sections (or immunocytochemistry, which is the staining of cells), is one of the most commonly applied immunostaining technique. The IHC staining can be done using fluorescent dyes or non-fluorescent methods using enzymes such as peroxidase and alkaline phosphatase. These enzymes are capable of catalysing reactions that give a coloured product that is easily detectable by light microscopy. Alternatively, radioactive elements can be used as labels, and the immunoreaction can be visualized by autoradiography. The antibodies used for specific detection can be polyclonal or monoclonal. For IHC detection strategies, antibodies are classified as primary or secondary reagents. Primary antibodies are raised against an antigen of interest and are typically unconjugated (unlabelled), while secondary antibodies are raised against immunoglobulins of the primary antibody species. The secondary antibody is usually conjugated to a linker molecule, such as biotin, that then recruits reporter molecules, or the secondary antibody itself is directly bound to the reporter molecule. Reporter molecules vary based on the nature of the detection method, the most popular are chromogenic and fluorescence detection mediated by an enzyme or a fluorophore, respectively. Both immonicytochemistry and immunohistochemistry were used in this thesis. Using specific antibodies we assessed the expression of proapoptotic factor Bax and antiapoptotic factor Bcl-xL in kidney tissue of mice inoculated with Stx2 and in Stx2-inoculated mice treated with ouabain. The expression of Bcl-xL and Bax was visualized by immunofluorescence. Semiquantitative evaluation of thefluorescence by ImageJ software was performed on one section from each kidney. Based on the same principle, detection of podocyte number (using specifi marker WT-1), level of cell proliferation (using Ki-67 and PCNA as a specific markers), level of glomerulosclerosis (using collagen IV as a marker), fibrosis (using TGF-beta 1 as a marker) were done in kidney tissue of rats with induced Passive Heymann Nephritis.

3.5. Morphometric analysis.

This is a method whereby the amounts of particular tissue or subcellular components are quantified. These components may be, for example, particular cell types (at the tissue level), or the nucleus, mitochondria or secretory vesicles, for example, at the cellular level. To do this, the area of the particular component of interest and the total (tissue or cellular) area need to be determined. This used to be achieved by what was termed 'point counting', which involved the overlaying of an acetate sheet - with points regularly dotted upon it - over a photographic image. The subsequent counting of points over the component of interest and the whole tissue/cell was rather tedious and time-consuming. We used a morphometric analysis in order to be able to evaluate the level of glomerular-tubular disconnection in kidney tissue of rats with PHN.

3.6. TUNEL assay. ApopTag® technology.

Terminal deoxynucleotidyl transferase dUTP nick end labeling (TUNEL) is a method for detecting DNA fragmentation by labeling the terminal end of nucleic acids. TUNEL is a common method for detecting DNA fragmentation that results from apoptotic signaling cascades. The assay relies on the presence of nicks in the DNA which can be identified by terminal deoxynucleotidyl transferase or terminal deoxynucleotidyl transferase (TdT), an enzyme that will catalyze the addition of dUTPs that are secondarily labeled with a marker. It may also label cells that have suffered severe DNA damage.

ApopTag detects single-stranded and double-stranded breaks associated with apoptosis. Drug-induced DNA damage is not identified by the TUNEL assay unless it is coupled to the apoptotic response. The betefit of this technique for our project is that this method can detect early-stage apoptosis in systems where chromatin condensation has begun and strand breaks are fewer, even before the nucleus undergoes major morphological changes. ApopTag Apoptosis Detection distinguishes apoptosis from necrosis by specifically detecting DNA cleavage and chromatin condensation associated with apoptosis. Visualization of positive ApopTag® results should reveal focal *in situ* staining inside early apoptotic nuclei and apoptotic bodies. This positive staining directly correlates with the more typical biochemical and morphological aspects of apoptosis.

The reagents provided in all ApopTag® assay are designed to label the free 3'OH DNA termini *in situ* with chemically labeled and unlabeled nucleotides. The nucleotides contained in the Reaction Buffer are enzymatically added to the DNA by TdT. TdT catalyzes a template-independent addition of nucleotide triphosphates to the 3'-OH ends of double-stranded or single-stranded DNA. The incorporated nucleotides form an oligomer composed of digoxigenin or fluorescein nucleotide and unlabeled nucleotide in a random sequence.

3.7. NF-κB activity.

Low concentrations of ouabain activate the survival factor p65, a subunit of the pleiotropic transcriptional factor NF-κB. Because NF-κB units under nonstimulated conditions are located in the cytoplasm, we immunostained RPTCs with a p65-specific antibody and compared the nuclear/cytoplasmic ratio of the immunosignal. Images of immune-labeled cells were recorded with confocal microscopy. The ratio of the immunosignal between nucleus and cytosol was measured using ImageJ software. An area corresponding to 90% of the nucleus and an identical area in the cytoplasm were used for the measurements. NF-kB p65 subunit DNA binding in nuclear protein extracts was assessed using a commercially available NF-kBp65 transcription factor assay has been use to assess the NF-κB activity in Stx2-treated RPTC with or without ouabain.

3.8. Mitochondria labeling. BacMam technology.

The BacMam technology is based on double-stranded DNA insect viruse (Baculovirus) as vehicles to efficiently deliver and express genes in mammalian cells. The baculovirus has been modified by engineering of a mammalian expression cassette for transgene expression in mammalian cells. Baculoviruses are non-replicating in mammalian cells and thus have an excellent safety profile combined with being well-tolerated by cells. BacMam reagents have been used in cell based assays, live cell imaging, stem cell biology and many other applications. To introduce genes into mammalian cells, a standard transduction process is used. BacMam particles are taken up by endocytosis and released for transcription and expression following migration to the nucleus. Gene expression begins within 4–6 hours of transduction and is at near maximum level within 24 hours of transduction. In our study we used BacMam technology in order to label mitochondria in RPTC (Figure 3.1).

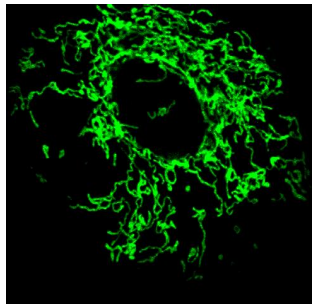

Figure 3.1. Mitochindria in RPTC labeled using BacMam technology.

3.9. Mitochondrial membrane potential assessment.

The membrane-permeant JC-1 dye is widely used in apoptosis studies to monitor mitochondrial health. JC-1 dye can be used as an indicator of mitochondrial membrane potential in a variety of cell types, including myocytes and neurons, as well as in intact tissues and isolated mitochondria. A distinctive feature of the early stages of programmed cell death is the disruption of active mitochondria. This mitochondrial disruption includes changes in the membrane potential and alterations to the oxidation–reduction potential of the mitochondria. Changes in the membrane potential are presumed to be due to the opening of the mitochondrial permeability transition pore, allowing passage of ions and small molecules. The resulting equilibration of ions leads in turn to the decoupling of the respiratory chain and the release of cytochrome c into the cytosol. Probes that detect mitochondrial membrane potential are positively charged, causing them to accumulate in the electronegative interior of the mitochondrion. Changes in the mitochondrial membrane potential can be measure by a variety of fluorescent techniques such as flow cytometry and fluorescent imaging. Mitochondrion-selective reagents enable researchers to probe mitochondrial activity, localization and abundance, as well as to monitor the effects of some pharmacological agents, such as anesthetics that alter mitochondrial function.

The membrane-permeant JC-1 dye is widely used in apoptosis studies to monitor mitochondrial health. JC-1 dye exhibits potential-dependent accumulation in mitochondria, indicated by a fluorescence emission shift from green (~529 nm) to red (~590 nm). Consequently, mitochondrial depolarization is indicated by a decrease in the red/green fluorescence intensity ratio. The potential-sensitive color shift is due to concentration-dependent formation of red fluorescent J-aggregates. JC-1 dye can be

used as an indicator of mitochondrial potential in a variety of cell types, including myocytes and neurons, as well as in intact tissues and isolated mitochondria. JC-1 dye is more specific for mitochondrial versus plasma membrane potential and more consistent in its response to depolarization than some other cationic dyes such as DiOC6 and rhodamine. The ratio of green to red fluorescence depends only on the membrane potential and not on other factors such as mitochondrial size, shape, and density, which may influence single-component fluorescence signals. In our project we used JC-1 dye in order to assess the mitochondrial potential changes in RPTC upon different influences (Figure 3.2). Use of fluorescence ratio detection therefore allows us to make comparative measurements of membrane potential and determine the percentage of mitochondria within a population that respond to an applied stimulus.

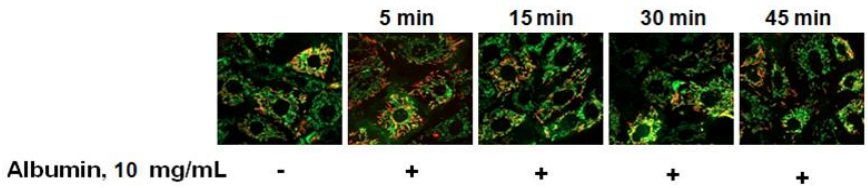

Figure 3.2. RPTC subjected to albumin and loaded with JC-1.

3.10. Ca^{2+} recording.

In eukaryotic cells Ca^{2+} is one of the most widespread second messengers used in signal transduction pathways. Intracellular levels of Ca^{2+} are usually kept low, as Ca^{2+} often forms insoluble complexes with phosphorylated and carboxylated compounds. Typically cytosolic Ca^{2+} concentrations are in the range of 100 nM. In response to stimuli Ca^{2+} may either be released from external medium or internal stores to raise the Ca^{2+} concentration. As Ca^{2+} cannot be visualized directly in living cells, it may be imaged indirectly by fluorescent Ca^{2+} indicators.

Ion sensitive dyes are fluorescent molecules which reversibly bind to specific ions. These dyes are sensitive to changes in ion concentration either by increase or decrease of fluorescence. A measure for the affinity of ion binding to the dye is the dissociation constant (Kd). The lower the Ca^{2+} binding affinity the higher the Kd (Ca^{2+}). There are two major groups of ion-sensitive dyes: 1. Single wavelength dyes, like Fluo3 and Calcium Green which are suitable for non-ratiometric measurements. The intensity of

the emitted fluorescence light increases proportional to free ion concentration. 2. Dual wavelength dyes are used for ratiometric measurements.

In our work we used Fura-2, an aminopolycarboxylic acid, is a ratiometric fluorescent dye which binds to free intracellular calcium. Fura-2 is excited at 340 nm and 380 nm of light, and the ratio of the emissions at those wavelengths is directly correlated to the amount of intracellular calcium. Regardless of the presence of calcium, Fura-2 emits at 510 nm of light. The use of the ratio automatically cancels out confounding variables, such as variable dye concentration and cell thickness, making Fura-2 one of the most appreciated tools to quantify calcium levels.

3.11. Confocal microscopy.

Confocal microscopy is an optical imaging technique used to increase optical resolution and contrast of a micrograph by using point illumination and a spatial pinhole to eliminate out-of-focus light in specimens that are thicker than the focal plane. It enables the reconstruction of three-dimensional structures from the obtained images. This technique has gained popularity in the scientific and industrial communities and typical applications are in life sciences, semiconductor inspection and materials science. All parts of the specimen in the optical path are excited at the same time and the resulting fluorescence is detected by the microscope's photodetector or camera including a large unfocused background part. In contrast, a confocal microscope uses point illumination and a pinhole in an optically conjugate plane in front of the detector to eliminate out-of-focus signal - the name "confocal" stems from this configuration. As only light produced by fluorescence very close to the focal plane can be detected, the image's optical resolution, particularly in the sample depth direction, is much better than that of wide-field microscopes. We used confocal microscopy techniques in terms of imaging of intracellular proteins on a live cells and fixed samples.

4 SUMMARY AND DISCUSSION

4.1. Protective effect of ouabain against kidney damage induced by Shiga toxin.

Hemolytic uremic syndrome is a disease characterized by microangiopathic hemolytic anemia, thromobocytopenia, and acute renal failure. HUS is the most common cause of acute renal failure in children. It is associated with 5-10% mortality. The kidney is the most severely affected organ and many children with HUS require renal replacement therapy (Obrig, 2010; Karpman et al., 2010). Histopathological studies have shown that the renal injuries are most prominent in the cortex, affecting both glomerular endothelial cells and tubular epithelial cells (Karpman, Hakansson et al., 1998). Stx is considered to be a major determinant of HUS-related virulence and is generally believed to contribute to the severe glomerular and tubular pathology in HUS. Recent studies have shown that apoptosis of kidney cells is a prominent feature in acute renal damage triggered by Stx (Psotka et al., 2009). In experimental studies performed on mice it was shown that Stx2 triggers extensive apoptosis, primarily in cortical tubular cells. In a recent study in children with HUS caused by shiga toxin producing E.Coli, extensive apoptosis, predominantly in the renal tubular cells, was observed (Karpman, Hakansson et al., 1998).

In this study we tested whether Stx2 can induce apoptosis in RPRC in vitro. We made a semiquantitative estimation by calculating apoptotic index in TUNEL stained RPTC exposed to Stx in presence or absence of ouabain. RPTC were exposed to Stx in concentrations ranging from 2 ng/mL to 4 ng/mL. We found that Stx concentrations in the range of 3-4 ng/mL gave a reproducible level of apoptosis. In cells co-incubated with Stx and ouabain 5 nM the apoptotic effect was almost completely abolished (**Figure 4.1**).

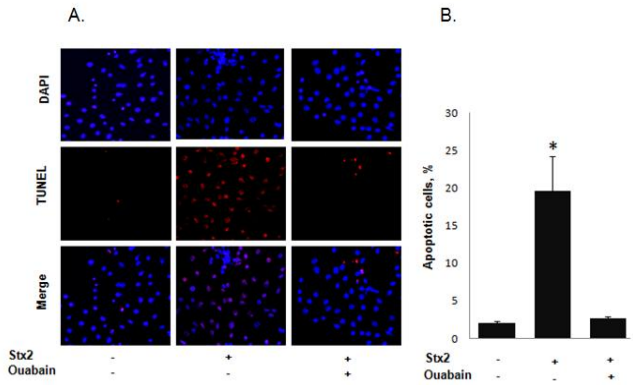

Figure 4.1. **A**. Stx2 induces apoptosis in rat proximal tubular cells and ouabain has a protective. RPTC were TUNEL-stained (red) to detect apoptotic cells and counterstained with DAPI (blue). **B**. AI was determined by analyzing five to seven randomly selected areas with 100 to 200 cells in each area.

Induction of apoptosis occurs via two major pathways, the extrinsic pathway, where activation of plasma membrane "death receptors" leads to the recruitment of caspase-8 (Sauter et al., 2008), and the intrinsic pathway, mitochondrial pathway, where the pro-apoptotic dimerizing factors Bax and Bak are recruited to the mitochondrial membrane (Kroemer et al., 2007). Both pathways will initiate signaling cascades that result in the cleavage of caspase-3 and cell death (Elmore, 2007).

In this study we found that Stx2 exposure for 16 h caused a prominent up-regulation of caspase-8, of Bax, and of caspase-3. We also detected a substantial down-regulation of Bcl-xL. The recordings made after 6 h of Stx2 exposure indicated that the effects on Bax and Bcl-xL preceded the effects on caspase-8 and 3. The up-regulation of Bax, but not of caspase-8, was attenuated by ouabain (**Figure 4.2**).

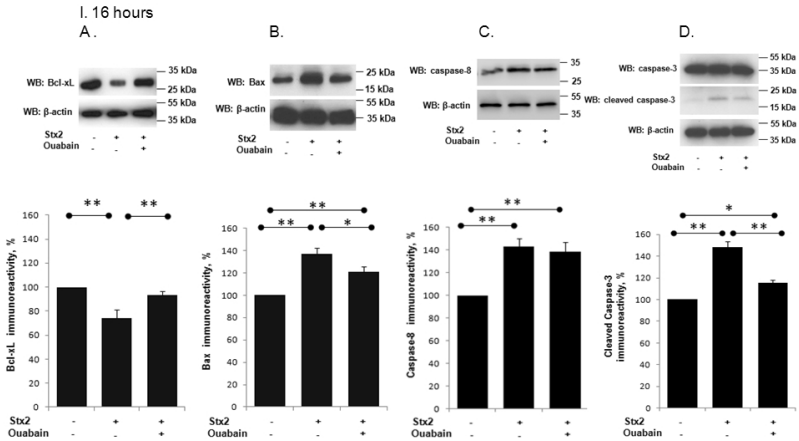

Figure 4.2. Expression of Bax, Bcl-xL, caspase-8, caspase-3 in Stx 2- and ouabain-treated cells. Expression of the Bax (A), Bcl-xL (B), caspase-8 (C) and caspase-3 (D) in presence of Stx2 and ouabain during 16 hours. Densitometric quantification of bands was done for the respective blots. The density of the band from control cells was set to 100%.

Caspase-8 can initiate both the extrinsic and intrinsic apoptotic pathway, since it may either bypass the mitochondrial pathway and directly cleave caspase-3, or via a series of events facilitate the translocation of Bax to the mitochondrial membrane (Elmore, 2007). Taken together these results imply that in Stx2-triggered apoptosis, caspase-8 may mainly act by stimulating Bax and the intrinsic apoptotic pathway. Little is known about the effect of Stx2 on the expression of the Bax inhibitor Bcl-xL, but over-expression of Bcl-xL by transient transfection was reported to protect against Stx-triggered apoptosis (Gordon et al., 2000). Here we could show that the down-regulation of this survival factor in Stx2-treated renal epithelial cells was almost completely abolished by ouabain treatment. Since there is little evidence for a more direct interaction between caspase-8 and Bcl-xL, we conclude that the anti-apoptotic effect of ouabain is due to inhibition of the intrinsic, mitochondrial apoptotic pathway, and that treatment with ouabain protects from apoptosis by reversing an imbalance between Bcl-xL and Bax, as shown both in the *in vitro* and *in vivo* studies (**Figure 4.3**).

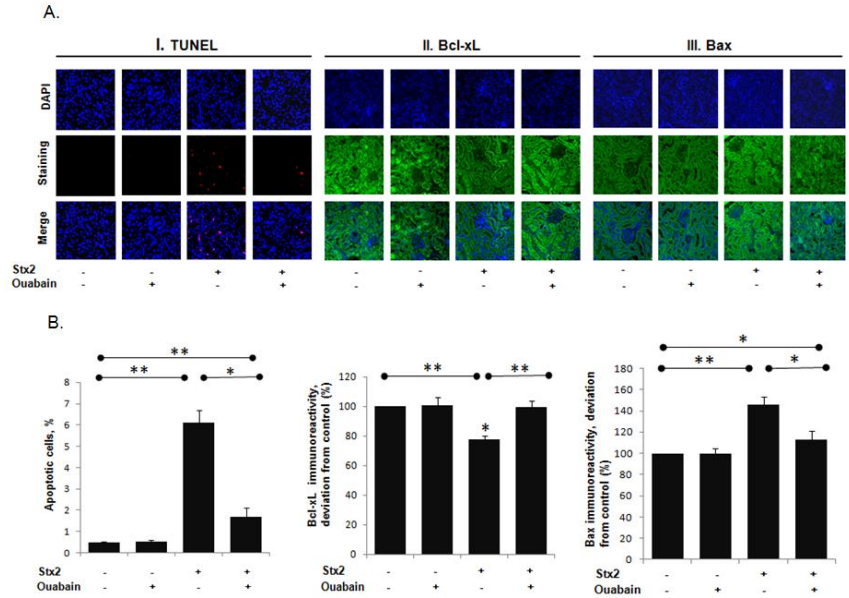

Figure 4.3. **A.** Expression of Bax, Bcl-xL, caspase-8, caspase-3 in Stx 2- and ouabain-treated cells. Representative confocal images of kidney sections from mice inoculated with Stx2 or PBS as vehicle, with and without continuous treatment with ouabain. Sections were labeled with terminal deoxynucleotidyl transferase-mediated dUTP nick-end labelling (TUNEL, red) to detect apoptotic cells (I), immunohistochemically stained for Bcl-xL (II) and Bax (III). Nuclei were counterstained with 4′,6-diamidino-2-phenylindole (DAPI, blue). **B.** AI is given as % apoptotic cells. Immunoreactivity for Bcl-xL and Bax is expressed as % deviation from control.

We describe the anti-apoptotic effect of ouabain to the signaling function of Na,K-ATPase. Exposure of renal cells to low concentrations of the highly specific Na,K-ATPase ligand, ouabain, will trigger a signaling cascade that involves interaction between the catalytic subunit of Na,K-ATPase and the inositol 1,4,5 triphosphate receptor, intracellular calcium oscillations and activation of the NF-kB p65 subunit. We showed that Stx2 does not affect the capacity of ouabain bound Na,K-ATPase to interact with IP3R. Bcl-xL is a target for the transcriptional effect of the NF-κB p65 subunit (Khoshnan et al., 2000). Here we showed that ouabain signaling triggers activation and translocation of NF-κB p65 subunit to the nucleus in cells exposed to Stx2 and ouabain, but found no evidence of NF-κB p65 subunit activation in cells exposed to Stx2 alone (**Figure 4.4**). The concentration of ouabain used in this study, 5nM, has no measurable effect on the pumping function of Na,K-ATPase in rat cells.

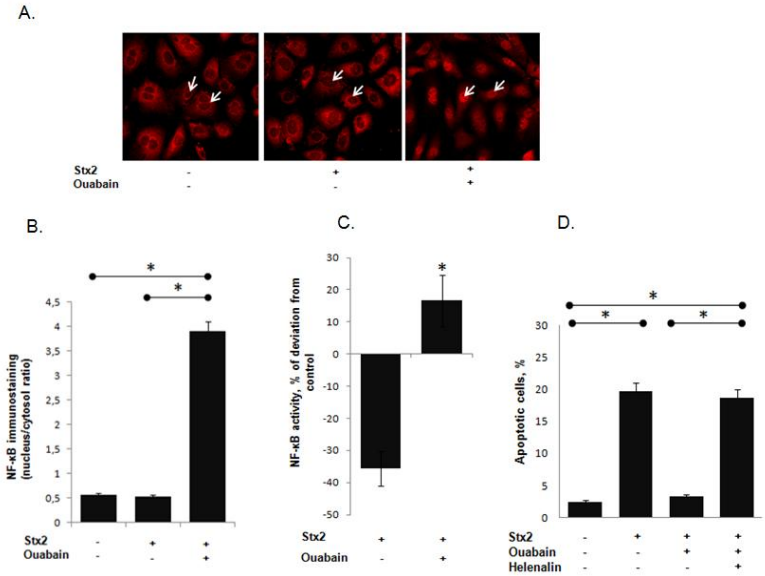

Figure. 4.4. **A**. Representative confocal images of NF-κB p65 subunit immunofluorescence signal in RPTC (marked with white arrow). Note the strong nuclear signal in ouabain-exposed cells in the right panel. **B.** Bars show mean nuclear/cytosol NF-κB p65 subunit signal. **C**. NF-κB p65 subunit activity in rat RPTC determined as NF-κB DNA binding capacity in nuclear protein extracts. The activity of the control was set to 100%. **D.** Helenalin is a specific NF-κB inhibitor that abolishes the antiapoptotic effect of ouabain. AI was determined by analyzing five to seven randomly selected areas with 50 to 200 cells enabling an analysis of around 5000 cells.

4.2. Future perspectives.

Currently HUS treatment is directed towards alleviating the acute functional consequences of kidney failure. Early peritoneal dialysis or hemodialysis has been widely used and has improved morbidity and mortality of HUS (Brunner et al., 2004; Amirlak, 2006). Treatment with antiplatelet factors such as aspirin and dipyridamole (Amirlak, 2006; Van Damme-Lombaerts et al., 1988), high dose intravenous furosemide (Rousseau et al., 1990), fresh frozen plasma and plasmapheresis have little or no proven therapeutic value (Bramlage et al., 2009). Other approaches to HUS management, such as monoclonal antibodies against Shiga toxin 2 are being tested on animal models (Sheoran et al., 2003) but have in healthy volunteers been shown to have side effects (Bitzan et al., 2009). Thus, there is currently no specific therapy that will protect kidney tissue from permanent damage.

Our in vivo study provided proof of principle that ouabain can protect proximal tubular cells from Stx2-triggered apoptosis, that Stx2 triggers an imbalance between Bax and Bcl-xL, and that this change in balance can be reversed by ouabain treatment. Continuous treatment with ouabain was started 24 h before the Stx2 injection. This is a time frame that may be relevant for the future therapeutic use of ouabain. The findings reported by us imply that renal cell apoptosis should be a major target for prevention of permanent renal damage in Stx2 triggered HUS and that ouabain, or maybe other cardiotonic steroids, might offer a novel therapeutic approach. Ouabain-induced triggered pathway will restore a physiological level of Bcl-xL and the balance between apoptotic and anti-apoptotic factors in HUS-injuried kidneys.

4.3. Cardiotonic steroids trigger Ca^{2+} oscillations in kidney epithelial cells.

Na,K-ATPase is a ubiquitous plasma membrane protein expressed in all eukaryotic cells. The pumping function of NKA is essential for regulation of cell ionic content, pH and for maintaining resting membrane potential. The CTS are highly specific NKA ligands that bind to all catalytic α-isoforms (Lingrel, 2010; Schoner, Scheiner-Bobis, 2007). All CTS can be divided into two families, the cardenolides, to which ouabain and digoxin belong and the bufadienolides, to which marinobufagenin belongs. There are data showing that different CTS have different binding the NKA catalytic subunit due to the number and nature of various sugar residues and changes in the position of hydroxyl groups of the steroid core (Cornelius et al., 2013). Studies from our group showed a new property of CTS (ouabain) to trigger slow regular Ca^{2+} oscillations within a period of range between 3 to 5 minutes that elicit activation of the transcription factor, NF-κB (Aaizman et al., 2001).

In this study we tested whether other CTS beside ouabain can play role in NKA-triggered Ca^{2+} oscillations. We found that cardenolide digoxin and the bufadienolide marinobufagenin may also trigger Ca^{2+} oscillations of similar frequency (**Figure 4.5**).

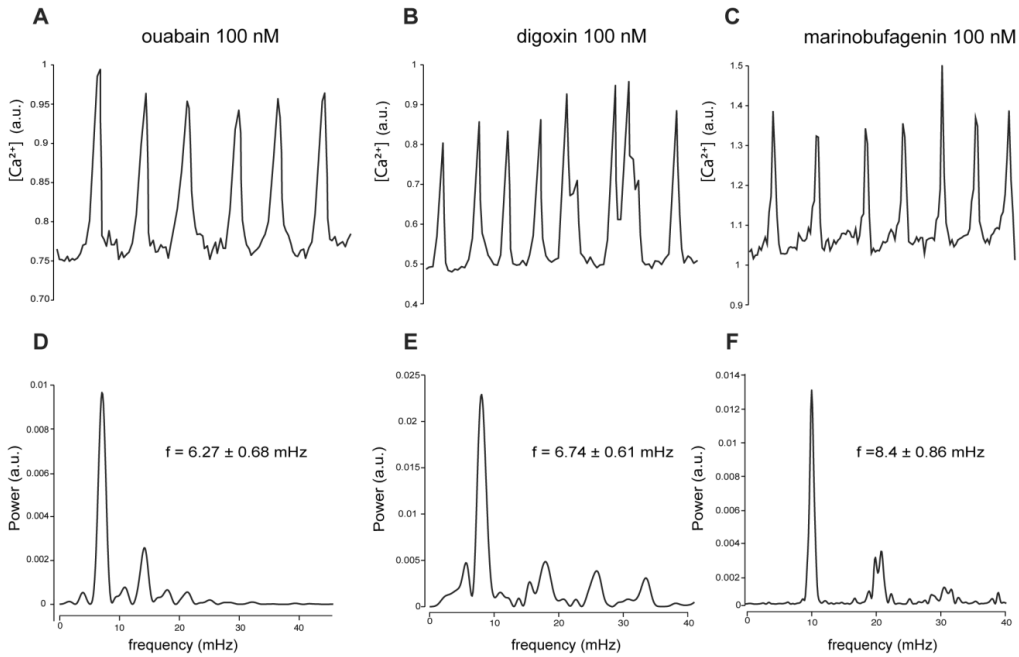

Figure 4.5. Effect of different CTS on NKA-dependent Ca^{2+} oscillations in COS-7 cells. Each plot corresponds to the single-cell recording above. *D*, *E* and *F* power spectral analysis of the three CTS-evoked Ca^{2+} oscillations depicted in *A*, *B* and *C*.

Binding of cardiotonic steroids to NKA will also stimulate tyrosine phosphorylation. These observations originally made by Xie and Askari at Toledo University (Kometiani et al., 1998; Haas et al., 2000). In this study we tested whether Src phosphorylation is required for the initiation of the CTS evoked Ca^{2+} signaling pathway. Our results show that that this is likely the case. We have shown that pre-treatment of COS-7 with PP2, an inhibitor of Src, significantly reduced the number of cells responding with Ca^{2+} oscillations. We have also tested the effect of inhibitors of signaling molecules that are known to be activated by the EGF receptor, but have not found an evidence for their involvement in the triggering of Ca^{2+} oscillations (**Figure 4.6**).

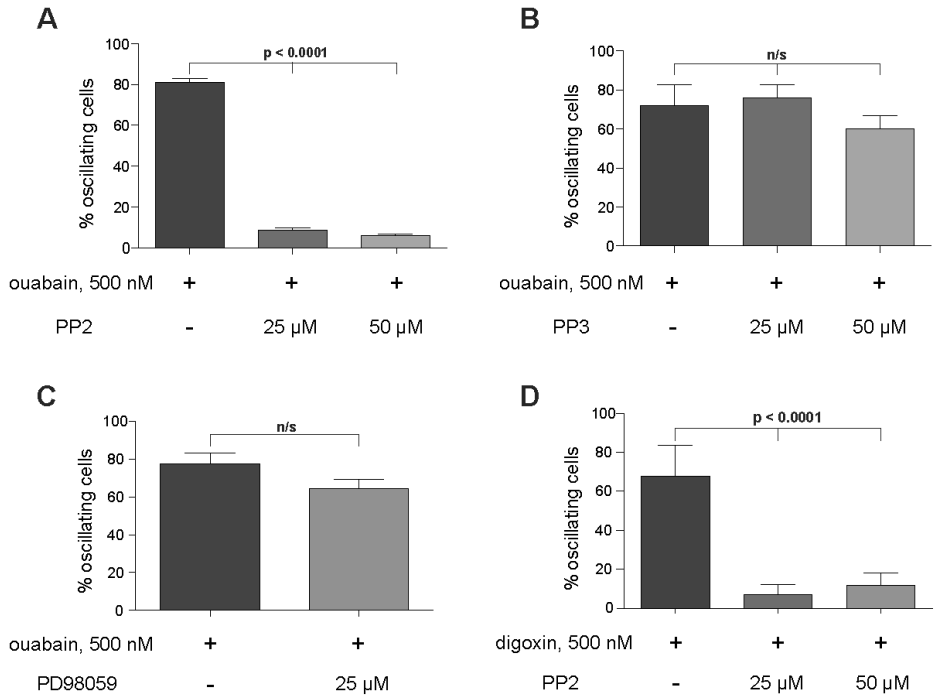

Figure 4.6. Effects of kinase inhibitors on ouabain- or digoxin-induced $[Ca^{2+}]_i$ oscillations. Data are mean ± SEM of the percentage of cells oscillating from at least 3 independent experiments, and the figure shows a representative recording of both control and the cells that were pretreated with different concentrations (25 and/or 50 µM) of inhibitor. *A*, Ouabain-induced Ca^{2+} oscillations are significantly suppressed by the Src kinase inhibitor PP2 but not by its inactive equivalent PP3, *B*, or the ERK 1/2 inhibitor PD98059 (C). *D*, Digoxin-induced Ca^{2+} oscillations are significantly suppressed by PP2.

4.4. Future perspectives.

In this study we have shown that two other cardiotonic steroids from the same class of family as ouabain initiate a similar calcium signaling pathway. This is one of the first functional studies of the endogenous cardiotonic steroid marinobufagenin. Secondly, we have found that the ouabain/calcium signaling pathway includes the Src activation but not the activation of Erk. The results derived from this study have provided novel information that is important and useful when the clinical study with ouabain or other CTS in terms of CKD treatment will be planned.

4.5. Suppression of albumin-triggered apoptosis slows down the progression of Chronic Kidney Disease.

Chronic kidney disease (CKD) is the 12th most common cause of death and the incidence is increasing worldwide. CKD has a progressive course, irrespective of the origin of the disease. Treatment with inhibitors of the renal angiotensin system will, by decreasing glomerular pressure and reducing the albuminuria, slow the progression, but can not stop it. Apoptosis and fibrosis are typical pathological features in CKD. Morphologically CKD is characterized by loss of podocytes, glomerular sclerosis and glomerular-tubular disconnection. The albuminuria is a predictor of the progressive loss of kidney function, and is also considered a major cause of the progression of CKD (Anderson et al., 2009).

To understand whether treatment of chronic kidney disease should primarily target fibrosis or apoptosis, or both, information is required about the initial cellular response to albumin overload. To address this important question we have exposed primary rat proximal tubule cells (RPTC) to albumin for 0 – 8 hours. A time and dose dependent increase in apoptotic index is observed and early signs of apoptosis precede early signs of fibrosis (**Figure 4.7**).

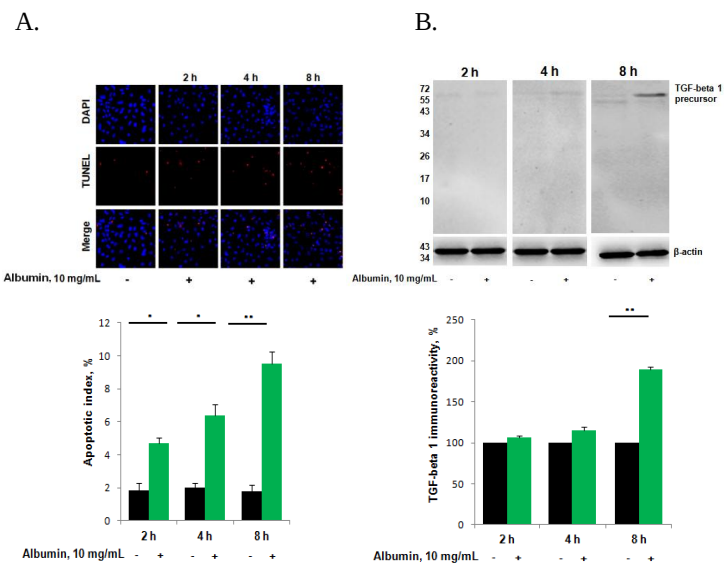

Figure 4.7. **A.** Time dependence of albumin-induced apoptosis in RPTC cells. RPTC cells were incubated for 0-8 hours with 10 mg/ml albumin in serum-free medium. RPTC were TUNEL-

stained (red) to detect apoptotic cells and counterstained with DAPI (blue). **B**. Time dependence of changes of albumin-induced expression of TGF-beta 1 in RPTC cells. RPTC cells were incubated for 0-8 hours with 10 mg/ml albumin in serum-free medium. Experiments were repeated four times.

To document the uptake of albumin, we used Alexa-555 tagged albumin. A massive uptake was noted already at 2 hours (**Figure 4.8**).

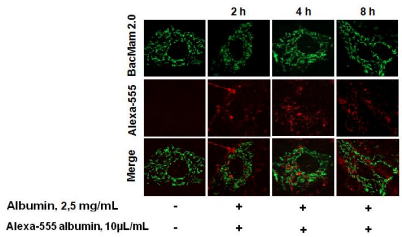

Figure 4.8. Time dependence of Alexa Fluor 555-coupled albumin internalization by RPTC. Cells were subjected to live cell imaging. All images represent a single section through the focal plane.

We next studied the capacity of ouabain to rescue from albumin-triggered apoptosis in RPTC exposed to albumin. The apoptotic effects of albumin were time- and dose-dependent. Co-incubation with ouabain resulted in substantial reduction of the apoptotic index at all time points and for all concentrations of albumin (**Figure 4.8**). The same effect has been obtained with TGF-beta expression in cells incubated with albumin 10 mg/mL for 8 and 18 hours.

A.

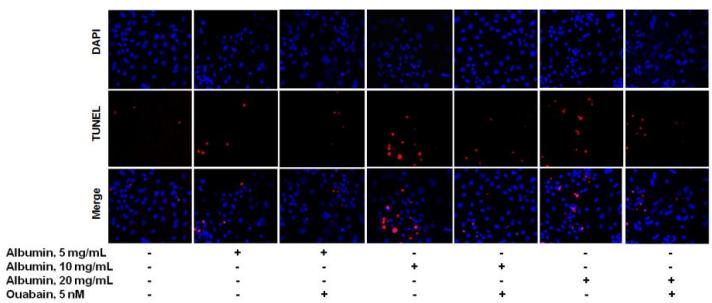

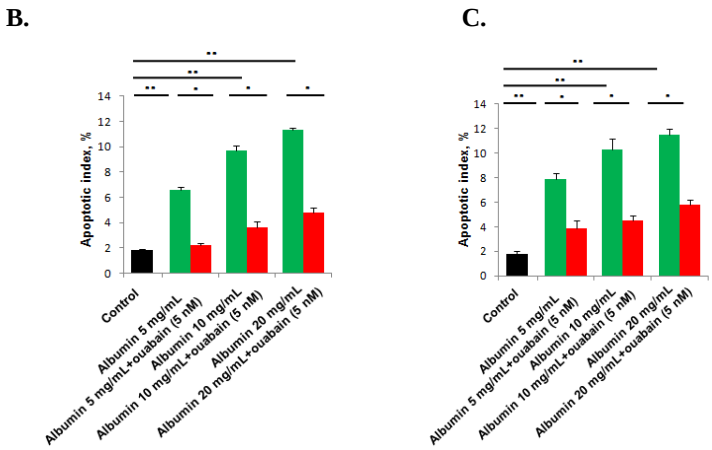

Figure 4.8. **A**. Representative images of the dose dependence of albumin-induced apoptosis in RPTC cells incubated for 18 hours with 0 to 20 mg/ml albumin with or without ouabain (5 nM) in serum-free medium. RPTC cells were incubated for 8 hours (**B**) or 18 hours (**C**) with 0 to 20 mg/ml albumin with or without ouabain (5 nM) in serum-free medium. AI was determined by analyzing five to seven randomly selected areas with 100 to 200 cells in each area. Histograms represent means ± SEM. ** - $p<0.001$, * - $p<0.01$. Statistical analysis was performed using one-way ANOVA. Experiments were repeated four times.

The intrinsic apoptotic pathway is initiated by the translocation of apoptotic factor Bax to the mitochondria, where it permeabilizes the outer mitochondrial membrane to promote apoptosis (Edlich et al., 2001). In this study we used an albumin to induce apoptosis in RPTC. We found that albumin enters the cells. We documented an almost immediate translocation of Bax to the mitochondria accompanied by a depolarization of the mitochondrial membrane. From our previous studies we know that ouabain triggers an anti-apoptotic signaling pathway (Zhang et al., 2006; Li et al., 2006; Lie at al., 2010). We have shown that nM ouabain can provide protection against apoptosis in fetal rat kidneys exposed to malnutrition and in adult mouse kidneys exposed to Shiga toxin by activating the anti-apoptotic factor Bcl-xL, which counteracts the effects of the apoptotic factor Bax (Burlaka et al., 2013). Here we present evidence that ouabain counteracts the translocation of Bax to mitochondria and the change in mitochondrial membrane potential in albumin exposed rat proximal tubular cells. Changes were more significant after 1 hour with albumin 10 mg/mL and after 2 hours with albumin 2,5

mg/mL. The rescuing effect of ouabain was more pronounced in cells incubated with albumin 2,5 mg/mL (**Figure 4.9**).

A.

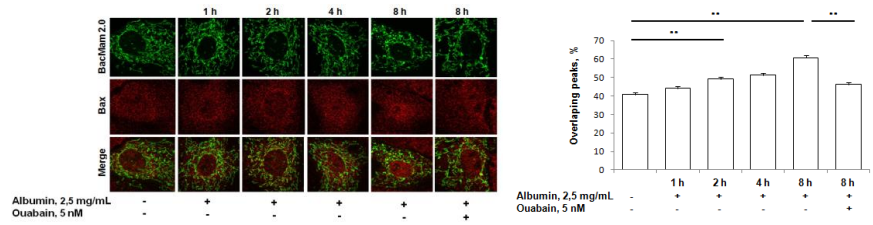

B.

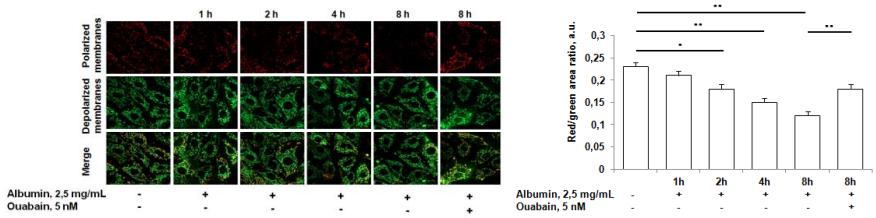

C.

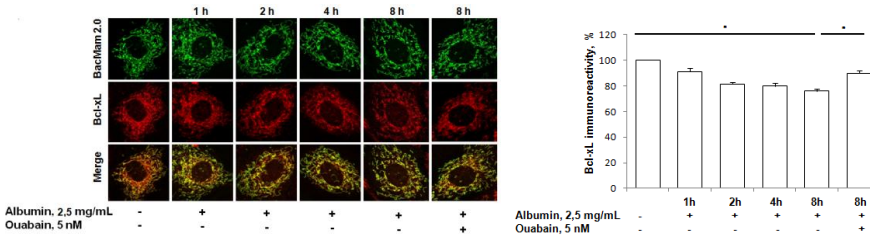

Figure 4.9. **A**. Immunofluorescence staining of proapoptotic factor Bax (red) in RPTC incubated with 2,5 mg/ml albumin. Cells were transfected with mitochondrial marker BacMam 2.0 (green). Number of co-localized Bax/mitochondrial peaks was counted. **p<0.01. Statistical analysis was performed using the Mann-Whitney U test. Experiments were repeated four times. **B.** Demonstration of the time course of the mitochondrial membrane potential changes in RPTC incubated with 2,5 mg/ml albumin. **p<0.01. Statistical analysis was performed using the Mann-Whitney U test. Experiments were repeated three times. **C.** Representative confocal images of Bcl-xL immunofluorescense signal (red) in RPTC. Cells were transfected with mitochondrial marker BacMam 2.0 (green). RPTC were incubated for 8 hours with 2,5 mg/ml albumin with or without ouabain (5 nM) in serum-free medium. Bars show mean immunosignall. 30 cells were analyzed in each experiment. Histograms represent means ± SEM. ** p<0.01. Statistical analysis was performed using the one-way ANOVA. Experiments were repeated three times.

To examine whether ouabain will also protect from loss of renal cells in proteinuric CKD, we have used a well known model of a human proteinuric disease, Passive Heymann Nephritis. The rats were treated with ouabain for 16 weeks and studied with regard to number of podocytes, glomerular-tubular disconnection and extent of fibrosis, apoptosis, the level of cell proliferation. The PHN rats were together with a control group, followed for four months before sacrifice. The PHN rats were divided into two groups, one that received ouabain in dose 15 µg/kg/day and one that received vehicle via subcutaneous mini-pumps. The vehicle-treated rats displayed at the same time of sacrifice for PHN typical renal pathology (**Figure 4.10A**). Significant albuminuria started to appear two weeks after induction of disease and was present throughout the observation period in both PHN groups. The mean value of albuminuria in the ouabain-treated groups was slightly lower than of untreated PHN (**Figure 4.10B**).

A. B.

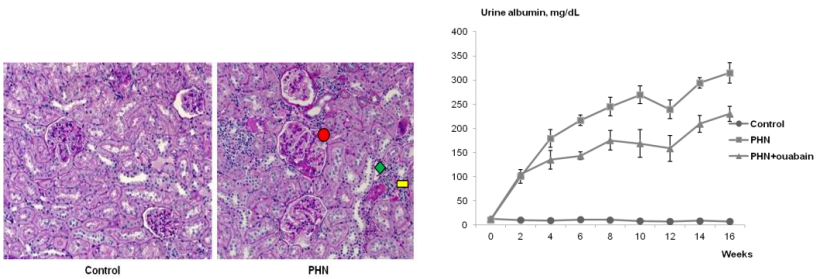

Figure 4.10. **A**. PAS staining of kidney sections (×200), showing segmental glomerulosclerosis and tubulointerstitial damage (fibrosis, infiltration with inflammatory cells) in control rats, rats with accelerated PHN and under treatment with ouabain. The depicted pictures are representative. **B**. Concentration of albumin in urine in control rats, rats with accelerated PHN and under treatment with ouabain. Data presented as means ± SEM. Statistical analysis was performed using the two-way ANOVA.

It is known that podocytes (Chang et al., 2011) and proximal tubular cells (Chevalier et al., 2008) at the glomerular-tubular junction are generally assumed to be the main targets for albumin toxicity. We quantified the level of apoptosis for these cell types in kidneys from control rats, PHN vehicle-treated rats and PHN ouabain-treated rats at the time of sacrifice. The apoptotic index was 3-fold higher in kidneys from vehicle-treated than in kidneys from ouabain-treated PHN rats (**Figure 4.11A**). Podocytes in control rats demonstrated little or no podocyte

apoptosis. In vehicle-treated PHN rats podocyte AI was dramatically increased. However, in ouabain-treated PHN rats podocyte AI was significantly lower that in vehicle-treated PHN rats (**Figure 4.11B**).

A.

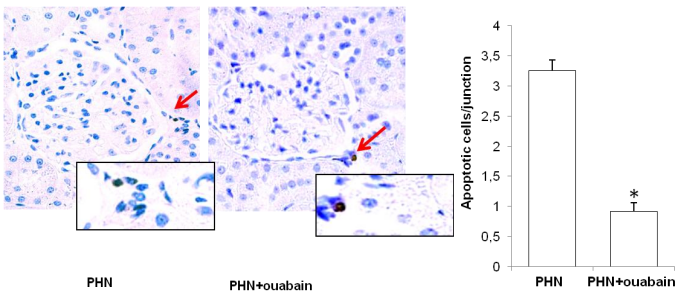

B.

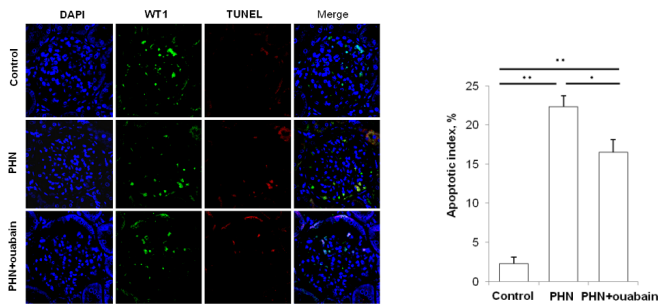

Figure 4.11. **A.** Representative TUNEL staining of proximal tubules connected to an atrophic tubule of PHN rats at four month and under the ouabain treatment. Quantitative determination of apoptotic proximal tubule cells. Histograms represent means ± SEM. * - $p<0.01$. Statistical analysis was performed using the Mann-Whitney U test. Original magnifications, x400. **B.** Representative micrographs demonstrate apoptotic podocytes in control rats, rats with accelerated PHN and under treatment with ouabain. Kidney sections were subjected to terminal deoxynucleotidyl transferase–mediated dUTP nick-end labeling (TUNEL) staining to identify apoptotic cells and WT-1 staining to recognize podocytes. Merging of the TUNEL and WT-1 staining images is presented. Quantitative determination of apoptotic podocytes. Histograms represent means ± SEM. **- $p<0.01$, * - $p<0.05$. Statistical analysis was performed using the Mann-Whitney U test.

Fibrosis is a typical feature of CKD (Eddy, 2000). Renal cortical expression of the pro-fibrotic factor TGF-beta 1 was detected in all groups. Semi-quantitative evaluation of the fluorescence was performed on one section from each kidney, and in each section

three areas corresponding to 75% of cortex were analyzed. In vehicle-treated PHN rats the TGF-beta 1 signal was 53% higher than in kidneys from control rats. In contrast no significant up-regulation of TGF-beta 1 was observed in kidneys from PHN rats treated with ouabain (**Figure 4.12A**).

Glomerular-tubular disconnection and loss of podocytes are indicators of permanent renal damage (Chevalier et al., 2008; Chang et al., 2011). In order to evaluate the extent of glomerular-tubular disconnection we used morphometric analysis for evaluation the type of connections between glomeruli and tubuli in individual nephrons. The prevalence of atubular glomeruli and the prevalence of glomeruli connected to atrophic tubuli were detected in kidneys from vehicle-treated PHN rats. These phenomena were reduced by almost 50% in ouabain-treated rats in comparison to what was found in the vehicle-treated PHN rats (**Figure 4.12B**). Serum creatinine, which was used as another end-point parameter in this study, was significantly lower in PHN rats treated with ouabain that in PHN rats treated with vehicle.

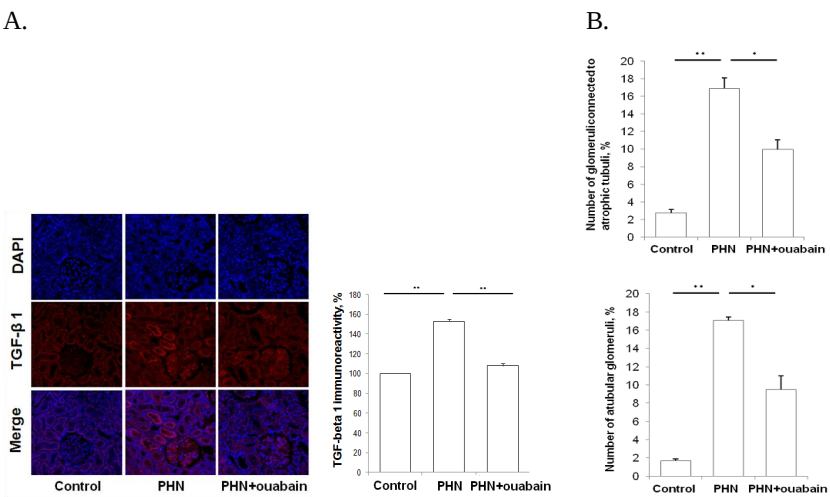

Figure 4.12. **A.** Representative confocal images of kidney sections from rats with PHN with and without continuous treatment with ouabain. Sections were immunohistochemically stained for TGF-β1 (red). Nuclei were counterstained with 4′,6-diamidino-2-phenylindole (DAPI, blue). Immunoreactivity for TGF-β1 is expressed as % deviation from control. Histograms represent means ± SEM**.** Statistical analysis was performed using the Mann-Whitney U test. Histograms represent means ± SEM. ** - p<0.001**. B.** Summary of Morphometric Studies. Quantitative determination of glomeruli. Histograms represent means ± SEM. ** - p<0.001, * - p<0.01.

4.6. Future perspectives.

Currently treatment of CKD is based on angiotensin-converting enzyme inhibitors and angiotensin-II receptor antagonist administration which are the most effective because of their unique ability to decrease proteinuria (Damman, Lambers-Heerspink, 2014). However, currently there are virtually no anti-apoptotic drugs available that do not have serious side effects. The use of caspase inhibitors is for most part prohibited because of the risk of preventing a physiological apoptotic process in premalignant cells. In contrast to caspase inhibitors, that would completely block the apoptotic pathway, ouabain would protect from glomerular damage due to prevention of podocytes apoptosis and glomerular-tubular disconnection by prevention of proximal tubular cells apoptosis in a proteinuric forms of CKD.

5 ACKNOWLEDGEMENTS

This work is a result of contributions from many people.

To my supervisors:

My main supervisor **Dr. Anita Aperia;** Thank you for accepting me as a student; for your continuous support of my PhD study and research; for your never ending encouragement and inspiration; for your patience, motivation, enthusiasm, and immense knowledge. I am deeply grateful for teaching me the art of scientific communication. Thank you for the great diplomatic experience I've learned from you.

Dr. Ulla Holtbäck; For your fantastic ability to share knowledges; your inspiring and always positive suggestions; your enthusiasm, fruitful ideas and positive attitude.

Dr. Xioa Li Liu; For teaching me how to plan and run complicated experiments, for encourage me to find solutions myself, for giving me useful explanations.

Dr. Vitaliy Maidannyk; For always finding time to listen, disscuss my theories and ideas; for sharing your great clinical experience and experimental knowledge; for our great conversations; for your great support during the entire PhD study.

To my co-authors:

Dr. Hjalmar Brismar; I would like to express my deep gratitude and respect to my teacher in imaging techniques. Thank you very much for exposing me to the world of confocal microscopy. I am grateful for your support, ideas and sharing insight into the imaging world.

Dr. Ann-Christine Eklöf; For giving me encourage to work with animals; for sharing your knowledge and experience. Thank you for always finding a time for disscussions.

Dr. Agnes Fogo; Thank you very much for teaching me pathology techniques. Thank you for making me feel at home while being and working during 2 weeks in Nashville with you and your awesome team.

Dr. Jacopo Fontana; For the help and a great time while working together.

I thank my co-authors from Lund University **Dr. Diana Karpman, Dr. Johan Rebetz, Dr. Ida Arvidsson** for the stimulating discussions, for the sleepless nights we were working together before deadlines.

In particular, I am grateful to **Dr. Liping Yang** for the productive and challenging discussions of the project.

To all my current and former colleagues at KI and SciLifeLab:

Dr. Lena Scott; For always sharing your knowlenges and experience; you are an amazing scientist and wonderful person.

Dr. Hans Blom; For helping me with microscopes; for your never ending jokes and positive attitudes.

Lill-Britt Svensson; For always helping and keeping thing in order; for your assistance any time it was necessary; for our warm conversations and your great support.

Raija Wallenborg; For the excellent secretary work.

Dr. Otto Manneberg; For your support with essentially everything in the lab.

Kristoffer Bernhem; For sharing your great experience in data analysis.

I am grateful to **Dr. Tommy Linne**. Thanks a lot that you've started Ukrainian-Swedish collaboration part of which my PhD is. I would like to express my deep gratitude and respect to you. Thank you for always finding time to listen me and giving me support in good and bad moments.

My thanks to **Dr. Guillame Azarias, Dr. Siobhan Conner, Dr. Susanne Crambert, Dr. Nicolas Fritz, Dr. Georgiy Khodus, Dr. Thomas Liebmann, Dr. Markus Kruusmägi, Dr. Daria Davydova, Dr. Zuzana Khorshidi, Eivow Zettenger Markus, Nina Illarionova, Linda Westin, Dr. Carolina Rigos, Dr. Evgeny Akkuratov, Dr. Alexandr Bondar, Dr. Eli Gunnarson, Dr. Sergey Zelenin, Dr. Marina Zelenina, David Unnersjö-Jess, Ludwig Brandt, Hans-Christian Smahl Hanssen, Linnea Nilsson, Jana Hanke.**

To my American friend **Dr. Gerald DiBona**. Thank you very much for sharing your time, ideas and experience. You are an amazing scientist and wonderful person.

Finally I dedicate this PhD thesis to my lovely family (my parents and my brother). Thank you for always believing in me, for your support in my decisions. Thank you for your endless love.

6 REFERENCES

- Aizman O, Uhlen P, Lal M, Brismar H, Aperia A: Ouabain, a steroid hormone that signals with slow calcium oscillations. Proc Natl Acad Sci USA 98: 13420–13424, 2001.
- Alvarez J, Montero M: Measuring [Ca^{2+}] in the endoplasmic reticulum with aequorin. Cell Calcium 32: 251–260, 2002.
- Amirlak I, Amirlak B: Haemolytic uraemic syndrome: An overview. Nephrology 11: 213–218, 2006.
- Anderson S, Halter JB, Hazzard WR, Himmelfarb J, Horne FMc, Kaysen JA, Kusek JW, Nayfield SJ, Schmader K, Tian Y, Ashworth JR, Clayton CP, Parker RP, Tarver ED, Woolard NF, High KP and for the workshop participants: Prediction, Progression, and Outcomes of Chronic Kidney Disease in Older Adults J Am Soc Nephrol 20 (6): 1199-1209, 2009.
- Bassik MC, Scorrano L, Oakes SA, Pozzan T, Korsmeyer SJ: Phosphorylation of Bcl-2 regulates ER Ca^{2+} homeostasis and apoptosis. EMBO J 23: 1207–1216, 2004.
- Berridge MJ, Bootman MD, Roderick HL: Calcium signalling: dynamics, homeostasis and remodelling. Nature Reviews Molecular Cell Biology 4(7): 517-529, 2003.
- Berridge MJ, Lipp P, Bootman MD: The versatility, universality of calcium signalling. Nat Rev Mol Cell Biol. 1:11–21, 2000.
- Berridge MJ: Elementary and global aspects of calcium signalling. J Physiol 499: 291–306, 1997.
- Bezprozvanny I: The inositol 1,4,5-trisphosphate receptors. Cell Calcium 38: 261–272, 2005.
- Billen LP, Kokoski CL, Lovell JF, Leber B, Andrews DW: Bcl-XL inhibits membrane permeabilization by competing with Bax. PLoS Biol 6: e147, 2008.
- Bitzan M, Poole R, Mehran M, et al: Safety and pharmacokinetics of chimeric anti-Shiga toxin 1 and anti-Shiga toxin 2 monoclonal antibodies in healthy volunteers. Antimicrouabain Agents Chemother 53(7): 3081-3087, 2009.
- Blanco G, Mercer RW: Isozymes of the Na-K-ATPase: heterogeneity in structure, diversity in function. Am. J. Physiol 275 (5 Pt 2), 633–650, 1998.
- Bootman MD, Fearnley C, Smyrnias I, Macdonald F, Roderick HL: An update on nuclear calcium signalling. J Cell Sci 122, 2337-2350, 2009.
- Boulanger BR, Lilly MP, Hamlyn JM, Laredo J, Shurtleff D, Gann DS: Ouabain is secreted by the adrenal gland of the awake dogs. Am. J. Physiol. 264, 413–419, 1993.
- Bramlage CP, Schröder K, Bramlage P, Ahrens K, Zapf A, Müller GA, Koziolek MJ: Predictors of comp-lications in therapeutic plasma exchange. Journal of Clinical Apheresis 24(6): 225-231, 2009.
- Brasier A.R: "The NF-κB regulatory network". Cardiovasc. Toxicol. **6** (2): 111–130, 2006.
- Brunner K, Bianchetti MG, Neuhaus TJ: recovery of renal function after long-term dialysis in hemolytic uremic syndrome. Pediatr. Nephrol 19: 229-231, 2004.
- Burlaka Ie, Liu XL, Rebetz J, Arvidsson I, Yang L, Brismar H, Karpman D, Aperia A. Ouabain protects from Shiga toxin-triggered apoptosis by reversing the imbalance between Bax and Bcl-xL. J Am Soc Nephrol 24: 1413–1423, 2013.

- Bygrave FL, Benedetti A: What is the concentration of calcium ions in the endoplasmic reticulum? Cell Calcium 19: 547–551, 1996.
- Chang AM, Ohse T, Krofft RD, Wu JS, Eddy AA, Pippin JW and Shankland SJ: Albumin-induced apoptosis of glomerular parietal epithelial cells is modulated by extracellular signal-regulated kinase 1/2. Nephrol Dial Transplant 0: 1–13, 2011.
- Chen Y-F, Chen Y-T, Chiu W-T, and Shen M-R: Remodeling of calcium signaling in tumor progression. Journal of Biomedical Science, 20:23, 2013.
- Chevalier RL, Forbes MS: Generation and Evolution of Atubular Glomeruli in the Progression of Renal Disorders. JASN 19(2): 197-206, 2008.
- Contreras RG, Shoshani L, Flores-Maldonado C, Lazaro A, Cereijido M: Relationship between Na(+),K(+)-ATPase and cell attachment. J Cell Sci 112:4223- 4232, 1999.
- Cornelius F, Kanai R, Toyoshima CA: Structural View on the Functional Importance of the Sugar Moiety and Steroid Hydroxyls of Cardiotonic Steroids in Binding to Na,K-ATPase. J Biol Chem 288: 6602–6616, 2013.
- Crompton M: The mitochondrial permeability transition pore and its role in cell death. Biochem J 341: 233–249, 1999.
- Damman K, Lambers-Heerspink HJ: Are Renin–Angiotensin–Aldosterone System Inhibitors Lifesaving in Chronic Kidney Disease? J Am College Cardiol: 63(7), 2014.
- Danial NN, Korsmeyer SJ: Cell death: critical control points. Cell 116: 205–219, 2004.
- Das R, Xu S, Quan X, Nguyen TT, Kong ID, Chung CH, Lee EY, Cha SK, Park KS: Upregulation of mitochondrial Nox4 mediates TGF-β-induced apoptosis in cultured mousepodocytes. Am J Physiol Renal Physiol. 06 (2): 155-167, 2014.
- De Giorgi F, Lartigue L, Bauer MK, Schubert A, Grimm S, Hanson GT, Remington SJ, Youle RJ, Ichas F: The permeability transition pore signals apoptosis by directing Bax translocation and multimerization. FASEB J: **16**: 607–609, 2002.
- Dean OM, Data-Franco J, Giorlando F, Berk M: Minocycline: therapeutic potential in psychiatry. CNS Drugs 26 (5): 391–401, 2012.
- Desagher S, Martinou J-C: Mitochondria as the central control point of apoptosis. Trends Cell Biol 10: 369–377, 2000.
- Dixon R, Brunskill NJ: Albumin stimulates p44/p42 extracellular-signal-regulated mitogen-activated protein kinase in opossum kidney proximal tubular cells. Clin Sci (Lond) 98: 295-303, 2000.
- Dlugosz PJ, Billen LP, Annis MG, Zhu W, Zhang Z, Lin J: Bcl-2 changes conformation to inhibit Bax oligomerization. EMBO J 25: 2287–2296, 2006.
- Donadelli R, Zanchi C, Morigi M, Buelli S, Batani C, Tomasoni S, Corna D, Rottoli D, Benigni A, Abbate M, Remuzzi G, Zoja C: Protein Overload Induces Fractalkine Upregulation in Proximal Tubular Cells through Nuclear Factor kappaB- and p38 Mitogen-Activated Protein Kinase-Dependent Pathways. J Am Soc Nephrol 14: 2436-2446, 2003.
- Doris PA, Hayward-Lester A, Bourne D, Stocco DM: Ouabain production by cultured adrenal cells. Endocrinology 137, 533–539, 1996.
- Dostanic I, Schultz JEJ, Lorenz JN, Lingrel JB: The α1 isoform of NaK-ATPase regulates cardiac contractility and functionally interacts and co-localizes with the Na/Ca exchanger in heart. J. Biol. Chem 279: 54053–54061, 2004.
- Dvorak HF: Discovery of vascular permeability factor (VPF). Exp Cell Res 312: 522–526, 2006.

- Eddy AA, Giachelli CM: Renal expression of genes that promote interstitial inflammation and fibrosis in rats with protein-overload proteinuria. Kidney Int 47: 1546-1557, 1995.
- Eddy AA: Molecular basis of renal fibrosis. Pediatr Nephrol 15: 290–301, 2000.
- Edlich F, Banerjee S, Suzuki M, Cleland MM, Arnoult D, Wang C, Neutzner A, Tjandra N, Youle RJ: Bcl-xL retrotranslocates Bax from the mitochondria into the cytosol. Cell 1; 145(1): 104–116, 2011.
- Elmore S: Apoptosis: A Review of Programmed Cell Death Apoptosis: A Review of Programmed Cell Death. Toxicol Pathol 35(4): 495-516, 2007.
- Erkan E, Devarajan P, Schwartz GJ: Mitochondria Are the Major Targets in Albumin-Induced Apoptosis in Proximal Tubule Cells. J Am Soc Nephrol 18: 1199–1208, 2007.
- Falcke M, Tsimring L, Levine H: Stochastic spreading of intracellular Ca($^{2+}$) release. Phys Rev E Stat Phys Plasmas Fluids Relat Interdiscip Topics. 62: 2636–2643, 2000.
- Fewtrell C: Ca^{2+} oscillations in non-excitable cells. Annu Rev Physiol. 55: 427–454, 1993.
- Garrido C, Galluzzi L, Brunet M, Puig PE, Didelot C, Kroemer G: Mechanisms of cytochrome c release from mitochondria. Cell Death Differ 13: 1423–1433, 2006.
- Gilmore TD: Introduction to NF-κB: players, pathways, perspectives Oncogene 25 (51): 6680–6684, 2006.
- Goilav B, Satlin LM, Wilson PD: Pathways od apoptosis in human autosomal recessive and autosomal dominant polycystic kidney diseases Pediatr. Nephrol 23: 1473–1482, 2008.
- Gonzalez-Michaca L, Farrugia G, Croatt AJ, Alam J, Nath KA: Heme: a determinant of life and death in renal tubular epithelial cells. Am J Physiol Renal Physiol 286: 370-377, 2004.
- Gordon J, Challa A, Levens JM, Gregory CD, Williams JM, Armitage RJ, Cook JP, Roberts LM, Lord JM: CD40 ligand, Bcl-2, and Bcl-xL spare group I Burkitt lymphoma cells from CD77-directed killing via Verotoxin-1 B chain but fail to protect against the holotoxin. Cell Death and Differentiation 7: 785-794, 2000.
- Goto A, Yamada K, Ishii M, Yoshioka M, Ishiguro T, Eguchi C, Sugimoto T: Purification and characterization of human urine-derived digitalis-like factor. Biochem. Biophys. Res. Commun 154: 847–853, 1998.
- Greef K, Wirth KE: Pharmakokinetics of strophanthin glycosides. Handbook Exp. Pharmacol 56/II: 57–85, 1981.
- Green D: Means to an End: Apoptosis and other Cell Death Mechanisms. Cold Spring Harbor, NY: Cold Spring Harbor Laboratory Press, 2011.
- Haas M, Askari A, Xie Z: Involvement of Src and epidermal growth factor receptor in the signal-transducing function of Na+/K+-ATPase. J Biol Chem 275: 27832–27837, 2000.
- Habib R: Pathology of the hemolytic uremic syndrome. In: Kaplan BS, Trompeter RS, Moake JL, editors. Hemolytic uremic syndrome and thrombotic thrombocytopenic purpura. New York, N.Y: Marcel Dekker Inc.: 315–353, 1992.
- Halestrap AP, McStay GP, Clarke SJ: The permeability transition pore complex: Another view. Biochimie 84: 153–166, 2002.
- Hawrysh PJ, Buck LT: Anoxia-mediated calcium release through the mitochondrial permeability transition pore silences NMDA receptor currents in turtle neurons. J Exp Biol 216(23): 4375-4387, 2013

- Horisberger JD: Recent insights into the structure and mechanism of the sodium pump. Physiology (Bethesda) 19: 3773-87, 2004.
- Hu Q, Deshpande S, Irani K, Ziegelstein RC: [Ca($^{2+}$)](i) oscillation frequency regulates agonist-stimulated NF-kappaB transcriptional activity. J Biol Chem 274: 33995–33998, 1998.
- Hughes AK, Stricklett PK, Kohan DE: Cytotoxic effect of Shiga toxin-1 on human proximal tubule cells. Kidney Int 54: 426–437, 1998.
- Inagami T, Tamura M: Purification and characterization of specific endogenous ouabain-like substance from bovine adrenal. Am. J. Med. Sci 295: 400–405, 1988.
- Inker LA: Albuminuria: time to focus on accuracy. Am J Kidney Dis 63(3): 378-81, 2014.
- Jafar TH, Stark PC, Schmid CH, Landa M, Maschio G, de Jong PE, de Zeeuw D, Shahinfar S, Toto R, Levey AS: Progression of chronic kidney disease: the role of blood pressure control, proteinuria, and angiotensin-converting enzyme inhibition: a patient-level meta-analysis. Ann Intern Med 139: 244-252, 2003.
- Joza N, Susin SA, Daugas E, Stanford WL, Cho SK, Li CY, Sasaki T, Elia AJ, Cheng HY, Ravagnan L, Ferri KF, Zamzami N, Wakeham A, Hakem R, Yoshida H, Kong YY, Mak TW, Zuniga- Pflucker JC, Kroemer G, Penninger JM: Essential role of the mitochondrial apoptosis-inducing factor in programmed cell death. Nature 410: 549–554, 2001.
- Kajiya H: Calcium signaling in osteoclast differentiation and bone resorption. Adv Exp Med Biol 740: 917-932, 2012.
- Karpman D, Hakansson A, Perez M-TR, Isaksson C, Carlemalm E, Caprioli A, Svanborg C: Apoptosis of renal cortical cells in the hemolytic-uremic syndrome: In vivo and in vitro studies. Infect Immun 66: 636–644, 1998.
- Karpman D, Sartz L, Johnson S: Pathophysiology of Typical Hemolytic Uremic Syndrome. Semin Thromb Hemost 36(6): 575-585, 2010.
- Kaur J1: Sanyal SN. Intrinsic mitochondrial membrane potential change and associated events mediate apoptosis in chemopreventive effect of diclofenac in colon cancer. Oncol Res 18(10): 481-492, 2010.
- Khoshnan A, Tindell C, Laux I, Bae D, Bennett B, Nel AE: The NF-kB Cascade Is Important in Bcl-xL Expression and for the Anti-Apoptotic Effects of the CD28 Receptor in Primary Human CD41 Lymphocytes. J. Immunol 165: 1743-1754, 2000.
- Kitano S, Morimoto S, Nishibe A, Fukuo K, Hirotani A, Nakahashi T, Ysuda O, Ogihara T: Exogenous ouabain is accumulated in the adrenals and mimics the kinetics of endogenous digitalis-like factor in rats. Hypertens. Res 21, 47–56, 1998.
- Kluz J, Kopec W, Jakobsche-Policht U, Adamiec R: Circulating endothelial cells, endothelial apoptosis and soluble markers of endothelial dysfunction in patients with systemic lupus erythematosus-related vasculitis. Int Angiol 28: 192-201, 2009.
- Kometiani P, Li J, Gnudi L, Kahn BB, Askari A, Xie Z: Multiple signal transduction pathways link Na+/K+-ATPase to growth-related genes in cardiac myocytes. The roles of Ras and mitogen-activated protein kinases. J Biol Chem 273, 15249–15256, 1998.
- Komiyama Y, Nishimura N, Munakata M, Mori T, Okuda K, Nishino N, Hirose S, Kosaka C, Masuda M, Takahashi H: Identification of endogenous ouabain in culture supernatant of PC12 cells. J. Hypertens 19: 229–236, 2001.

- Komiyama, Y, Nishimura N, Munakata M, Okuda K, Nishino N, Kosaka C, Masuda M, Mori T, Matsuda T, Takahashi HL: Increases in plasma ouabainlike immunoreactivity during surgical extirpation of pheochromocytoma. Hypertens. Res 22: 135–139, 1999.
- Kroemer G, Gallunzi L, Brenner C: Mitochondrial Membrane Permeabilization in Cell Death. Physiol Rev 87: 99–163, 2007.
- Lamkanfi M, Festjens N, Declercq W, Vanden Berghe T, Vandenabeele P: Caspases in cell survival, proliferation and differentiation. Cell Death and Differentiation 14 (1): 44–55, 2007.
- Landeta O, Landajuela A, Gil D, Taneva S, DiPrimo C, Sot B, Valle M, Frolov VA, Basañez G: Reconstitution of proapoptotic BAK function in liposomes reveals a dual role for mitochondrial lipids in the BAK-driven membrane permeabilization process. J Biol Chem 286: 8213–8230, 2011.
- Laredo J, Hamilton BP, Hamlyn JM: Ouabain is secreted by bovine adrenocortical cells. Endocrinology 135: 794–797, 1994.
- Li J, Khodus GR, Markus Kruusmägi M, Kamali-Zare P , Liu X, Eklöf A-Ch, Zelenin S, Brismar H, Aperia A: Ouabain protects against adverse developmental programming of the kidney. Nature Communications 27, 2010.
- Li J, Zelenin S, Aperia A, Aizman O: Low doses of ouabain protect from serum deprivation–triggered apoptosis and stimulate kidney cell proliferation via activation of NF-κB. J Am Soc Nephrol 17: 1848-1857, 2006.
- Li LY, Luo X, Wang X: Endonuclease G is an apoptotic DNase when released from mitochondria. Nature 412: 95–99, 2001.
- Lingrel JB: The physiological significance of the cardiotonic steroid/ouabain-binding site of the Na,K-ATPase. Annu Rev Physiol 72: 395–412, 2010.
- Llambi F, Moldoveanu T, Tait SW, Bouchier-Hayes L, Temirov J, McCormick LL, Dillon CP, Green DR: A unified model of mammalian Bcl-2 protein family interactions at the mitochondria. Mol Cell 44: 1–15, 2011.
- López-Novoa JM, Rodríguez-Peña AB, Ortiz A, Martínez-Salgado C, and Hernández FJL: Etiopathology of chronic tubular, glomerular and renovascular nephropathies: Clinical implications J Transl Med 9: 13, 2011.
- Lovell JF, Billen LP, Bindner S, Shamas-Din A, Fradin C, Leber B, Andrews DW: Membrane binding by tBid initiates an ordered series of events culminating in membrane permeabilization by Bax. Cell 135: 1074–1084, 2008.
- Manunta P, Evans G, Hamilton BP, Gann D, Resau J, Hamlyn JM: A new syndrome with elevated plasma ouabain and hypertension secondary to an adrenocortical tumor. J. Hypertens 10: 27, 1992.
- Mao H, Li Z, Zhou Y, Li Z, Zhuang S, An X, Zhang B, Chen W, Nie J, Wang Z, Borkan SC, Wang Y, Yu X: HSP72 attenuates renal tubular cell apoptosis and interstitial fibrosis in obstructive nephropathy. Am J Physiol Renal Physiol 295(1): 202-214, 2008.
- Martinou JC, Youle RJ: Mitochondria in apoptosis: Bcl-2 family members and mitochondrial dynamics. Dev Cell 21: 92–100, 2011.
- Masugi, F, Ogihara T, Hasegawa T, Sagakuchi K, Kumahara Y: Normalization of high plasma level of ouabainlike immunoreactivity in primary aldosteronism after removal of adenoma. J. Hum. Hypertens 2: 17–20, 1988.
- Mathews WR, DuCharme DW, Hamlyn JM, Harris DW, Mandel F, Clark M.A, Ludens JA: Mass spectral characterization of an endogenous digitalis-like factor from human plasma. Hypertension 17: 930–935, 1991.

- Mbaya E, Oulès B, Caspersen C, Tacine R, Massinet H, Pennuto M, Chrétien D, Munnich A, Rötig A, Rizzuto R, Rutter GA, Paterlini-Bréchot P, Chami M: Calcium signalling-dependent mitochondrial dysfunction and bioenergetics regulation in respiratory chain Complex II deficiency. Cell Death Differ. 17(12): 1855-1866, 2010.
- Meguid El, Nahas A, Bello AK: Chronic kidney disease: the global challenge. Lancet 365: 331-340, 2005.
- Melton-Celsa A, Mohawk K, Teel L, O'Brien A: Pathogenesis of Shiga-toxin producing escherichia coli. Curr Top Microbiol Immunol 357: 67-103, 2012.
- Miyakawa-Naito A, Uhlen P, Lal M, Aizman O, Mikoshiba K, Brismar H, Zelenin S, and Aperia A: Cell signaling microdomain with Na,K-ATPase and inositol 1,4,5-trisphosphate receptor generates calcium oscillations. J Biol Chem 27: 50355-50361, 2003.
- Montero M, Brini M, Marsault R, Alvarez J, Sitia R, Pozzan T, Rizzuto R: Monitoring dynamic changes in free Ca2+ concentration in the endoplasmic reticulum of intact cells. EMBO J 14: 5467–5475, 1995.
- Morigi M, Macconi D, Zoja C, Donadelli R, Buelli S, Zanchi C, Ghilardi M, Remuzzi G: Protein overload-induced NF-kappaB activation in proximal tubular cells requires $H(_2)O(_2)$ through a PKC-dependent pathway. J Am Soc Nephrol 13: 1179-1189, 2002.
- Moriwaki Y, Inokuchi T, Yamamoto A, Ka T, Tsutsumi Z, Takahashi S, Yamamoto T: Effect of TNF-alpha inhibition on urinary albumin excretion in experimental diabetic rats. Acta Diabetol 44: 215–218, 2007.
- Morth JP, Pedersen BP, Toustrup-Jensen MS, Sorensen TL, Petersen J, Andersen JP, Vilsen B, Nissen P: Crystal structure of the sodium-potassium pump. Nature 450(7172): 1043-1049, 2007.
- Müller R, Daniel C, Hugo C, Amann K, Mielenz D, Endlich K, Braun T, van der Veen B, Heeringa P, Schett G, Zwerina J. The mitogen-activated protein kinase p38α regulates tubular damage in murine anti-glomerular basement membrane nephritis. PLoS One. 8(2):e56316, 2013.
- Mundel P, Shankland SJ: Podocyte biology and response to injury. J Am Soc Nephrol 13 : 3005–3015, 2002.
- Nakanishi C, Toi M: Nuclear factor-kappaB inhibitors as sensitizers to anticancer drugs. Nat Rev Cancer 5: 297–309, 2005.
- Naoi M, Maruyama W, Youdim MB, Yu P, Boulton A.A: Anti-apoptotic function of propargylamine inhibitors of type-B monoamine oxidase. Inflammopharmacology 11 (2): 175-181, 2003.
- Naraghi M, Neher E: Linearized buffered Ca^{2+} diffusion in microdomains and its implications for calculation of $[Ca^{2+}]$ at the mouth of a calcium channel. J Neurosci 17: 6961–6973, 1997.
- Neher E: Vesicle pools and Ca^{2+} microdomains: new tools for understanding their roles in neurotransmitter release. Neuron 20: 389–399, 1998.
- Oberbauer R, Schwarz C, Regele HM, Hansmann C, Meyer TW, Mayer G: Regulation of renal tubular cell apoptosis and proliferation after ischemic injury to a solitary kidney. Journal of Laboratory and Clinical Medicine 5: 343–351, 2001.
- Obrig TG: Escherichia coli Shiga Toxin Mechanisms of Action in Renal Disease: Toxins 2(12): 2769-2794, 2010.
- Oeckinghaus A, Hayden MS, Ghosh S: Crosstalk in NF-κB signaling pathways. Nat Immunol 12: 695–708, 2011.

- Ogawa H, Shinoda T, Cornelius F, Toyoshima C: Crystal structure of the sodium-potassium pump (Na+,K+-ATPase) with bound potassium and ouabain. Proc Natl Acad Sci USA 106(33): 13742-13247, 2009.
- Oldfield V, Keating GM, Perry CM: Rasagiline: a review of its use in the management of Parkinson's disease. Drugs 67 (12): 1725-1747, 2007.
- Paci A, Marrone O, Lenzi S, Prontera C, Nicolini G, Ciabatti G, Ghione S, Bonsignore G: Endogenous digitalis-like factors in obstructive sleep apnea. Hypertens. Res 23: 87–91, 2000.
- Paredes SD, Korkmaz A, Manchester LC, Tan DX, Reiter RJ: Phytomelatonin: a review. J. Exp. Bot. 60 (1): 57–69, 2009.
- Porcheray F, Fraser JW, Gao B, McColl A, DeVito J, Dargon I, Helou Y, Wong W, Girouard TC, Saidman SL, Colvin RB, Palmisano A, Maggiore U, Vaglio A, Smith RN and Zorn E: Polyreactive Antibodies Developing Amidst Humoral Rejection of Human Kidney Grafts Bind Apoptotic Cells and Activate Complement American Journal of Transplantation 13: 2590–2600, 2013.
- Pravst I, Zmitek K, Zmitek J: Coenzyme Q10 Contents in Foods and Fortification Strategies. Critical Reviews in Food Science and Nutrition 50 (4): 269-280, 2010.
- Price EM, Lingrel JB: Structure-function relationships in the Na,K-ATPase alpha subunit: site-directed mutagenesis of glutamine-111 to arginine and asparagine-122 to aspartic acid generates a ouabain resistant enzyme. Biochemistry. 27: 8400–8408, 1988.
- Psotka MA, Obata F, Kolling GL, Gross LK, Saleem MA, Satchell SC, Mathieson PW, Obrig TG: Shiga toxin 2 targets the murine renal collecting duct epithelium. Infect Immun 77(3):959-69 2009.
- Rajasekaran SA, Barwe SP, Rajasekaran AK: Multiple functions of Na,K-ATPase in epithelial cells. Semin Nephrol 25:328-334, 2005
- Robb EL, Page MM, Wiens BE, Stuart JA: Molecular mechanisms of oxidative stress resistance induced by resveratrol: Specific and progressive induction of MnSOD. Biochem. Biophys. Res. Commun 367 (2): 406-412, 2008.
- Roderick HL, Berridge MJ, Bootman MD: Calcium-induced calcium release. Current Biology 13(R425), 2003.
- Rodriguez RR: "Warning Letter". Inspections, Compliance, Enforcement, and Criminal Investigations. U.S. Food and Drug Administration, 2010.
- Rousseau E, Blais N, O'Regan S: Decreased necessity for dialysis with loop diuretic therapy in hemolytic uremic syndrome. Clin. Nephrol 34: 22–25, 1990.
- Rubio-Moscardo F, Blesa D, Mestre C, Siebert R, Balasas T, Benito A, Rosenwald A, Climent J, Martinez JI, Schilhabel M, Karran EL, Gesk S, Esteller M, deLeeuw R, Staudt LM, Fernandez-Luna JL, Pinkel D, Dyer MJ, Martinez-Climent JA: Characterization of 8p21.3 chromosomal deletions in B-cell lymphoma: TRAIL-R1 and TRAIL-R2 as candidate dosage-dependent tumor suppressor genes. Blood 106: 3214–3222, 2005.
- Ruggenenti P, Noris M, Remuzzi G: Thrombotic microangiopathy, hemolytic uremic syndrome, and thrombotic thrombocytopenic purpura. Kidney Int. 60: 831–846, 2001.
- Saelens X, Festjens N, Vande Walle L, van Gurp M, van Loo G, Vandenabeele P: Toxic proteins released from mitochondria in cell death. Oncogene 23: 2861–2874, 2004.
- Sanchez G, Nguyen AN., Timmerberg B, Tash JS, Blanco G: The Na,K-ATPase alpha4 isoform from humans has distinct enzymatic properties and is important for sperm motility. Mol. Hum. Reprod 12: 565–576, 2006.

- Sauter KAD, Melton-Celsa AR, Larkin K, Troxell ML, O'Brien AD, Magun BE: Mouse Model of Hemolytic-Uremic Syndrome Caused by Endotoxin-Free Shiga Toxin 2 (Stx2) and Protection from Lethal Outcome bynti-Stx2 Antibody. Infection and Immunity 76(10): 4469–4478, 2008.
- Scaffidi C, Schmitz I, Krammer PH, Peter ME: The role of c-FLIP in modulation of CD95-induced apoptosis. J Biol Chem 274: 1541–1548, 1999.
- Schimmer AD. Inhibitor of apoptosis proteins: translating basic knowledge into clinical practice.Cancer Res 64: 7183–7190, 2004.
- Schlondorff DO: Overview of factors contributing to the pathophysiology of progressive renal disease. Kidney International 74: 860–866, 2008.
- Schoner W, Scheiner-Bobis G: Endogenous cardiac glycosides: Hormones using the sodium pump as signal transducer. Semin Nephrol 25: 343-351, 2005.
- Schoner W: Endogenous cardiac glycosides, a new class of steroid hormones. Eur. J. Biochem 269: 2440–2448, 2002
- Schultz DR, Harrington WJ: Apoptosis: programmed cell death at a molecular level. Semin Arthritis Rheum 32: 345–369, 2003.
- Schuster S, Marhl M, Hofer T: Modelling of simple, complex calcium oscillations. From single-cell responses to intercellular signalling. Eur J Biochem. 269: 1333–1355, 2002.
- Shah SV, Baliga R, Rajapurkar M, Fonseca VA: Oxidants in chronic kidney disease. J Am Soc Nephrol 18: 16-28, 2007.
- Shamas-Din A, Brahmbhatt H, Leber B, Andrews DW: BH3-only proteins: orchestrators of apoptosis. Biochim Biophys Acta Mol Cell Res 1813: 508–520, 2011.
- Sheoran AS, Chapman S, Singh P, Donohue-Rolfe A, Tzipori S: Stx2-specific human monoclonal antibodies protect mice against lethal infection with Escherichia coli expressing Stx2 variants. Infect. Immun 71: 3125–2130, 2003.
- Shibolet, O, Shina A, Rosen S, Clearly TG, Brezis M, Ashenazi S: Shiga toxin induces medullary tubular injury in isolated perfused rat kidneys. FEMS Immunol Med Microbiol 18: 55–60, 1997.
- Shull GE, Schwartz A, Lingrel JB: Amino-acid sequence of the catalytic subunit of the (Na^{++} K^{+})ATPase deduced from a complementary DNA. Nature 316: 691–695, 1982.
- Skou JC: The influence of some cations on an adenosine triphosphatase from peripheral nerves. Biochim. Biophys. Acta 1000: 439–446, 1989.
- Sneyd J, Tsaneva-Atanasova K: Modeling calcium waves. In: Falcke M, Malchow D (eds) Understanding Calcium Dynamics - Experiments and Theory, Lecture Notes in Physics, Springer, Berlin: 179-199, 2003.
- Sun SC, Liu ZG: A special issue on NF-κB signaling and function. Cell Res 21: 1–2, 2011.
- Sun SC: Non-canonical NF-κB signaling pathway. Cell Res 21: 71–85, 2011.
- Sweadner KJ: Isozymes of the Na+/K+-ATPase. Biochim. Biophys. Acta 988: 185–220, 1989.
- Takeda T, Dohi, S, Igarashi T, Yoshiya K, Kobayashi N: Impairment by verotoxin of tubular function contributes to the renal damage seen in haemolytic uraemic syndrome. J Infect 27: 339–341, 1993.
- Tarr PI, Gordon CA, Chandler WL: Shiga-toxin-producing Escherichia coli and haemolytic uraemic syndrome. Lancet 365, 1073–1086, 2005.

- Taylor CW, da Fonseca PC, Morris EP: Ip(3) receptors: the search for structure. Trends in Biochemical Sciences 29(4): 210-219, 2004.
- Tergaonkar V, Correa RG, Ikawa M, Verma IM: Distinct roles of IκB proteins in regulating constitutive NF-κB activity. Nat Cell Biol **7**: 921–923, 2005.
- Tian J, Xie Z-J: The Na-K-ATPase and Calcium-Signaling Microdomains. Physiology 23: 205-211, 2008.
- Tomé-Carneiro J, Gonzálvez M, Larrosa M, Yáñez-Gascón MJ, García-Almagro FJ, Ruiz-Ros JA, Tomás-Barberán FA, García-Conesa MT, Espín JC: Resveratrol in primary and secondary prevention of cardiovascular disease: a dietary and clinical perspective. Annals of the New York Academy of Sciences 1290: 37–51, 2013.
- Trevisi L, Visentin B, Cusinato F, Pighin I, Luciani S: Antiapoptotic effect of ouabain on human umbilical vein endothelial cells. Biochem Biophys Res Commun 321: 716–21, 2004.
- Uhlen P, Burch PM, Zito CI, Estrada M, Ehrlich BE, Bennett AM: Gain-of-function/Noonan syndrome SHP-2/Ptpn11 mutants enhance calcium oscillations, impair NFAT signaling. Proc Natl Acad Sci USA 103: 2160–2165, 2006.
- Uhlen P, Fritz N: Biochemistry of calcium oscillations. Biochem Biophys Res Commun 396: 28–32, 2010.
- United States Renal Data System. USRDS 2013 Annual Data Report: Atlas of Chronic Kidney Disease and End-Stage Renal Disease in the United States. National Institutes of Health. National Institute of Diabetes and Digestive and Kidney Diseases. Bethesda, MD, 2013.
- Van Damme-Lombaerts R, Proesmans W, Van Damme B, Eeckels R, Binda Ki Muaka P, Mercieca V, Vlietinck R, Vermylen J: Heparin plus dipyridamole in childhood hemolytic-uremic syndrome: A prospective, randomized study. J. Pediatr 113: 913–918, 1988.
- Wajant H: The Fas signaling pathway: more than a paradigm. Science 296: 1635–1666, 2002.
- Wang L, Hong Q, Lv Y, Feng Z, Zhang X, Wu L, Cui S, Hou K, Su H, Huang Z, Wu D, Chen X: Autophagy can repair endoplasmic reticulum stress damage of the passive Heymann nephritis model as revealed by proteomics analysis 75(13): 3866-3876, 2012.
- Ward SC, Hamilton BP, Hamlyn JM: Novel receptors for ouabain: Studies in adrenocortical cells and membranes. Hypertension 39:536-542, 2002.
- Wohlfarth V, Drumm K, Mildenberger S, Freudinger R, Gekle M. Protein uptake disturbs collagen homeostasis in proximal tubule-derived cells. Kidney Int Suppl 103-109, 2003.
- Woo AL, James PF, Lingrel JB: Sperm motility is dependent on a unique isoform of the Na,K-ATPase. J. Biol. Chem. 275: 20693–20699, 2000.
- Zandi-Nejad K, Eddy AA, Glassock RJ, Brenner BM: Why is proteinuria an ominous biomarker of progressive kidney disease? Kidney Int Suppl 76-89, 2004.
- Zhang S, Malmersjo S, Li J, Ando, H., Aizman, O, Uhlen P, Mikoshiba, K, Aperia A: Distinct role of the N-terminal tail of the Na,K-ATPase catalytic subunit as a signal transducer. J Biol Chem 281: 21954-21962, 2006.

I

BASIC RESEARCH www.jasn.org

Ouabain Protects against Shiga Toxin–Triggered Apoptosis by Reversing the Imbalance between Bax and Bcl-xL

Ievgeniia Burlaka,* Xiao Li Liu,* Johan Rebetz,† Ida Arvidsson,† Liping Yang,‡ Hjalmar Brismar,§ Diana Karpman,† and Anita Aperia*

*Department of Women's and Children's Health, Karolinska Institutet, Astrid Lindgren Children's Hospital, Research Lab, Stockholm, Sweden; †Department of Pediatrics, Clinical Sciences Lund, Lund University, Lund, Sweden; ‡Key Laboratory of Cancer Research Center Nantong, Affiliated Tumor Hospital of Nantong University, Nantong, China; and §Science for Life Laboratory, Department of Applied Physics, Royal Institute of Technology, Stockholm, Sweden

ABSTRACT

Hemolytic uremic syndrome, a life-threatening disease often accompanied by acute renal failure, usually occurs after gastrointestinal infection with Shiga toxin 2 (Stx2)–producing *Escherichia coli*. Stx2 binds to the glycosphingolipid globotriaosylceramide receptor, expressed by renal epithelial cells, and triggers apoptosis by activating the apoptotic factor Bax. Signaling *via* the ouabain/Na,K-ATPase/IP3R/NF-κB pathway increases expression of Bcl-xL, an inhibitor of Bax, suggesting that ouabain might protect renal cells from Stx2-triggered apoptosis. Here, exposing rat proximal tubular cells to Stx2 *in vitro* resulted in massive apoptosis, upregulation of the apoptotic factor Bax, increased cleaved caspase-3, and downregulation of the survival factor Bcl-xL; co-incubation with ouabain prevented all of these effects. Ouabain activated the NF-κB antiapoptotic subunit p65, and the inhibition of p65 DNA binding abolished the antiapoptotic effect of ouabain in Stx2-exposed tubular cells. Furthermore, *in vivo*, administration of ouabain reversed the imbalance between Bax and Bcl-xL in Stx2-treated mice. Taken together, these results suggest that ouabain can protect the kidney from the apoptotic effects of Stx2.

J Am Soc Nephrol 24: 1413–1423, 2013. doi: 10.1681/ASN.2012101044

Hemolytic uremic syndrome (HUS) is a life-threatening disease, with acute renal failure as one of the most prominent symptoms. HUS generally occurs after a gastrointestinal infection with Shiga toxin 2 (Stx2)–producing *Escherichia coli*.[1,2] Stx2 penetrates the intestine, enters the circulation, and binds with high affinity to glycosphingolipid globotriaosylceramide receptors (Gb3), which are expressed in many tissues but are particularly abundant in renal epithelial cells. The Stx2/Gb3 complex is endocytosed and then translocated *via* the Golgi apparatus and the endoplasmic reticulum to the cytosol, where the toxic A subunit will exert its effects by acting on ribosomes.[3] Apoptosis is a major manifestation of Stx2 toxicity, as shown in biopsy samples from patients with HUS and in kidneys from mice inoculated with Stx2-producing versus Stx-nonproducing *E. coli* O157:H7, those treated with Stx2, and Stx2-exposed cells.[1,4,5]

The mechanism by which Stx2 activates apoptotic pathways is not fully understood, but several lines of evidence suggest that it involves activation of caspase-8 and the intrinsic, mitochondrial pathway. It is well documented that Stx2 increases caspase-8 expression.[6,7] Caspase-8 may trigger a signaling cascade that results in caspase-3 cleavage and cell death without involving the mitochondrial pathway (the extrinsic apoptotic pathway), or it may

Received October 31, 2012. Accepted March 27, 2013.

Published online ahead of print. Publication date available at www.jasn.org.

Correspondence: Dr. Anita Aperia, Department of Women's and Children's Hospital, Karolinska Institutet, Astrid Lindgren Children's Hospital, Research Lab, Q2:09, SE-171 76 Stockholm, Sweden. Email: Anita.Aperia@ki.se

act by stimulating the apoptotic oligomerizing factors Bax and Bak, which bind to the mitochondrial membrane and make it permeable. This leads to a series of events that also result in caspase-3 cleavage and cell death (the intrinsic apoptotic pathway).[7] Bax belongs to the Bcl-2 family, which includes both pro- and antiapoptotic factors. Bcl-xL is an antiapoptotic member of the Bcl-2 family and a potent inhibitor of Bax.[8,9] Little is known about the effect of Stx2 on Bax and Bcl-xL expression. Two independent studies found that the overexpression of Bcl-xL by transient transfection protected from Stx2 B subunit–mediated apoptosis.[10,11] HUS was previously more common in children, but the recent large outbreak of food-borne Stx2-producing *E. coli* O104:H4 infection suggested that severe HUS might affect adults as well as children. No available therapy protects patients from acute toxin-mediated cellular injury, including apoptosis.[12,13] Chronic renal affection or failure occurs in up to 10% of patients who survive the acute manifestations of the disease.[13]

Our group has identified a novel signaling system that protects against apoptosis.[14,15] The signal is activated by the cardiotonic steroid ouabain. The signaling pathway involves interaction between Na,K-ATPase and the inositol 1,4,5-triphosphate receptor (IP3R), triggering of slow intracellular calcium oscillations, and activation of the NF-kB p65 subunit (or RelA).[16–19] Because NF-κB p65 is known to increase the expression of Bcl-xL,[20] we hypothesized that ouabain-triggered Na,K-ATPase signaling may counteract the apoptotic action of Stx2 by upregulation of Bcl-xL and downregulation of Bax. Here we present a series of studies in support of this hypothesis. We show that ouabain in nM concentrations protects Stx2-exposed rat renal epithelial cells from apoptosis by reversing an imbalance between Bax and Bcl-xL. Studies on mice inoculated with Stx2 provide proof of principle and show that treatment with ouabain protects against apoptosis and reverses the imbalance between Bax and Bcl-xL.

RESULTS

Stx2 Binds to Rat Proximal Tubular Cells

Stx binds to the globotriaosylceramide (Gb3) receptor in the plasma membrane in human as well as rodent cells.[21–23] To examine whether Gb3 is also expressed in primary rat proximal tubular cells (RPTCs), these cells were fixed with 2% paraformaldehyde, exposed to Stx2, and immunostained. As shown in Figure 1, approximately 50% of cells incubated with Stx2, an Stx2-specific antibody, and secondary antibody exhibited a strong immunosignal, both in the presence and the

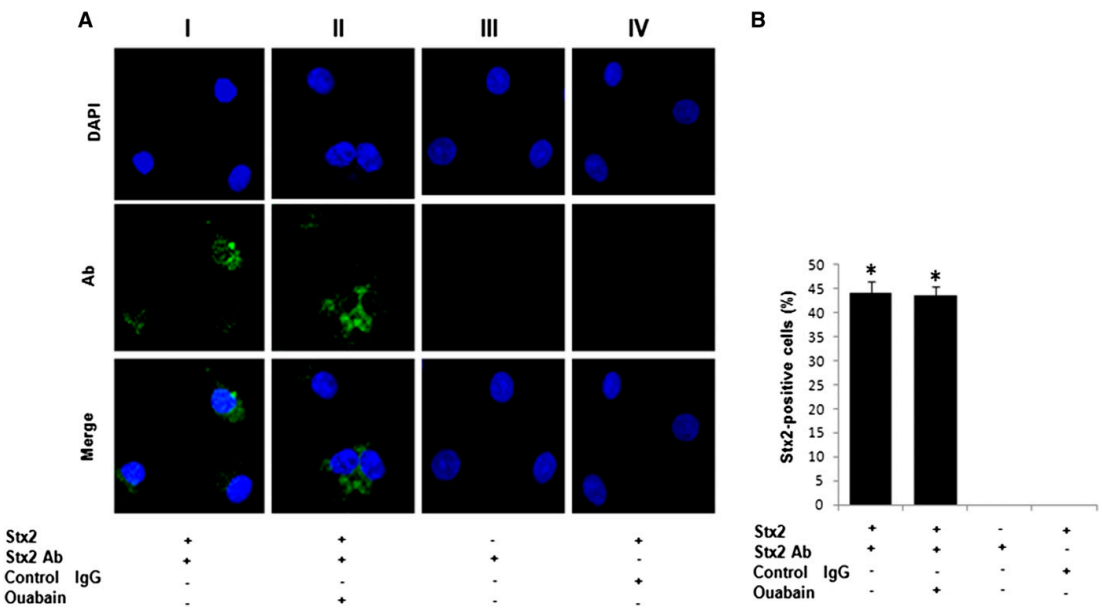

Figure 1. Stx2 binds to rat proximal tubular cells. (A) Panel I: cells exposed to Stx2, Stx2 antibody, and Alexa-conjugated secondary antibody (Ab). Stx2 immunostaining is shown in green. Panel II: cells exposed to Stx2, ouabain, Stx2 antibody, and Alexa-conjugated secondary antibody. Stx2 immunostaining is shown in green. Panel III: cells not exposed to Stx2 but exposed to the anti-Stx2 antibody and secondary antibody. Panel IV: cells not exposed to Stx2, control IgG antibody, and secondary antibody. All cells are counterstained with DAPI (blue). Cells were observed with fluorescent microscope using 40×/1.2NP water-immersion objective. For lower magnification, see Supplemental Figure 4. (B) Histograms represent means ± SEM. *P<0.001. Statistical analysis was performed using the Mann-Whitney U test. Experiments were repeated three times.

absence of ouabain. No signal was detected when the primary antibody was omitted or replaced with a control IgG antibody.

Stx2 2 Induces Apoptosis in Rat Proximal Tubular Cells, and Ouabain Has a Protective Effect

The apoptotic effect of Stx2 was first studied in RPTCs, which 2 days after plating were incubated with standard medium containing Stx2 or Stx2 and ouabain. Cells incubated with standard medium without these additives served as controls. Three days after plating, the cells were prepared for terminal deoxynucleotidyl transferase dUTP nick end labeling (TUNEL) staining for semiquantitative assessment of the level of apoptosis (Figure 2). In control cells, the mean ± SEM apoptotic index was 2.1%±0.2%. Stx2, 4 ng/ml, caused extensive apoptosis (apoptotic index, 19.6%±4.6%). In cells co-incubated with Stx2 and ouabain, 5 nM, the apoptotic effect was almost completely abolished (apoptotic index, 2.7%±0.4%). In pilot studies, a Shiga toxin 2 concentration of 4 ng/ml had pronounced and reproducible apoptotic effects (Supplemental Figure 1). This concentration was therefore used in all subsequent experiments.

To further examine the nature of cell death caused by Stx2 exposure, flow cytometry analysis was performed (Figure 3). Cells were treated as described above. Annexin V was used as a marker of early apoptosis, and 7-aminoactinomycin D (7-AAD) as a marker of late apoptosis/necrosis. The number of cells that exhibited an annexin V signal was significantly ($P<0.05$) higher in cells exposed to Stx2 alone (19.9%±0.7%) than in control cells (7.3%±0.6%) and cells exposed to Stx2 and ouabain (9.7%±0.9%). In a similar fashion, the number of cells that exhibited a 7-AAD signal was also significantly ($P<0.05$) higher in cells exposed to Stx2 alone (6.5%±0.1%) than in control cells (1.0%±0.4%) and cells exposed to Stx2 and ouabain (1.2%±0.1%).

NF-κB p65 Subunit Activity

Low concentrations of ouabain activate the survival factor p65,[20,24] a subunit of the pleiotropic transcriptional factor NF-κB. Because NF-κB units under nonstimulated conditions are located in the cytoplasm, we immunostained RPTCs with a p65-specific antibody and compared the nuclear/cytoplasmic ratio of the immunosignal. The ratio was similar in control cells and in cells exposed to Stx2 alone (0.57±0.04 and 0.53±0.03, respectively) but was significantly higher in cells exposed to Stx2 and ouabain (3.9±0.2) than in the other groups (Figure 4, A and B). We then determined the p65 DNA–binding activity in nuclear extracts from RPTCs; we found that it was significantly reduced in cells exposed to Stx2 compared with control cells but similar in cells co-incubated with Stx2 and ouabain and in control cells (Figure 4C). To test the functional role of NF-κB activation, the anti-apoptotic effect of ouabain on Stx2-exposed RPTCs was determined in the presence or absence of helenalin, a specific inhibitor of the transcriptional effect of the NF-κB (Figure

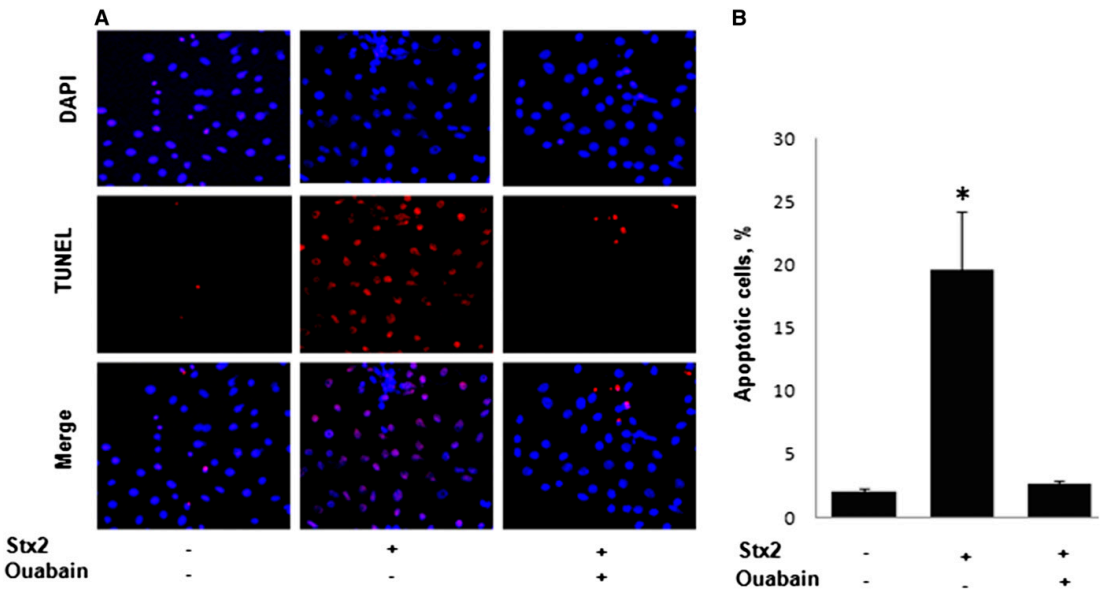

Figure 2. Stx2 induces apoptosis in rat proximal tubular cells, and ouabain has a protective effect. (A) RPTCs were TUNEL-stained (red) to detect apoptotic cells and counterstained with DAPI (blue). Apoptotic index was determined by analyzing five to seven randomly selected areas with 100–200 cells in each area. (B) Histograms represent means ± SEM. *$P<0.001$ for Stx2 versus control, Stx2 versus Stx2 plus ouabain. Statistical analysis was performed using the Mann-Whitney *U* test. Experiments were repeated eight times.

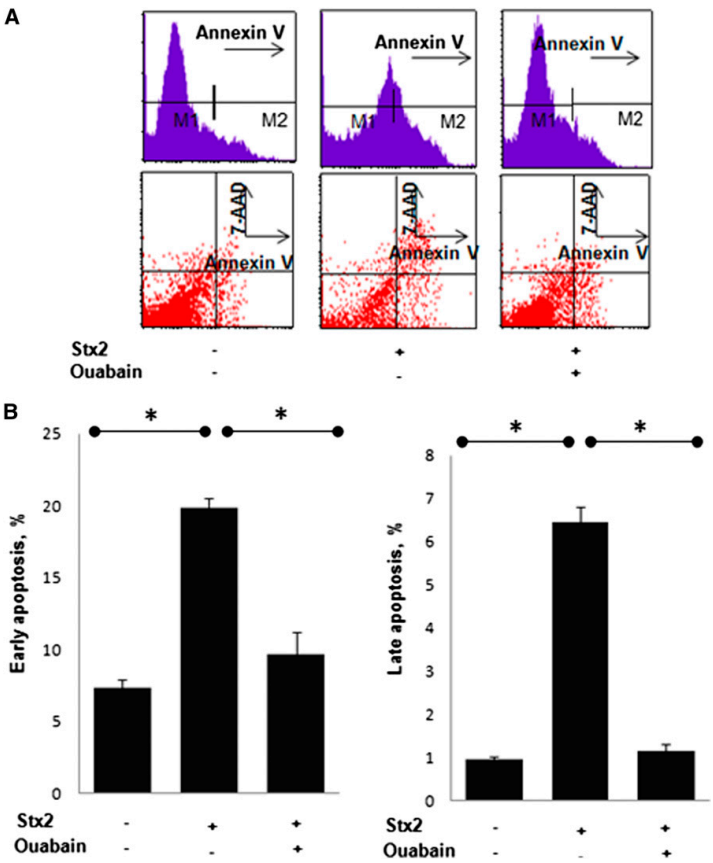

Figure 3. Ouabain increases cell viability. (A) Representative histogram and scatter plots of flow cytometer analysis from different experimental groups. Normal cells (in gate M1) and total apoptotic cells (in gate M2) are shown in the histograms; the early apoptosis (the lower right quadrants) and the late apoptosis and/or dead cells (the upper right quadrant) are shown in the scatter plots. (B) Histograms represent means ± SEM. *$P<0.05$. Statistical analysis was performed using the Mann-Whitney *U* test. Experiments were repeated three times.

4D).[25,26] Preincubation with helenalin completely abolished the antiapoptotic effect of ouabain in Stx2-exposed cells.

Expression of Bcl-xL, Bax, Caspase-8, and Caspase-3 in Stx2- and Ouabain-Treated Cells

The expression of apoptotic and antiapoptotic factors was determined with immunoblotting. After 16 hours of incubation of RPTCs with Stx2 alone, the expression of Bcl-xL was decreased by 23.7%±5.9% compared with control cells. In contrast, Bcl-xL expression was similar in cells co-incubated with Stx2 and ouabain and in control cells. In cells exposed to Stx2 alone, expression of Bax was increased by 37.0%±5.2%, but no such increase was observed in cells exposed to Stx2 and ouabain. Bax can initiate a cascade of events that eventually involves cleavage of caspase-3. The expression of cleaved caspase-3 was significantly increased (48.1%±5.4%) in cells exposed to Stx2 alone compared with control cells, but no such increase was observed in cells exposed to Stx2 and ouabain. The apoptotic factor caspase-8, an activator of Bax,[27] was increased with 42.7%±5.1% in cells exposed to Stx2 alone and with 38.4%±5.0% in cells exposed to Stx2 and ouabain (Figure 5, A–D). The effects of Stx2 incubation on Bcl-xL and Bax were significant at 6 hours but were not significant in comparison with control cells for caspase-3 and caspase-8 (Figure 5, E–H). Incubation with ouabain alone caused an increase in Bcl-xL and decrease in Bax expression after 16 hours of incubation (Supplemental Figure 2).

Ouabain Protects Kidneys from Apoptosis in Stx2-Treated Mice

To study the *in vivo* effects of Stx2 and ouabain treatment, mice were given an intraperitoneal injection of Stx2 (285 ng/kg) (n=9) or PBS (n=9) at day 0. A mini-pump that delivered ouabain (15 μg/kg per day) or PBS was inserted subcutaneously 1 day earlier. Mice given an intraperitoneal injection of PBS (n=6) and receiving PBS *via* mini-pumps (n=6) were controls. The mice were observed for 2 days and then euthanized. Mice injected with this dose of Stx2 usually develop symptoms after 3–4 days.[4,28] Mice were euthanized before symptoms developed in order to detect early apoptotic changes.

Kidneys were immediately removed, fixed, and stained for evaluation of the apoptotic index or for evaluation of Bcl-xL and Bax expression. Two sections from each kidney were used for TUNEL assay of the apoptotic index, which was determined in the renal cortex as the number of TUNEL-positive tubular cells in relation to the total number of tubular cells (Figure 6A). The apoptotic index was significantly higher in mice given Stx2 alone (n=9) than in mice given Stx2 and ouabain (n=9) (6.1%±0.6% and 1.7%±0.4%, respectively, $P<0.001$). In the control group the apoptotic index was 0.48%±0.06% (Figure 6A).

The expression of Bcl-xL and Bax was visualized by immunofluorescence. Renal cortical expression of Bcl-xL and Bax was detected in all groups studied (Figure 6B). Semiquantitative evaluation of the fluorescence by ImageJ software was performed on one section from each kidney. In mice inoculated with Stx2 and receiving PBS from the mini-pump, the Bcl-xL signal was significantly lower (22.5%±2.6%) than in

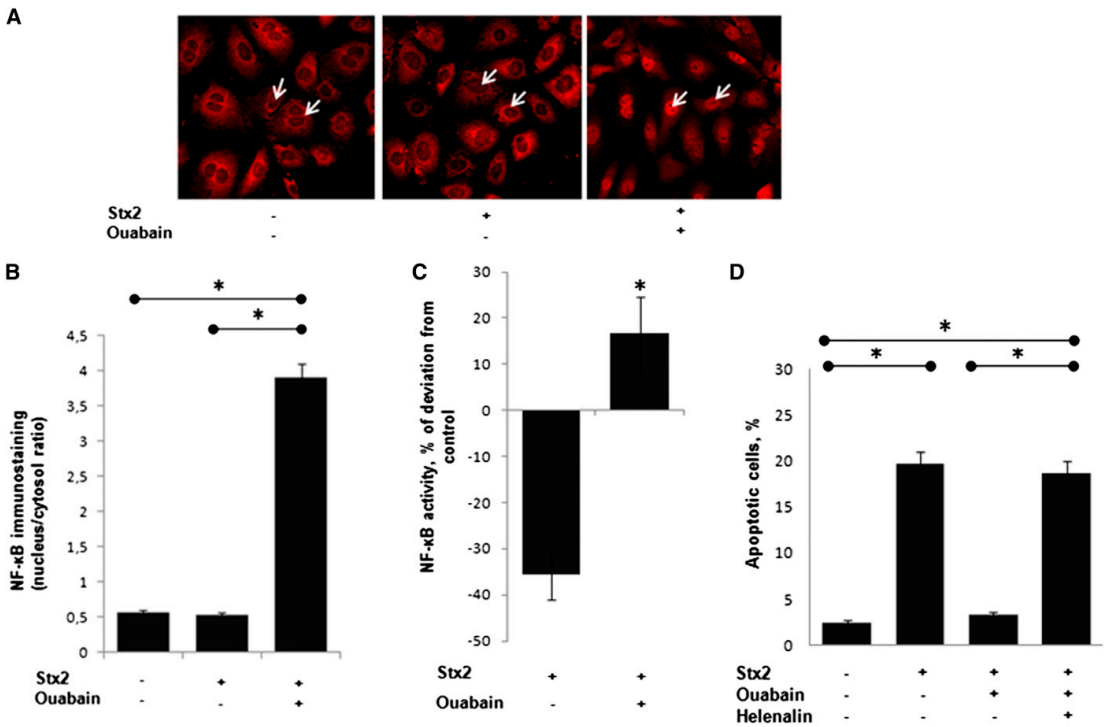

Figure 4. Ouabain activates NF-κB p65 subunit. (A) Representative confocal images of NF-κB p65 subunit immunofluorescence signal in RPTCs (white arrows). Note the strong nuclear signal in ouabain-exposed cells in the right panel. (B) Bars show mean nuclear/cytosol NF-κB p65 subunit signal. Each experiment analyzed 30–50 cells. Histograms represent means ± SEM. *$P<0.001$ for Stx2 plus ouabain versus control, Stx2 plus ouabain versus Stx2. Experiments were repeated four times. (C) NF-κB p65 subunit activity in rat RPTCs determined as NF-κB DNA-binding capacity in nuclear protein extracts. The activity of the control was set to 100%. Histograms represent means ± SEM. *$P<0.01$. Statistical analysis was performed using the one-way ANOVA followed by *post hoc* test. Experiments were repeated three times. (D) Helenalin is a specific NF-κB inhibitor that abolishes the antiapoptotic effect of ouabain. Apoptotic index was determined by analyzing five to seven randomly selected areas with 50–200 cells, enabling an analysis of around 5000 cells. Histograms represent means ± SEM. *$P<0.01$. Experiments were repeated three times.

kidneys from the mice in the control group. In contrast, the intensity of the fluorescent signal from Bcl-xL was similar in Stx2-inoculated mice treated with ouabain and in control mice. Kidneys from control mice exhibited low levels of Bax expression. In mice inoculated with Stx2 alone, expression of Bax was increased by 46.1%±7.1%. Bax was not upregulated in kidneys from mice treated with Stx2 and ouabain. The mice receiving an intraperitoneal injection of PBS and ouabain in the mini-pump did not differ from the control group with regard to any measures studied (Figure 6B).

Ouabain Protects against Podocyte Depletion and Attenuates Renal Function Impairment in Stx2-Treated Mice

The visceral epithelial cells in the glomeruli, the podocytes, are of critical importance for the filtering process but have a limited capacity to regenerate. Podocyte depletion is one of the major mechanisms behind progressive kidney disease. The number of podocytes was counted in the control group and the two groups inoculated with Stx2. The number of podocytes in 12–15 glomeruli from two kidney sections from each animal included in the study was reduced by 25.2% ($P^*0.01$) in the Stx2 group receiving vehicle compared with the control group but was significantly less reduced (7.7%) in the group receiving ouabain (Figure 7A). Stx2-treated mice with vehicle had a moderate but significant increase in plasma creatinine. This was not observed in Stx2-inoculated mice treated with ouabain (Figure 7B).

DISCUSSION

Shiga toxin is an important virulence factor of *E. coli* strains that are associated with HUS, and Stx2-triggered apoptosis is considered one of the causes of renal damage during HUS.[1,2]

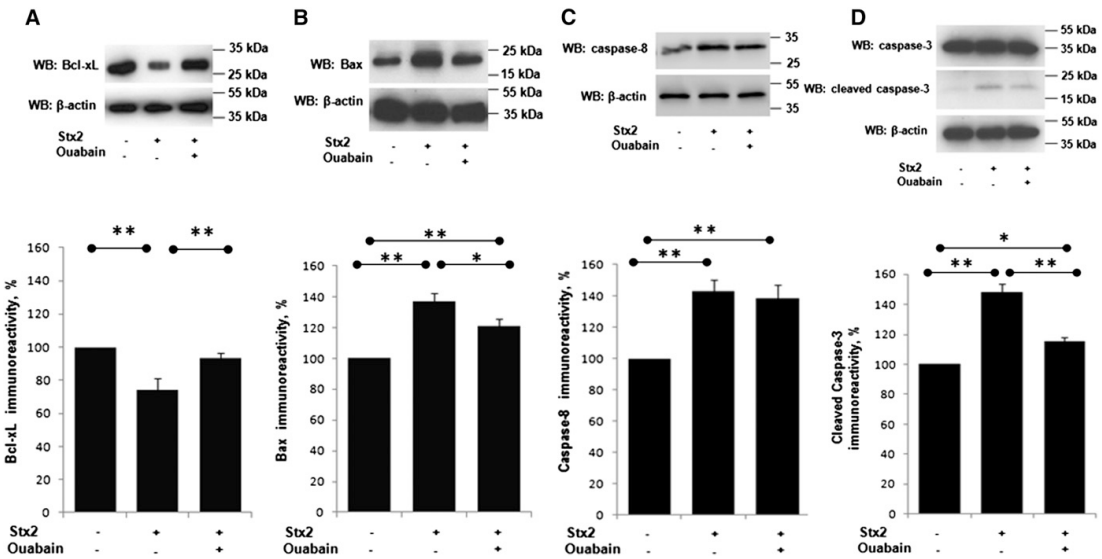

Figure 5. Ouabain regulates the balance between apoptotic and antiapoptotic factors in Stx-2-treated RPTCs. Panel I: Expression of the Bax (A), Bcl-xL (B), caspase-8 (C), and caspase-3 (D) in the presence of Stx2 and ouabain during 16 hours. Densitometric quantification of bands was done for the respective blots. The density of the band from control cells was set to 100%. Histograms represent means ± SEM. $^{**}P<0.01$, $^{*}P<0.05$. Statistical analysis was performed using the Mann-Whitney *U* test. Experiments were repeated five times. Panel II: Expression of the Bax (A), Bcl-xL (B), caspase-8 (C), and caspase-3 (D) in the presence of Shiga toxin 2 and ouabain during 6 hours. Densitometric quantification of bands was done for the respective blots. Histograms represent means ± SEM. $^{*}P<0.05$. Statistical analysis was performed using the Mann-Whitney *U* test. Experiments were repeated five times.

The results from this study confirm the apoptotic effect of Stx2 on renal epithelial cells and indicate that the apoptosis is due to an imbalance between the apoptotic factor Bax and the antiapoptotic factor Bcl-xL. The cardiotonic steroid ouabain reverses the imbalance and protects against this manifestation of Stx2 pathology.

Apoptosis is induced *via* two major pathways: the extrinsic pathway, where activation of plasma membrane "death receptors" leads to the recruitment of caspase-8,[29] and the intrinsic pathway (the mitochondrial pathway), where the proapoptotic dimerizing factors Bax and Bak are recruited to the mitochondrial membrane.[30] Both pathways will initiate signaling cascades that result in the cleavage of caspase-3 and cell death.[29] Here we found, in line with several previous studies, that Stx2 exposure for 16 hours caused a large upregulation of caspase-8,[6] of Bax,[9,31] and of caspase3.[6] We also recorded a substantial downregulation of Bcl-xL. The recordings made after 6 hours of Stx2 exposure indicated that the effects on Bax and Bcl-xL preceded the effects on caspase-8 and -3. Ouabain attenuated the upregulation of Bax, but not of caspase-8. Caspase-8 can initiate both the extrinsic and the intrinsic apoptotic pathway because it may bypass the mitochondrial pathway and directly cleave caspase-3, or, *via* a series of events, facilitate the translocation of Bax to the mitochondrial membrane.[29] Taken together, these results imply that in Stx2-triggered apoptosis, caspase-8 may mainly act by stimulating Bax and the intrinsic apoptotic pathway. Little is known about the effect of Stx2 on the expression of the Bax inhibitor Bcl-xL, but overexpression of Bcl-xL by transient transfection was reported to protect against Stx-triggered apoptosis.[10] Here we could show that the downregulation of this survival factor in Stx2-treated renal epithelial cells was almost completely abolished by ouabain treatment. Because there is little evidence for a more direct interaction between caspase-8 and Bcl-xL, we conclude that the antiapoptotic effect of ouabain is due to inhibition of the intrinsic, mitochondrial apoptotic pathway and that treatment with ouabain protects against apoptosis by reversing an imbalance between Bcl-xL and Bax, as shown in both the *in vitro* and *in vivo* studies.

We ascribe the antiapoptotic effect of ouabain to the signaling function of Na,K-ATPase. Exposure of renal cells to low concentrations of the highly specific Na,K-ATPase ligand, ouabain, will trigger a signaling cascade that involves interaction between the catalytic subunit of Na,K-ATPase and the inositol 1,4,5-triphosphate receptor, intracellular calcium oscillations and activation of the NF-kB p65 subunit (Supplemental Figure 3). We showed that Stx2 does not affect the capacity of ouabain-bound Na,K-ATPase to interact with IP3R. Bcl-xL is a target for the transcriptional effect of the NF-κB p65 subunit.[32] The calcium oscillations triggered by ouabain/Na,K-ATPase/IP3R signaling have a frequency of approximately 1 peak every 3–5 minutes, and calcium

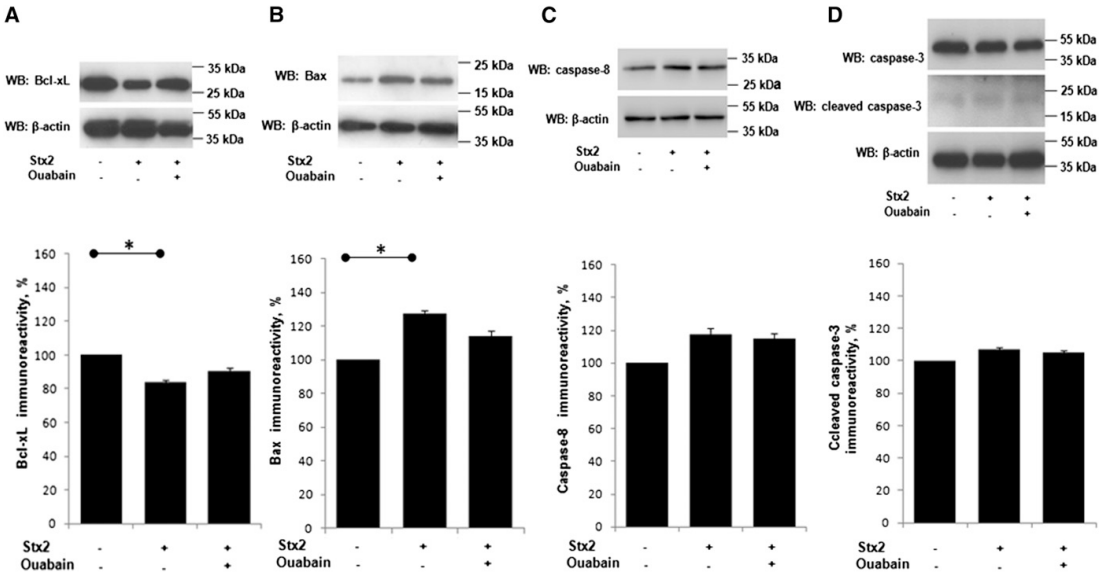

Figure 5. Continued.

oscillations with this periodicity have previously been reported to activate NF-κB.[16–19] Here we showed that ouabain signaling triggers activation and translocation of NF-κB p65 subunit to the nucleus in cells exposed to Stx2 and ouabain but found no evidence of NF-κB p65 subunit activation in cells exposed to Stx2 alone. Helenalin inhibits the transcriptional effect of NF-κB p65 subunit; in cells co-incubated with Stx2, ouabain, and helenalin, the capacity of ouabain to protect against apoptosis was lost. The concentration of ouabain used in this study, 5 nM, has no measurable effect on the pumping function of Na,K-ATPase in rat cells.[18,19]

The *in vivo* study provided proof of principle that ouabain can protect proximal tubular cells from Stx2-triggered apoptosis, that Stx2 triggers an imbalance between Bax and Bcl-xL, and that ouabain treatment can reverse this change in balance. Continuous treatment with ouabain was started 24 hours before the Stx2 injection. This time frame may be relevant for a future therapeutic use of ouabain because patients with Stx2-producing *E. coli* infection seek care after the onset of hemorrhagic diarrhea and before or at the onset of Stx2-triggered pathology. Loss of podocytes is a hallmark of permanent renal damage because these cells have a very low capacity to regenerate.[33] The number of podocytes decreased in both groups of Stx2-inoculated mice, but this reduction was significantly less pronounced in the ouabain-treated group. Taken together, these results imply that the antiapoptotic effect of ouabain will, at least partially, protect against acute and permanent renal damage caused by exposure to Stx2.

The results from this study may have implications that go beyond the treatment of HUS-associated renal apoptosis. Many disease conditions in the kidney are associated with excessive apoptosis, such as diabetic nephropathy,[34,35] glomerular tubular disconnection in diseases with profound proteinuria,[36] polycystic kidney disease,[37] and AKI.[38] Expression of Bax is increased in many of these conditions, leading to the suggestion that the Bax inhibitor Bcl-xL would be a potential therapeutic target in renal diseases associated with apoptosis.[39] Almost all of the available antiapoptotic drugs have serious adverse effects. The use of caspase inhibitors is for the most part prohibited because of the risk of preventing a physiologic apoptotic process in premalignant cells. However, in contrast to caspase inhibitors, which would completely block the apoptotic pathway, ouabain would, by triggering a signal that results in physiologic upregulation of Bcl-xL, reset and normalize the balance between apoptotic and antiapoptotic factors.

CONCISE METHODS

Cells

RPTCs were prepared from kidneys of 20-day-old male Sprague-Dawley rats as described previously. Cells were plated on 12-mm glass coverslips in 24-well cell culture plates On day 2 *in vitro*, at which time they have been shown to maintain most of their phenotype as RPTCs, the cells were exposed to the indicated compounds (Stx2 with or without ouabain) or to vehicle (PBS).

Stx2 Binding to RPTCs

RPTCs were plated on 12-mm glass coverslips in 24-well cell culture plates. The cells were fixed in paraformaldehyde, washed once with cold

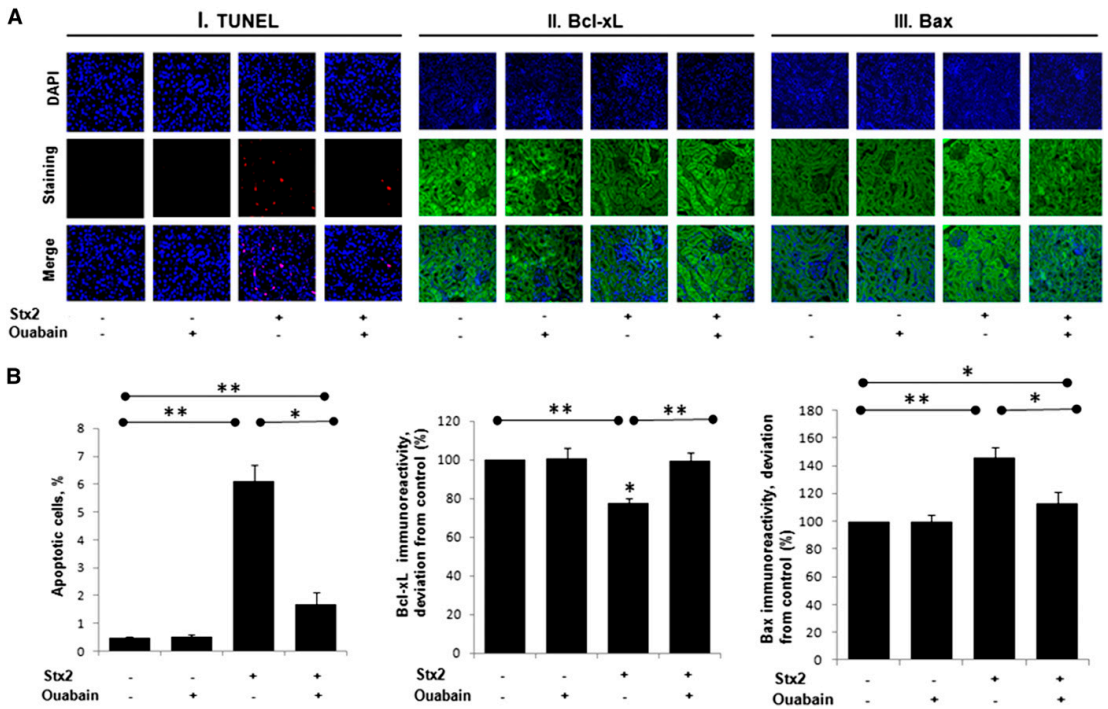

Figure 6. Ouabain protects kidneys from apoptosis in Stx2-treated mice. (A) Representative confocal images of kidney sections from mice inoculated with Stx2 or PBS as vehicle, with and without continuous treatment with ouabain. Sections were labeled with TUNEL (red) to detect apoptotic cells (I), immunohistochemically stained for Bcl-xL (II), and Bax (III). Nuclei were counterstained with DAPI (blue). (B) Apoptotic index is given as percentage apoptotic cells and was determined by analyzing 5–7 randomly selected areas, with 80–150 cells in each area, from two independent experiments. Immunoreactivity for Bcl-xL and Bax is expressed as percentage deviation from control. Histograms represent means ± SEM. Statistical analysis was performed using the Mann-Whitney *U* test. **P*<0.05, ***P*<0.001.

PBS, and incubated with Stx2 for 1 hour with gentle shaking. Cells were then incubated with mouse monoclonal anti-Stx2 IgG1 antibody or the isotype control antibody, followed by incubation with Alexa Fluor 488 fluorescence-conjugated goat antimouse IgG antibody.

Detection of Apoptotic Cells

RPTCs were plated on 12-mm glass coverslips in 24-well cell culture plates. On culture day 2, when cells had achieved approximately 50% confluence, indicated compounds were added to the medium. The ApopTag Red In Situ Apoptosis Detection kit was used to determine apoptotic cells. TUNEL assay was conducted according to the manufacturer's instructions. Nuclei were counterstained with DAPI. Cells were mounted in Immu-Mount and images were recorded with confocal microscopy. The apoptotic index was calculated as the percentage of TUNEL-positive cells; the total number of cells was determined by DAPI stain.

FACS Staining

Approximately 1 million RPTCs from each study group were harvested, washed, and labeled with fluorochrome-conjugated annexin V (an indicator of early apoptosis) and 7-AAD (viability dye) in the dark at room temperature for 15 minutes using Annexin V-PE Apoptosis detection Kit I. This procedure was followed by FACSCalibur analysis. The quantification analysis was performed with CellQuest software, version 3.3.

NF-κB p65 Subunit Activity

NF-κB p65 subunit translocation to nucleus was used as an index of NF-κB p65 subunit activation. RPTCs were labeled with rabbit polyclonal NF-κB p65 antibody, and secondary antibody was antirabbit Alexa 546. Images of immune-labeled cells were recorded with confocal microscopy. The ratio of the immunosignal between nucleus and cytosol was measured using ImageJ software. An area corresponding to 90% of the nucleus and an identical area in the cytoplasm were used for the measurements. NF-κB p65 subunit DNA binding in nuclear protein extracts was assessed using a commercially available NF-κB p65 transcription factor assay according to the manufacturer's instructions.

The ApopTag Red In Situ Apoptosis Detection kit was used to determine apoptotic cells. TUNEL assay was conducted according to the manufacturer's instructions. RPTCs were preincubated with helenalin, an NF-κB inhibitor (1 μM). Cells were mounted in Immu-Mount, and images were recorded with confocal microscopy. The

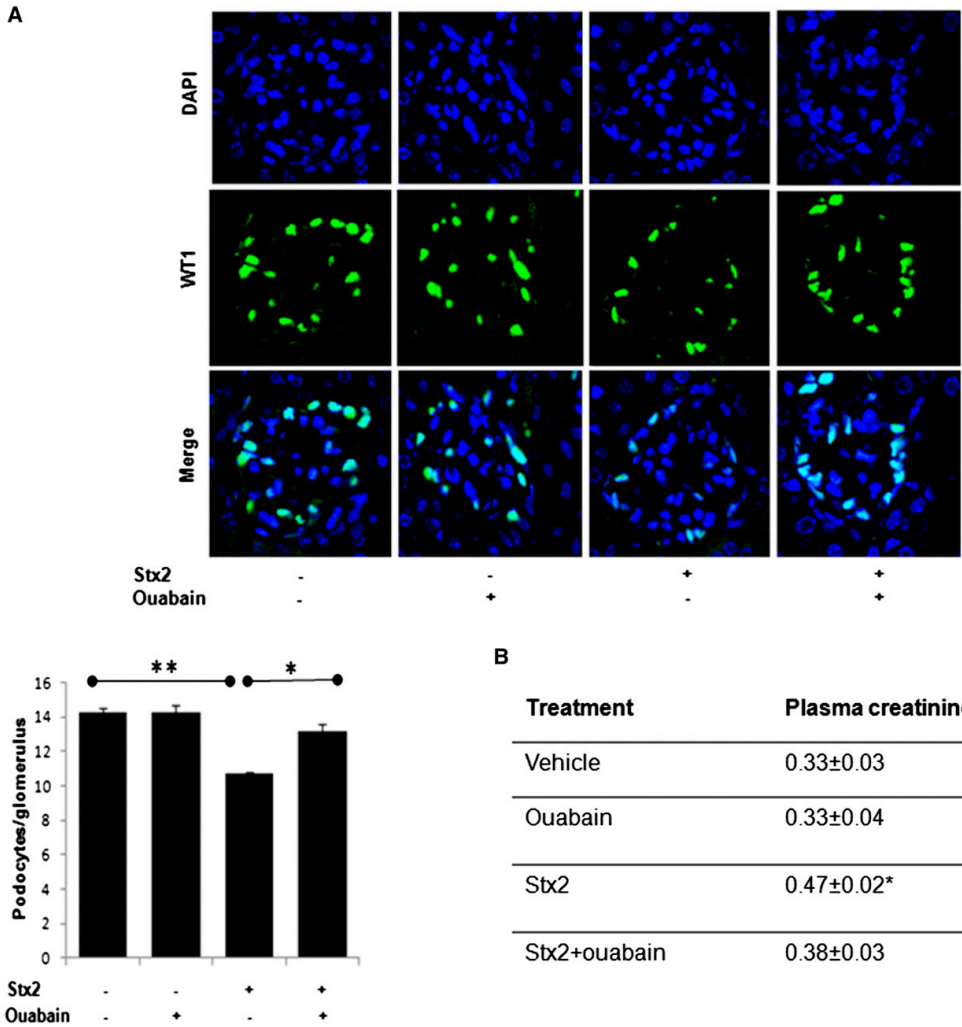

B

Treatment	Plasma creatinine, mg/dL
Vehicle	0.33±0.03
Ouabain	0.33±0.04
Stx2	0.47±0.02*
Stx2+ouabain	0.38±0.03

Figure 7. Ouabain prevents podocyte loss and attenuates renal function impairment. (A) Representative micrographs demonstrate podocytes from mice treated with Stx2 or PBS as vehicle, with and without continuous treatment with ouabain. WT-1 staining has been used to recognize podocytes. Histograms represent means ± SEM. $^{**}P<0.01$, $^{*}P<0.05$. Statistical analysis was performed using the Mann-Whitney *U* test. (B) Plasma creatinine values in Stx2- and ouabain-treated mice. Data presented as means ± SEM. $^{*}P<0.05$ for Stx2 versus control, ouabain, and Stx2 plus ouabain. Statistical analysis was performed using the Mann-Whitney *U* test.

apoptotic index was calculated as the percentage of ApopTag-positive cells; the total number of cells was determined by DAPI stain.

Immunoprecipitation of NKA and IP3R

After incubation with Stx2 and ouabain for 24 hours, RPTCs were washed twice with PBS, lysed on ice in cold buffer, sonicated, and centrifuged. Immune complexes were then incubated with 30 μg/L of 50% slurry of protein A/GPLUS-agarose beads. On the next day the beads were processed for SDS-PAGE and immunoblotting. The protein bands were visualized by chemiluminescence using secondary antibodies labeled with horseradish peroxidase. Densitometric quantification of films was done, correction for total protein was made, and control values were set to 100%.

Immunoblotting for Detection of Bax, Bcl-xL, Caspase-3, and Caspase-8

Proteins solubilized in Laemmli sample buffer were resolved in polyacrylamide gels by SDS-PAGE and transferred to a polyvinylidene

difluoride membrane. The protein bands were visualized by chemiluminescent substrate.

Animal Studies

Experiments were conducted on C57BL/6 male mice weighing 22–24 g. Mice received an intraperitoneal injection of Shiga toxin 2 at 285 ng/kg. PBS injection was used for control mice. Ouabain was delivered in a dose corresponding to 15 μg/kg per day using subcutaneous neck mini-pumps. Controls received PBS vehicle in the pump. All mice were euthanized at day 3 after inoculation with Stx2. Mouse kidneys were removed and fixed in 4% paraformaldehyde in PBS (pH, 7.4) immediately after euthanasia. Tissues were then embedded in paraffin and sectioned.

TUNEL Assay

Renal tissue (3-μm sections) used for TUNEL assay was deparaffinized and rehydrated before processing. Two sections from each mouse kidney were used for TUNEL assay. The ApopTag Red In Situ Apoptosis Detection kit was used to determine the apoptotic index. TUNEL assay was conducted according to the manufacturer's instructions. Nuclei were counterstained with DAPI. Sections were mounted in Immu-Mount and recorded with confocal microscopy. Cells were considered apoptotic when they exhibited ApopTag Red staining and characteristic apoptotic structure.

Apoptotic index was calculated as the percentage of TUNEL-positive cells; the total number of cells was determined by DAPI stain. In each slice, five to seven randomly selected areas were examined, and in each area, between 80 and 150 DAPI-stained cells were counted.

Immunohistochemistry

Renal tissue (3-μm sections) was deparaffinized and rehydrated before processing. Antigens were retrieved by boiling in citrate buffer. Sections were treated with Triton X-100 0.3% in PBS for 20 minutes. After three PBS washes, sections were incubated with blocking buffer (5% bovine serum albumin and Triton X-100 0.1% in PBS) for 1 hour. The rabbit polyclonal anti-Bcl-xL primary antibody and rabbit polyclonal anti-Bax were applied overnight at 4°C. After three PBS washes, sections were incubated with a secondary Alexa Fluor 488 goat antirabbit IgG) for 1 hour at room temperature. Nuclei were counterstained with DAPI. All samples were stained using identical protocols. Sections were mounted in Immu-Mount and images were recorded with confocal microscopy. All microscopy recordings were done during one session using identical microscope parameters. Image analysis was performed using ImageJ software. Three areas in each section were analyzed.

For podocyte immunostaining, the rabbit polyclonal anti–Wilms tumor-1 (WT1) primary antibody was applied overnight to kidney sections at 4°C. Controls were performed in the same conditions, but the primary antibody was omitted. After three PBS washes, sections were incubated with a secondary antirabbit Alexa Fluor 488 IgG. Nuclei were counterstained with DAPI. The immune-labeled cells were observed with Zeiss LSM 510 laser scanning confocal microscope using a 63×/1.2NA oil-immersion objective. For quantitative determination of podocyte numbers, the WT-1–positive cells were counted in at least 12–15 randomly chosen glomeruli. Two sections from each kidney were analyzed.

Analyticals

Blood was collected by cardiac puncture of anesthetized animals. Plasma creatinine was determined using a Mouse Creatinine (Cr) ELISA kit (Cusabio, Biotech Co., LTD, China). Reaction was analyzed on automated spectrophotometer (Wallac Victor^3 1420 Multilabel Counter).

Statistical Analyses

Statistical analysis was performed with Statistica 6.0 software (Statsoft, Tulsa, OK) and SAS statistical software, version 9.1 (SAS Institute, Cary, NC). A *t* test was used to compare quantitative variables between groups if the distribution was parametric; ANOVA followed by the *post hoc* test and nonparametric test (Mann-Whitney *U* test) were used to test significance of differences. Statistical significance was determined as $P<0.05$. Values are expressed as means ± SEM.

A complete description of the Methods is provided in the Supplemental Material.

ACKNOWLEDGMENTS

This study has been supported by grants from the Swedish Research Council to Anita Aperia (K2011-54X-03644-40-6), the Swedish Research Council (K2010-65X-14008-10-3), the Torsten Söderberg Foundation, Konung Gustaf V:s 80-årsfond, Fanny Ekdahl's Foundation and Crown Princess Lovisa's Society for Child Care to D.K.; by grants from the Family Erling-Persson Foundation to Anita Aperia; and by a Karolinska Institute KIRT fellowship to I.B.

REFERENCES

1. Obrig TG: *Escherichia coli* Shiga Toxin Mechanisms of Action in Renal Disease. *Toxins (Basel)* 2: 2769–2794, 2010
2. Karpman D, Sartz L, Johnson S: Pathophysiology of typical hemolytic uremic syndrome. *Semin Thromb Hemost* 36: 575–585, 2010
3. Bergan J, Dyve Lingelem AB, Simm R, Skotland T, Sandvig K: Shiga toxins. *Toxicon* 60: 1085–1107, 2012
4. Psotka MA, Obata F, Kolling GL, Gross LK, Saleem MA, Satchell SC, Mathieson PW, Obrig TG: Shiga toxin 2 targets the murine renal collecting duct epithelium. *Infect Immun* 77: 959–969, 2009
5. Karpman D, Håkansson A, Perez MT, Isaksson C, Carlemalm E, Caprioli A, Svanborg C: Apoptosis of renal cortical cells in the hemolytic-uremic syndrome: in vivo and in vitro studies. *Infect Immun* 66: 636–644, 1998
6. Fujii J, Wood K, Matsuda F, Carneiro-Filho BA, Schlegel KH, Yutsudo T, Binnington-Boyd B, Lingwood CA, Obata F, Kim KS, Yoshida S, Obrig T: Shiga toxin 2 causes apoptosis in human brain microvascular endothelial cells via C/EBP homologous protein. *Infect Immun* 76: 3679–3689, 2008
7. Lee SY, Cherla RP, Caliskan I, Tesh VL: Shiga toxin 1 induces apoptosis in the human myelogenous leukemia cell line THP-1 by a caspase-8-dependent, tumor necrosis factor receptor-independent mechanism. *Infect Immun* 73: 5115–5126, 2005
8. Taylor RC, Cullen SP, Martin SJ: Apoptosis: controlled demolition at the cellular level. *Nat Rev Mol Cell Biol* 9: 231–241, 2008

9. Schinzel A, Kaufmann T, Borner C: Bcl-2 family members: Intracellular targeting, membrane-insertion, and changes in subcellular localization. *Biochim Biophys Acta* 1644: 95–105, 2004
10. Gordon J, Challa A, Levens JM, Gregory CD, Williams JM, Armitage RJ, Cook JP, Roberts LM, Lord JM: CD40 ligand, Bcl-2, and Bcl-xL spare group I Burkitt lymphoma cells from CD77-directed killing via Verotoxin-1 B chain but fail to protect against the holotoxin. *Cell Death Differ* 7: 785–794, 2000
11. Jones NL, Islur A, Haq R, Mascarenhas M, Karmali MA, Perdue MH, Zanke BW, Sherman FM: Escherichia coli Shiga toxins induce apoptosis in epithelial cells that is regulated by the Bcl-2 family. *AJP GI* 278: 811–819, 2000
12. Bitzan M, Schaefer F, Reymond D: Treatment of typical (enteropathic) hemolytic uremic syndrome. *Semin Thromb Hemost* 36: 594–610, 2010
13. Boyer O, Niaudet P: Hemolytic uremic syndrome: New developments in pathogenesis and treatment. *Int J Nephrol* 2011: 908407, 2011
14. Aperia A: New roles for an old enzyme: Na,K-ATPase emerges as an interesting drug target. *J Intern Med* 261: 44–52, 2007
15. Zhang S, Malmersjö S, Li J, Ando H, Aizman O, Uhlén P, Mikoshiba K, Aperia A: Distinct role of the N-terminal tail of the Na,K-ATPase catalytic subunit as a signal transducer. *J Biol Chem* 281: 21954–21962, 2006
16. Miyakawa-Naito A, Uhlén P, Lal M, Aizman O, Mikoshiba K, Brismar H, Zelenin S, Aperia A: Cell signaling microdomain with Na,K-ATPase and inositol 1,4,5-trisphosphate receptor generates calcium oscillations. *J Biol Chem* 278: 50355–50361, 2003
17. Aizman O, Uhlén P, Lal M, Brismar H, Aperia A: Ouabain, a steroid hormone that signals with slow calcium oscillations. *Proc Natl Acad Sci U S A* 98: 13420–13424, 2001
18. Li J, Zelenin S, Aperia A, Aizman O: Low doses of ouabain protect from serum deprivation-triggered apoptosis and stimulate kidney cell proliferation via activation of NF-kappaB. *J Am Soc Nephrol* 17: 1848–1857, 2006
19. Li J, Khodus GR, Markus Kruusmägi M, Kamali-Zare P, Liu X, Eklöf A-Ch, Zelenin S, Brismar H, Aperia A. Ouabain protects against adverse developmental programming of the kidney. *Nature Communications 27*, 2010.
20. Tamatani M, Che YH, Matsuza0ki H, Ogawa S, Okado H, Miyake S, Mizuno T, Tohyama M: Tumor necrosis factor induces Bcl-2 and Bcl-x expression through NFkappaB activation in primary hippocampal neurons. *J Biol Chem* 274: 8531–8538, 1999
21. Keepers TR, Psotka MA, Gross LK, Obrig TG: A murine model of HUS: Shiga toxin with lipopolysaccharide mimics the renal damage and physiologic response of human disease. *J Am Soc Nephrol* 17: 3404–3414, 2006
22. Dahiya R, Brasitus TA: Dexamethasone-induced alterations in the glycosphingolipids of rat kidney. *Lipids* 23: 863–868, 1988
23. Lindberg AA, Brown JE, Strömberg N, Westling-Ryd M, Schultz JE, Karlsson KA: Identification of the carbohydrate receptor for Shiga toxin produced by Shigella dysenteriae type 1. *J Biol Chem* 5;262: 1779–1785, 1987
24. Sarnico I, Lanzillotta A, Benarese M, Alghisi M, Baiguera C, Battistin L, Spano P, Pizzi M: NF-kappaB dimers in the regulation of neuronal survival. *Int Rev Neurobiol* 85: 351–362, 2009
25. Lyss G, Knorre A, Schmidt TJ, Pahl HL, Merfort I: The anti-inflammatory sesquiterpene lactone helenalin inhibits the transcription factor NF-kappaB by directly targeting p65 *J Biol Che* 11: 273(50): 33508-335016, 1998.
26. Lyß G, Knorre A, Schmidt TJ, Pahl HL, Merfort I: The anti-inflammatory sesquiterpene lactone helenalin inhibits the transcription factor NF-kB by directly targeting p65. *J Biol Chem* 273: 50: 33508–33516, 1998
27. Gustafsson AB, Gottlieb RA: Bcl-2 family members and apoptosis, taken to heart. *Am J Physiol Cell Physiol* 292: C45–C51, 2007
28. Sauter KAD, Melton-Celsa AR, Larkin K, Troxell ML, O'Brien AD, Magun BE: Mouse model of hemolytic-uremic syndrome caused by endotoxin-free Shiga toxin 2 (Stx2) and protection from lethal outcome by anti-Stx2 antibody. *Infect Immun* 76: 4469–4478, 2008
29. Elmore S: Apoptosis: A review of programmed cell death. *Toxicol Pathol* 35: 495–516, 2007
30. Kroemer G, Galluzzi L, Brenner C: Mitochondrial membrane permeabilization in cell death. *Physiol Rev* 87: 99–163, 2007
31. Tironi-Farinati C, Loidl CF, Boccoli J, Parma Y, Fernandez-Miyakawa ME, Goldstein J: Intracerebroventricular Shiga toxin 2 increases the expression of its receptor globotriaosylceramide and causes dendritic abnormalities. *J Neuroimmunol* 222: 48–61, 2010
32. Khoshnan A, Tindell C, Laux I, Bae D, Bennett B, Nel AE: The NF-kappa B cascade is important in Bcl-xL expression and for the anti-apoptotic effects of the CD28 receptor in primary human CD4+ lymphocytes. *J Immunol* 165: 1743–1754, 2000
33. Pavenstädt H, Kriz W, Kretzler M: Cell biology of the glomerular podocyte. *Physiol Rev* 83: 253–307, 2003
34. Sanchez-Niño MD, Bozic M, Córdoba-Lanús E, Valcheva P, Gracia O, Ibarz M, Fernandez E, Navarro-Gonzalez JF, Ortiz A, Valdivielso JM: Beyond proteinuria: VDR activation reduces renal inflammation in experimental diabetic nephropathy. *Am J Physiol Renal Physiol* 15; 302: 647–657, 2012
35. Sanchez-Niño MD, Sanz AB, Lorz C, Gnirke A, Rastaldi MP, Nair V, Egido J, Ruiz-Ortega M, Kretzler M, Ortiz A: BASP1 promotes apoptosis in diabetic nephropathy. *J Am Soc Nephrol* 21: 610–621, 2010
36. Chevalier RL, Forbes MS: Generation and evolution of atubular glomeruli in the progression of renal disorders. *J Am Soc Nephrol* 19: 197–206, 2008
37. Ostrom L, Tang MJ, Gruss P, Dressler GR: Reduced Pax2 gene dosage increases apoptosis and slows the progression of renal cystic disease. *Dev Biol* 219: 250–258, 2000
38. Srichai MB, Hao C, Davis L, Golovin A, Zhao M, Moeckel G, Dunn S, Bulus N, Harris RC, Zent R, Breyer MD: Apoptosis of the thick ascending limb results in acute kidney injury. *J Am Soc Nephrol* 19: 1538–1546, 2008
39. Sanz AB, Santamaría B, Ruiz-Ortega M, Egido J, Ortiz A: Mechanisms of renal apoptosis in health and disease. *J Am Soc Nephrol* 19: 1634–1642, 2008

This article contains supplemental material online at http://jasn.asnjournals.org/lookup/suppl/doi:10.1681/ASN.2012101044/-/DCSupplemental.

II

the FEBS Journal
REVIEW ARTICLE

Calcium oscillations triggered by cardiotonic steroids

Jacopo M. Fontana[1], Ievgeniia Burlaka[1], Georgiy Khodus[1,2], Hjalmar Brismar[1,2] and Anita Aperia[1]

1 Department of Women and Children's Health, Karolinska Institutet, Stockholm, Sweden
2 Department of Cell Physics, Royal Institute of Technology, Stockholm, Sweden

Keywords
apoptosis; Ca^{2+} signaling; cardiotonic steroids; inositol trisphosphate receptor; intracellular Ca^{2+} oscillations; Na^+–K^+–ATPase; NF-κB; organ development; ouabain; Src kinase

Correspondence
A. Aperia, Department of Women and Children's Health, Karolinska Institutet, 171 76 Stockholm, Sweden
Fax: +46 8 5177 7328
Tel.: +46 8 5177 7326
E-mail: anita.aperia@ki.se

(Received 12 March 2013, revised 18 July 2013, accepted 19 July 2013)

doi:10.1111/febs.12448

Na^+, K^+–ATPase (NKA) is well known for its function as an ion pump. Studies during the last decade have revealed an additional role for NKA as a signal transducer. In this brief review, we describe how cardiotonic steroids, which are highly specific NKA ligands, trigger slow Ca^{2+} oscillations by promoting the interaction between NKA and the inositol trisphosphate receptor, and how this Ca^{2+} signal activates the NF-κB subunit p65 and increases the expression of the antiapoptotic factor Bcl-xL. The potential tissue-protective effects of this signal are discussed.

Na^+,K^+–ATPase, a receptor for cardiotonic steroids

Na^+,K^+–ATPase (NKA) [1] belongs to the family of P-type ATPases and is a ubiquitous integral plasma membrane protein expressed in all eukaryotic cells. NKA uses the energy from ATP hydrolysis to export three Na^+ ions from the cell and to import two K^+ ions into the cell against an electrochemical gradient [2,3].

The pumping function of NKA is essential for the regulation of cell ionic content, pH and for maintaining resting membrane potential. NKA is a heterotrimeric protein complex consisting of a large catalytic α subunit, a heavily glycosylated β subunit and a tissue-specific regulatory subunit belonging to the FXYD proteins family. In mammals, there are four α subunits, three β subunits and seven FXYD [4].

The cardiotonic steroids (CTS) are highly specific NKA ligands that bind to all catalytic α-isoforms [5,6]. The CTS consist of a steroid core with a lactone ring and a sugar moiety. The CTS can be divided into two families, the cardenolides, to which ouabain and digoxin belong and the bufadienolides, to which marinobufagenin belongs. Ouabain, digoxin and marinobufagenin have been identified in human plasma. The cardenolides have a five-membered lactone ring and the bufadienolides a six-membered lactone ring. Ouabain, which is perhaps the best studied CTS, binds to the α subunit on the extracellular side in the cavity in the transmembrane domain at the interface created by six transmembrane segments αM1–6. Its lactone ring is buried within the transmembrane domain and

Abbreviations
CTS, cardiotonic steroid(s); Ins(1,4,5)P_3, inositol trisphosphate; Ins(1,4,5)P_3R, inositol trisphosphate receptor; NKA, Na^+,K^+–ATPase; Src, Src kinase.

the sugar moiety facing the extracellular side [7,8]. Recent studies have indicated differences in the capacity of the CTS to bind to the NKA catalytic subunit because of the number and nature of various sugar residues and changes in the position of hydroxyl groups of the steroid core [9].

The CTS are now generally considered as mammalian hormones. Studies using NMR and MS techniques have convincingly shown that ouabain, digoxin and marinobufagenin are present in human plasma and urine, bovine adrenal gland and hypothalamus, and rat adrenomedullary glands [10]. Their biological significance has been discussed for many years. CTS dose-dependently inhibit the activity of NKA. However, there is little support for the notion that CTS act as natriuretic hormones, because their circulating concentrations are most likely too low to induce an inhibitory effect on NKA ion transport. During the last decade, reports from several labs have revealed an additional role for NKA as a signal transducer [11–14]. Studies from our group have shed new light on the potential function of endogenous CTS as triggers of highly regular Ca^{2+} oscillations within a period range of 3–5 min.

Cardiotonic steroids trigger calcium oscillations

Several years ago our group reported that ouabain, in doses causing only partial NKA inhibition, acts as an inducer of regular, low-frequency intracellular Ca^{2+} oscillations that elicit activation of the transcription factor, NF-κB [15]. The study was performed on primary rat renal epithelial cells. This first unexpected finding was followed up by several studies on the role of the inositol 1,4,5-trisphosphate receptor [Ins(1,4,5)P_3R] in the generation of ouabain-triggered Ca^{2+} oscillations and the downstream effects of this signal pathway. Most of these studies were performed on COS-7 cells, a cell line derived from embryonic monkey kidney cells.

To examine whether the generation of the ouabain-induced Ca^{2+} oscillations required the generation of inositol 1,4,5-trisphosphate [Ins(1,4,5)P_3], cells were transfected with a construct encoding a hyperaffinity Ins(1,4,5)P_3 absorbent, 'an Ins(1,4,5)P_3 sponge' that has more than 1000-fold higher affinity for Ins(1,4,5)P_3 than Ins(1,4,5)P_3R, traps Ins(1,4,5)P_3 and abrogates Ins(1,4,5)P_3-induced Ca^{2+} release [16]. Because ouabain was found to trigger low-frequency Ca^{2+} oscillations in cells expressing the Ins(1,4,5)P_3 sponge, we concluded that the ouabain effect was at least partially independent of the generation of Ins(1,4,5)P_3 and we went on to explore the possibility that the ouabain-triggered Ca^{2+} oscillations might be initiated by direct interaction between NKA and Ins(1,4,5)P_3R. NKA coimmunoprecipitated with Ins(1,4,5)P_3R, and with the use of FRET measurements, a close spatial proximity between NKA and Ins(1,4,5)P_3R could be demonstrated, which was significantly enhanced in the presence of ouabain. The interaction between NKA and Ins(1,4,5)P_3R was found to be mediated by the N-terminus of the NKA catalytic α subunit and the N-terminus of the Ins(1,4,5)P_3R. The amino acid residues LKK in the α N-terminus tail, which are conserved in most species and all α-isoforms, were found to be essential for the binding. Ouabain-triggered Ca^{2+} signals were suppressed in cells overexpressing a peptide corresponding to the α-subunit N-terminal tail, but not in cells overexpressing a peptide in which the lysine-rich (LKK) motif had been deleted. It was concluded from these studies that NKA and Ins(1,4,5)P_3R can form a signaling microdomain that triggers Ca^{2+} oscillations [17]. It was later shown that ankyrin, which binds to the N-terminus of NKA and Ins(1,4,5)P_3R, acts as a stabilizing scaffolding protein within this signaling microdomain [18] (Fig. 1).

Taking into account the potential physiological and pharmacological role of NKA-triggered Ca^{2+} oscillations, it is important to consider whether this effect is specific for ouabain or can be extended to other CTS. In ongoing studies, we have tested whether the cardenolide digoxin and the bufadienolide marinobufagenin may also trigger Ca^{2+} oscillations. Both digoxin and marinobufagenin have been identified in human plasma. Figure 2 shows the effects of 100 nM ouabain, 100 nM digoxin and 100 nM marinobufagenin applied to COS-7 cells loaded with the Ca^{2+}-sensitive dye Fura-2AM. Results from these preliminary studies suggest that all tested CTS will trigger Ca^{2+} oscillations of similar frequency. Ouabain 100 nM has previously been found to cause ~ 10% inhibition of NKA activity in COS-7 cells [17]. Similar dose–response studies have not yet been performed on cells exposed to digoxin or marinobufagenin.

CTS stimulate Src-dependent tyrosine phosphorylation

Binding of CTS to NKA will also stimulate tyrosine phosphorylation. These observations, originally made by Xie and Askari at Toledo University [19,20], have since been confirmed by many laboratories. The tyrosine phosphorylation is mediated by the Src family of kinases, and coimmunoprecipitation and FRET studies indicate that the NKA catalytic α subunit and Src form a functional complex [21,22].

Several lines of evidence suggest that CTS activation of the NKA/Src complex causes transactivation of the

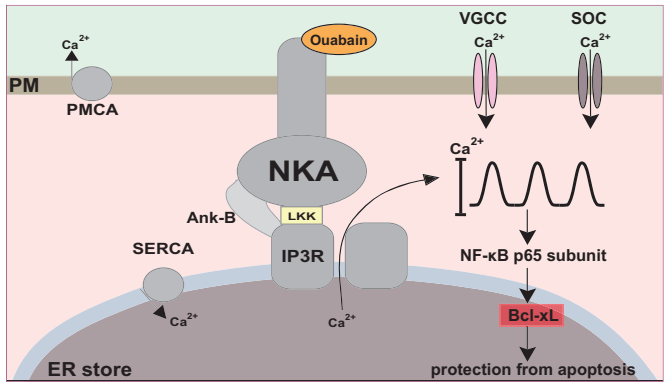

Fig. 1. NKA and Ca^{2+} signaling. Ouabain triggers the direct interaction between NKA and the Ins(1,4,5)P_3R. Amino acid residues LKK in the N-terminus of the catalytic α subunit of NKA are essential for binding with the Ins(1,4,5)P_3R N-terminus. This interaction is also supported by the scaffolding protein Ankyrin-B. The ouabain/NKA/Ins(1,4,5)P_3R complex will trigger slow Ca^{2+} oscillations that subsequently activate the NF-κB p65 and leads to protection from apoptosis. ER, endoplasmic reticulum; IP3R, inositol trisphosphate receptor; LKK, lysine-rich motif; PM, plasma membrane; PMCA, plasma membrane Ca^{2+} ATPase; SERCA, sarcoplasmic reticulum Ca^{2+} ATPase; SOC, store-operated channels; VGCC, voltage-gated Ca^{2+} channels.

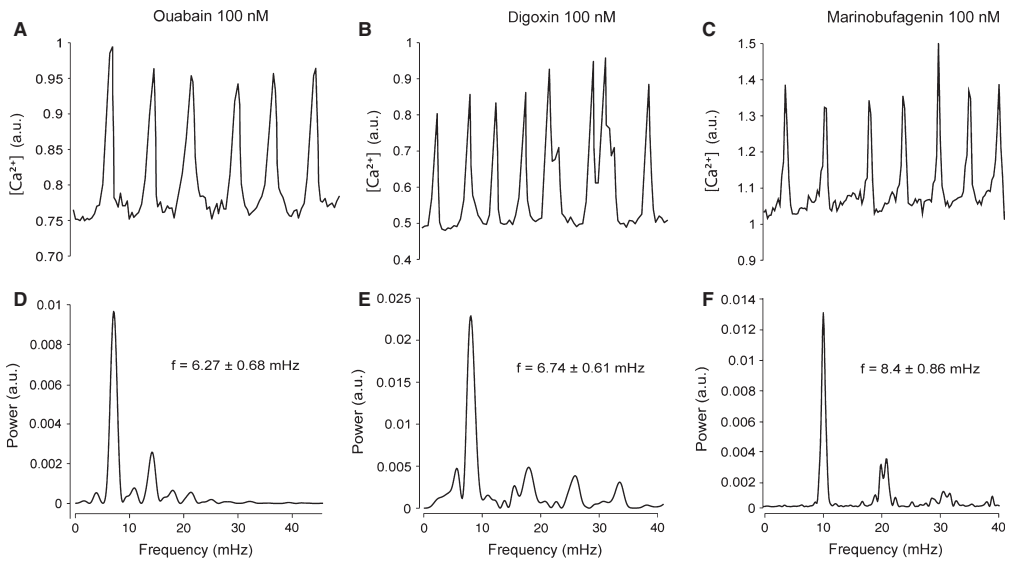

Fig. 2. Effect of ouabain-, digoxin- and marinobufagenin-induced Ca^{2+} oscillations in COS-7 cells. Cells were loaded with Fura-2AM and changes in $[Ca^{2+}]_i$ were recorded as a function of time after treatment with ouabain, digoxin and marinobufagenin. (A–C) Single-cell $[Ca^{2+}]_i$ tracings in response to the indicated ouabain, digoxin and marinobufagenin concentrations. Each plot corresponds to the single-cell recording above. (D–F) Power spectral analysis of the three CTS-evoked Ca^{2+} oscillations depicted in (A–C). For a methodological description see Zhang *et al.* [17]. Marinobufagenin was obtained from A. Y. Bagrov (National Institute of Health, Baltimore, MD, USA).

epidermal growth factor receptor and subsequent activation of signaling pathways downstream of the epidermal growth factor [21,23,24]. It has been suggested by Pierre and Xie that activation of Src may be the initiating event in downstream signaling invoked by interaction of the NKA with CTS [13]. In ongoing studies, we

haver tested whether Src phosphorylation is required for initiation of the CTS-evoked Ca^{2+} signaling pathway, and found that this is likely to be the case.

As shown in Fig. 3(A,D), pretreatment of COS-7 with 4-amino-5-(4-chlorophenyl)-7-(*t*-butyl)pyrazolo [3,4-*d*]pyrimidine (PP2), an inhibitor of Src, significantly reduced the number of cells responding with Ca^{2+} oscillations. We have also tested the effect of inhibitors of signaling molecules that are known to be activated by the epidermal growth factor receptor, but to date have found no evidence for their involvement in the triggering of Ca^{2+} oscillations (Fig. 3B,C).

Downstream effects of calcium oscillations triggered by CTS

Ca^{2+} is the most versatile of all intracellular signals, because the cell can decode the amplitude and duration of the signal [25]. Studies in cell-free systems have indicated that Ca^{2+}-binding proteins, with multiple Ca^{2+}-binding sites, such as CaM kinase II, can decode the frequency of an oscillatory Ca^{2+} signal [26]. Reduction of the frequency of Ca^{2+} oscillations, accomplished by dose-dependent application of an Ins(1,4,5)P_3R inhibitor, has been shown to promote the activation of NF-κB transcriptional activity [27]. Many G_q-coupled receptors, including the metabotropic glutamate receptors, are known to trigger regular Ca^{2+} oscillations that generally have a higher frequency (0.5–1 min) than the Ca^{2+} oscillations triggered by CTS. Studies from our group have shown that the slow Ca^{2+} oscillations triggered by CTS activate the NF-κB survival factor p65 in the nucleus and increase its transcriptional activity [28,29]. p65 is known to control the transcription of the antiapoptotic factor Bcl-xL.

Antiapoptotic effects of ouabain/NKA/Ins(1,4,5)P_3R signaling have been demonstrated in developmental programming of kidneys exposed to malnutrition [30], and in kidneys exposed to Shiga toxin, a well-known cause of apoptosis [29]. Organ development requires a well-controlled balance between proliferation, differentiation and apoptosis. Explant embryonic kidneys were studied with regard to the level of apoptosis and nephron formation, and malnutrition was mimicked by serum starvation. This caused a robust increase in apoptotic rate and retardation of nephron formation. Exposure to 10 nM ouabain during the serum starvation rescued the cell from apoptosis and retarded nephron formation. The effects of ouabain were abolished in the presence of a p65 inhibitor and following depletion of Ca^{2+} stores in the endoplasmic reticulum. Ouabain (10 nM) had no measurable effect on the NKA pumping function. The intracellular sodium concentration was maintained at a constant 5 mM level. *In vivo* studies of nephron endowment in offspring of rats that received low-pro-

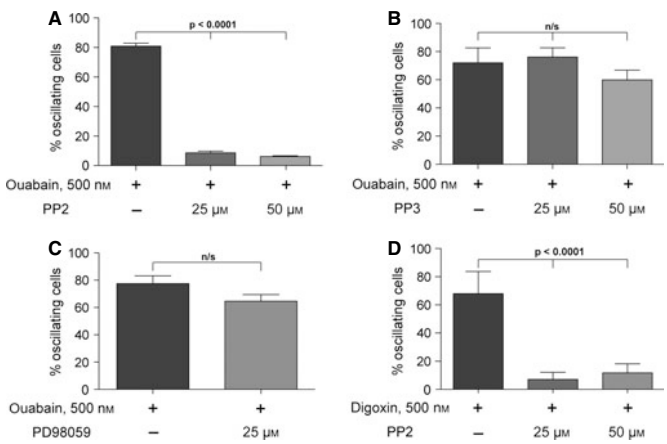

Fig. 3. Effects of one or more kinase inhibitors on ouabain- or digoxin-induced $[Ca^{2+}]_i$ oscillations. Cells were prepared as described in Fig. 2. Data are the mean ± SEM of the percentage of cells oscillating from at least three independent experiments, and the figure shows a representative recording of both the control and cells pretreated with different concentrations (25 and/or 50 μM) of inhibitor. (A) Ouabain-induced Ca^{2+} oscillations are significantly suppressed by the Src kinase inhibitor 4-amino-5-(4-chlorophenyl)-7-(*t*-butyl)pyrazolo[3,4-*d*] pyrimidine (PP2), but not by its inactive equivalent 4-amino-7-phenylpyrazol[3,4-*d*]pyrimidine (B) or the ERK 1/2 inhibitor 2′-amino-3′-methoxyflavone (PD98059) (C). (D) Digoxin-induced Ca^{2+} oscillations are significantly suppressed by PP2.

tein diet during pregnancy and were treated with either vehicle or ouabain confirmed the results from the *in vitro* studies. The metanephric mesenchymal cells that are about to differentiate into primitive nephrons exhibited Ca^{2+} activity that was enhanced by ouabain in both acute and chronic experiments.

Shiga toxin has a well-documented apoptotic effect. Shiga toxin is produced by the strain of *Escherichia coli* that causes hemolytic uremic syndrome. Shiga toxin binds to kidney epithelial cells and neurons and is a major contributor to loss of renal function and cognitive difficulties following the acute disease. Shiga toxin acts on the proapoptotic factor Bax to promote the intrinsic mitochondrial pathway [31]. Ouabain, in concentrations that should have little or no effect on the NKA pumping function in studies on rat primary renal epithelial cells and *in vivo* studies on mice, was shown to protect against Shiga-toxin-triggered apoptosis by upregulating Bcl-xL and downregulating Bax.

The downstream effects of ouabain-triggered Ca^{2+} oscillations cannot be attributed to inhibition of the NKA pumping function [17,28]. In acute experiments, the threshold concentration of ouabain required for triggering Ca^{2+} oscillations gives < 10% inhibition of Rb^+ uptake in COS-7 cells. If cells are exposed to 10–50 nM ouabain for several hours, Ca^{2+} oscillations are observed in ~ 5–30% of COS-7 cells [17]. Ouabain does not induce Ca^{2+} oscillations in cells in which the endoplasmic stores of Ca^{2+} are depleted. Treatment of COS-7 cells for 24 h with 1 nM ouabain activates the NF-κB p65 subunit and gives complete protection from apoptosis induced by serum starvation.

The plant-derived cardenolide digitalis has been used for more than a century to treat cardiac disease, and it seems likely, although is yet not proved, that at least some of the beneficial effects are related to the signaling function and tissue preserving effects of the CTS/NKA signaling. The cardiovascular effects of the CTS in humans are, however, somewhat controversial. Recent studies have drawn attention to the relationship between elevated serum values of the bufadienolide and increased risks of cardiovascular complications in end-stage kidney disease [32,33]. We speculate that the adverse effects of CTS may to some extent be related to Ca^{2+} homeostasis. There are reports indicating that digitalis toxicity is most commonly observed in patients with hypercalcemia [34]. Hypercalcemia related to hyperparathyroidism is a common complication in patients with end-stage kidney disease and an experimental study that showed the adverse cardiovascular effects of high circulating levels of marinobufagenin was performed on rats with severe kidney insufficiency and documented hyperparathyroidism [35].

Summary and perspectives

We have presented evidence for a signaling function of NKA that is activated by CTS and that involves the generation of slow Ca^{2+} oscillations, activation of the NF-κB survival factor p65 and generation of the antiapoptotic factor Bcl-xL, which counteracts the intrinsic mitochondrial apoptotic pathway. Evidence is also presented for a tissue-protective effect of NKA-generated Ca^{2+} oscillations during adverse developmental programming and following exposure to bacterial toxins. Important topics for future studies will be to clarify by which mechanisms Ca^{2+} oscillations activate p65 and to investigate how NKA Ca^{2+} signaling is related to mitochondrial function.

Acknowledgements

This study has been supported by the Swedish Research Council, the Family Erling-Persson Foundation and the Märta and Gunnar V Philipson Foundation.

References

1 Skou JC (1957) The influence of some cations on an adenosine triphosphatase from peripheral nerves. *Biochim Biophys Acta* **23**, 394–401.
2 Albers RW (1967) Biochemical aspects of active transport. *Annu Rev Biochem* **36**, 727–756.
3 Post RL, Hegyvary C & Kume S (1972) Activation by adenosine triphosphate in the phosphorylation kinetics of sodium and potassium ion transport adenosine triphosphatase. *J Biol Chem* **247**, 6530–654.
4 Geering K (2008) Functional roles of Na, K–ATPase subunits. *Curr Opin Nephrol Hypertens* **17**, 526–532.
5 Lingrel JB (2010) The physiological significance of the cardiotonic steroid/ouabain-binding site of the Na, K–ATPase. *Annu Rev Physiol* **72**, 395–412.
6 Schoner W & Scheiner-Bobis G (2007) Endogenous and exogenous cardiac glycosides and their mechanisms of action. *Am J Cardiovasc Drugs* **7**, 173–189.
7 Ogawa H, Shinoda T, Cornelius F & Toyoshima C (2009) Crystal structure of the sodium–potassium pump (Na+, K+–ATPase) with bound potassium and ouabain. *Proc Natl Acad Sci USA* **106**, 13742–13747.
8 Cornelius F, Mahmmoud YA & Toyoshima C (2011) Metal fluoride complexes of Na, K-ATPase: characterization of fluoride-stabilized phosphoenzyme analogues and their interaction with cardiotonic steroids. *J Biol Chem* **26**, 29882–29892.
9 Cornelius F, Kanai R & Toyoshima C (2013) A structural view on the functional importance of the sugar moiety and steroid hydroxyls of cardiotonic steroids in binding to Na, K–ATPase. *J Biol Chem* **288**, 6602–6616.

10 Bagrov AY, Shapiro JI & Fedorova OV (2009) Endogenous cardiotonic steroids: physiology, pharmacology, and novel therapeutic targets. *Pharmacol Rev* **61**, 9–38.
11 Aperia A (2007) New roles for an old enzyme: Na, K–ATPase emerges as an interesting drug target. *J Intern Med* **261**, 44–52.
12 Aperia A (2010) 2011 Homer Smith Award: to serve and protect: classic and novel roles for Na+, K+ -adenosine triphosphatase. *J Am Soc Nephrol* **23**, 1283–1290.
13 Pierre SV & Xie Z (2006) The Na, K–ATPase receptor complex: its organization and membership. *Cell Biochem Biophys* **46**, 303–316.
14 Li Z & Xie Z (2009) The Na/K-ATPase/Src complex and cardiotonic steroid-activated protein kinase cascades. *Pflugers Arch* **457**, 635–644.
15 Aizman O, Uhlén P, Lal M, Brismar H & Aperia A (2001) Ouabain, a steroid hormone that signals with slow calcium oscillations. *Proc Natl Acad Sci USA* **98**, 13420–13424.
16 Miyakawa-Naito A, Uhlén P, Lal M, Aizman O, Mikoshiba K, Brismar H, Zelenin S & Aperia A (2003) Cell signaling microdomain with Na, K–ATPase and inositol 1,4,5–trisphosphate receptor generates calcium oscillations. *J Biol Chem* **278**, 50355–50361.
17 Zhang S, Malmersjö S, Li J, Ando H, Aizman O, Uhlén P, Mikoshiba K & Aperia A (2006) Distinct role of the N–terminal tail of the Na, K–ATPase catalytic subunit as a signal transducer. *J Biol Chem* **281**, 21954–21962.
18 Liu X, Spicarová Z, Rydholm S, Li J, Brismar H & Aperia A (2008) Ankyrin B modulates the function of Na, K–ATPase/inositol 1,4,5–trisphosphate receptor signaling microdomain. *J Biol Chem* **283**, 11461–11468.
19 Kometiani P, Li J, Gnudi L, Kahn BB, Askari A & Xie Z (1998) Multiple signal transduction pathways link Na^+/K^+-ATPase to growth-related genes in cardiac myocytes. The roles of Ras and mitogen-activated protein kinases. *J Biol Chem* **273**, 15249–15256.
20 Haas M, Askari A & Xie Z (2000) Involvement of Src and epidermal growth factor receptor in the signal-transducing function of Na^+/K^+-ATPase. *J Biol Chem* **275**, 27832–27837.
21 Kotova O, Al-Khalili L, Talia S, Hooke C, Fedorova OV, Bagrov AY & Chibalin AV (2006) Cardiotonic steroids stimulate glycogen synthesis in human skeletal muscle cells via a Src- and ERK1/2-dependent mechanism. *J Biol Chem* **281**, 20085–20094.
22 Tian J, Cai T, Yuan Z, Wang H, Liu L, Haas M, Maksimova E, Huang XY & Xie ZJ (2006) Binding of Src to Na^+/K^+-ATPase forms a functional signaling complex. *Mol Biol Cell* **17**, 317–326.
23 Aydemir-Koksoy A, Abramowitz J & Allen JC (2001) Ouabain-induced signaling and vascular smooth muscle cell proliferation. *J Biol Chem* **276**, 46605–46611.
24 Haas M, Wang H, Tian J & Xie Z (2002) Src-mediated inter-receptor cross-talk between the Na^+/K^+-ATPase and the epidermal growth factor receptor relays the signal from ouabain to mitogen-activated protein kinases. *J Biol Chem* **277**, 18694–18702.
25 Berridge MJ, Lipp P & Bootman MD (2000) The versatility and universality of calcium signalling. *Nat Rev Mol Cell Biol* **1**, 11–21.
26 De Koninck P & Schulman H (1998) Sensitivity of CaM kinase II to the frequency of Ca^{2+} oscillations. *Science* **279**, 227–230.
27 Hu Q, Deshpande S, Irani K & Ziegelstein RC (1999) [Ca(2+)](i) oscillation frequency regulates agonist-stimulated NF-kappaB transcriptional activity. *J Biol Chem* **274**, 33995–33998.
28 Li J, Zelenin S, Aperia A & Aizman O (2006) Low doses of ouabain protect from serum deprivation-triggered apoptosis and stimulate kidney cell proliferation via activation of NF-kappaB. *J Am Soc Nephrol* **17**, 1848–1857.
29 Burlaka I, Liu XL, Rebetz J, Arvidsson I, Yang L, Brismar H, Karpman D & Aperia A (2013) Ouabain protects against Shiga toxin-triggered apoptosis by reversing the imbalance between Bax and Bcl-xL. *J Am Soc Nephrol*. Epub ahead of print.
30 Li J, Khodus GR, Kruusmägi M, Kamali-Zare P, Liu XL, Eklöf AC, Zelenin S, Brismar H & Aperia A (2010) Ouabain protects against adverse developmental programming of the kidney. *Nat Commun*, doi:10.1038/ncomms1043.
31 Tironi-Farinati C, Fabián Loidl C, Boccoli J, Parma Y, Fernandez-Miyakawa ME & Goldstein J (2010) Intracerebroventricular Shiga toxin 2 increases the expression of its receptor globotriaosylceramide and causes dendritic abnormalities. *J Neuroimmunol* **222**, 48–61.
32 Puschett JB, Agunanne E & Uddin MN (2010) Emerging role of the bufadienolides in cardiovascular and kidney diseases. *Am J Kidney Dis* **56**, 359–370.
33 Tian J, Haller S, Periyasamy S, Brewster P, Zhang H, Adlakha S, Fedorova OV, Xie ZJ, Bagrov AY, Shapiro JI, *et al.* (2010) Renal ischemia regulates marinobufagenin release in humans. *Hypertension* **56**, 914–919.
34 Vella A, Gerber TC, Hayes DL & Reeder GS (1999) Digoxin, hypercalcaemia, and cardiac conduction. *Postgrad Med J* **75**, 554–556.
35 Kennedy DJ, Vetteth S, Periyasamy SM, Kanj M, Fedorova L, Khouri S, Kahaleh MB, Xie Z, Malhotra D, Kolodkin NI, *et al.* (2006) Central role for the cardiotonic steroid marinobufagenin in the pathogenesis of experimental uremic cardiomyopathy. *Hypertension* **47**, 488–495.

III

Ouabain halts progression of chronic kidney disease by inhibition of albumin-triggered apoptosis

Ievgeniia Burlaka[1], Ulla Holtbäck[1], Ann-Christine Eklof[1], Agnes B. Fogo[2], Hjalmar Brismar[1,3], Anita Aperia[1]

[1]Science for Life Laboratory, Department of Women's and Children's Health, Karolinska Institutet, Solna, Sweden

[2]Department of Pathology, Microbiology and Immunology, Vanderbilt University Medical Center, Nashville, TN 37232 USA

[3]Science for Life Laboratory, Department of Applied Physics, Royal Institute of Technology, Stockholm, Sweden

Abstract

Increased albumin in primary urine leads to apoptosis and fibrosis of podocytes and tubule cells and is a main cause of functional deterioration in chronic kidney disease. Here we show that excessive albumin uptake into rat primary renal cells causes an almost immediate down-regulation of the anti-apoptotic factor Bcl-xL, accompanied by mitochondrial accumulation of the apoptotic factor Bax and mitochondrial membrane depolarization. A calcium signaling pathway, activated by ouabain, opposes these effects and protects albumin-exposed proximal tubule cells and podocytes from apoptosis but does not result in the up-regulation of Bcl-xL or re-location of Bax in control cells. The efficacy of ouabain as an anti-apoptotic and kidney-protective drug is tested in a rat model of proteinuric disease. Chronic ouabain treatment of rats preserves renal function and results in less apoptosis, a lower incidence of glomerular-tubular disconnections and more remaining podocytes than that observed in untreated rats. Thus, we have identified a novel clinically feasible approach to prevent apoptosis.

Introduction

Chronic kidney disease (CKD) is a rapidly increasing world-wide public health problem. CKD results from a variety of causes, including diabetes, glomerulonephritis, hypoxia, hypertension, infections and polycystic kidney disease[1]. Most forms of CKD are progressive[1,2] and are characterized by disrupted glomerular perm-selectivity[3], glomerular sclerosis, albuminuria, loss of podocytes and glomerular tubular disconnection[4,5]. Albuminuria, which is a well-documented predictor of the progressive loss of kidney function, is also considered to be a cause of structural kidney damage and loss of function[6,7]. The nature of albumin toxicity has been extensively studied in the past decade, and it is now well recognized that prolonged exposure of renal tubular cells to albumin results in both apoptosis and fibrosis[8-10]. The interrelationship between apoptosis and fibrosis is not yet fully understood.

There are several ongoing trials aimed at halting the progression of CKD using drugs that are targeted to inhibit pro-fibrotic and/or stimulate anti-fibrotic molecular pathways[11-14.] However, there have been few attempts to use drugs that target the apoptotic process, primarily because of the lack of non-toxic inhibitors of apoptosis. Recently, our group characterized and tested an anti-apoptotic signal that is triggered by the cardiotonic steroid ouabain[15-17]. The signaling pathway involves an interaction between Na, K-ATPase and the inositol 1,4,5-triphosphate receptor (IP3R), triggering slow intracellular calcium oscillations and the activation of the NF-κB p65 subunit, a transcriptional activator of Bcl-xL. Bcl-xL is an anti-apoptotic member of the Bcl2 family of proteins, which are involved in the control of the intrinsic mitochondrial apoptotic pathway. We have shown that ouabain may provide protection against apoptosis in fetal rat kidneys exposed to malnutrition[18] and in mouse kidneys exposed to Shiga toxin[19].

The activation of the intrinsic mitochondrial apoptotic pathway is initiated by the accumulation of Bax, a pro-apoptotic member of the Bcl2 family, in the outer mitochondrial membrane, where it oligomerizes and penetrates the inner mitochondrial membrane[20]. This results in the release of cytochrome C into the cytosol and activation of caspases, the apoptotic executors. Of particular importance is caspase 3, which plays a key role in DNA fragmentation. Bcl-xL exerts its anti-apoptotic effect by inhibiting binding of Bax to the membrane. Here we report the time sequence for mitochondrial Bax accumulation, depolarization of the mitochondrial membrane and changes in Bcl-xL expression following albumin uptake into rat primary proximal tubule cells (RPTC). The studies, which were performed in the presence and absence of 5 nM ouabain, demonstrate that albumin uptake into the cell almost immediately triggers the mitochondrial apoptotic pathway and that ouabain inhibits apoptosis by counteracting the down-regulation of Bcl-

xL expression and mitochondrial accumulation of Bax. The onset of apoptosis precedes the appearance of the precursor to TGF-beta 1, a pro-fibrotic factor typically expressed in injured renal epithelial cells.

To determine the therapeutic value of ouabain in proteinuric CKD, we used a well-established rat model of human proteinuric disease[21], passive Heymann nephritis (PHN). PHN rats were treated with ouabain or vehicle for 16 weeks. The results from a series of morphometric studies regarding podocyte and proximal tubule apoptosis, glomerular tubular disconnection and secondary fibrosis uniformly demonstrated the protective effect of ouabain.

Results

Albumin uptake into proximal tubular cells triggers apoptosis followed by increased expression of TGF-beta 1

It is well documented that excessive uptake of albumin into RPTC can trigger apoptosis[22,23] and the generation of pro-fibrotic factors, such as TGF-beta[24,25]. To determine the order in which these processes are initiated, we incubated primary RPTC with albumin (10 mg/mL) for 2, 4 and 8 hours and determined the apoptosis index (AI) with TUNEL staining and assessed the expression of the pro-fibrotic TGF-β 1 precursor by Western blotting **(Figure 1A, B)**. A significant, greater than 2-fold increase in the AI was observed after incubation with albumin for 2 hours, followed by additional increases after 4 and 8 hours of albumin incubation. In contrast, the expression of the TGF-beta precursor was not significantly increased until 8 hours of incubation with albumin **(Figure 1D)**.

We next studied the capacity of ouabain to rescue from albumin-triggered apoptosis in RPTC exposed to varying concentrations of albumin (5, 10 or 20 mg/mL) for 8 or 18 hours (**Figure 1E**). The apoptotic effect of albumin was time- and dose-dependent. The co-incubation of ouabain with any of the tested concentrations of albumin resulted in a reduction of the AI at both time points (**Figure 1H,I**). TGF-beta expression in cells exposed to albumin for 8 or 18 h was also significantly attenuated when the cells were co-incubated with ouabain.(**Figure 1F,G,J,K**).

Albumin also triggers apoptosis of primary rat podocytes in a time- and dose-dependent manner (**Supplementary Figure 1)**. The podocytes actually appear to be more sensitive to the apoptotic effect of albumin than proximal tubule cells. The rescuing effect of ouabain is similar in podocytes and RPTC**.**

Albumin initiates but ouabin inhibits the intrinsic apoptotic pathway.

The intrinsic apoptotic pathway is initiated by the activation and recruitment of Bax to the outer mitochondrial membrane[20,29], leading to membrane depolarization, mitochondrial damage, release of cleaved caspase-3 and initiation of the apoptotic process[29,30]. Bcl-xL prevents apoptosis by blocking the translocation of Bax from the cytosol to the mitochondria. In primary RPTC exposed to albumin (10 mg/ml) for 8 or 18 hours, immunoblotting studies revealed a decreased abundance of Bcl-xL and increased abundance of Bax. The amount of cleaved caspase-3 was also increased, indicating an ongoing apoptotic process. Ouabain up-regulated Bcl-xL and down-regulated Bax in albumin-exposed cells but had no such effect in control cells. The level of cleaved caspase 3 was significantly reduced in albumin-exposed cells co-treated with ouabain (**Figure 3**). The ouabain signaling pathway includes the activation of the 1,4,5-triphosphate receptor, release of calcium from intracellular stores and activation of the NF-κB p65 subunit[26,27] (**Supplementary Figure 2**). When these studies were repeated in cells in which intracellular stores of calcium had been depleted by inhibition of the SERCA pump with cyclopiazonic acid (CPA) or cells co-incubated with helenalin, a specific NF-κB p65 subunit inhibitor, the anti-apoptotic effect of ouabain was abolished (**Supplementary Figure 3,4**). Incubation with ouabain did not affect Bax and Bcl-xL levels in control cells, nor did it protect against LPS-triggered cytokine release (**Figure 3**).

To further characterize mitochondrial involvement in albumin toxicity, we performed time sequence studies, monitoring Bcl-xL abundance, Bax and mitochondria co-localization and mitochondrial membrane potential in albumin-exposed rat proximal tubule. Two concentrations of albumin were used, 2.5 mg/mL (the expected albumin concentration in primary filtrate in many cases of CKD) and 10 mg/mL. The observed pattern of changes was similar for both concentrations of albumin, but the effects were more pronounced and appeared earlier in cells exposed to 10 mg/mL albumin. The amount of Bcl-xL decreased in a time- and dose-dependent manner in albumin-exposed RPTC. Those changes were significant after 1 hour incubation with 10 mg/mL albumin and after 2 hours incubation with 2.5 mg/mL albumin (**Figure 2A,B,C**). The co-localization of immunolabeled Bax and mitochondria expressing GFP was analyzed in confocal micrographs (**Figure 2D,E,F**). Two perpendicular line traces across the nucleus were drawn for each cell. Using these line traces, the co-localization of mitochondria and Bax signals was analyzed. The weakest peaks, representing background fluctuations, were ignored. The peaks that were separated by no more than 140 nm were considered to be co-localized (**Figure 2G,H**). Co-localization increased in a time-dependent manner, and the increase was significant after 1 hour

incubation with 10 mg/mL albumin and after 2 hours incubation with 2.5 mg/mL albumin. Albumin exposure also caused a dose- and time dependent depolarization of the mitochondrial membrane (**Figure 2I,J,K**). Albumin exposure had no effect on the co-localization of Bcl-xL and the mitochondria (**Figure 2N**). Ouabain significantly attenuated the down-regulation of Bcl-xl, mitochondrial accumulation of Bax and depolarization of the mitochondrial membrane in the albumin-exposed cells (**Figure 2L,M**).

To identify the earliest time points for albumin-triggered mitochondrial dysfunction and onset of the apoptotic pathway, the study was repeated incubating cells with 10 mg/mL albumin for 5, 15, 30 and 45 min. Albumin was found in the RPTC at 15 min, and there was a significant mitochondrial depolarization and Bax accumulation detected after incubation with albumin for 45 min (**Supplementary Figure 5**).

Long-term treatment with ouabain attenuated apoptosis and tissue damage in a rat model of CKD associated with proteinuria

To study the nephro-protective effect of ouabain in an animal model, PHN, a well-documented model of membranous nephropathy with proteinuria[21,31], was induced in male rats by injection of an anti-Fx1A antibody. PHN and control rats were followed for four months before sacrifice. The PHN rats were divided into two groups, one group receiving ouabain (15 µg/kg/day) and one receiving vehicle via subcutaneous mini-pumps. Long-term treatment with this concentration of ouabain does not affect arterial blood pressure (**Supplementary Figure 6**). All of the animals survived the study. Significant albuminuria appeared two weeks after disease induction and was present throughout the observation period. The mean value of albuminuria was slightly lower in ouabain-treated PHN rats than in vehicle-treated PHN rats from the 4th week of observation until the end of the study (**Figure 4A**).

Podocytes[28,32] and proximal tubular cells at the glomerular-tubular junction[33] are considered the main targets for albumin toxicity. The AI in vehicle-treated PHN rats was 10-fold higher than in control rats. This increase in AI was much less pronounced in ouabain-treated PHN rats. The AI of the proximal tubular cells at the level of the glomerular-tubular junction was 3-fold higher in kidneys from vehicle-treated PHN rats than in kidneys from ouabain-treated PHN rats (**Figure 4C,G**).

Kidneys from adult rats have a certain regenerative capacity, which may be preserved in CKD[34,35]. We used two markers to identify proliferating cells, Ki-67 and PCNA. Kidneys from vehicle-treated PHN rats displayed approximately 5-fold more proliferating cells than kidneys from

control rats; the difference was statistically significant. The number of proliferating cells was significantly lower in kidneys from ouabain-treated PHN rats than in kidneys from vehicle-treated PHN rats (**Figure 4E,F,I,J**). Fibrosis is a typical feature of CKD[8,9]. Renal cortical expression of TGF-beta1 was detected in all groups. Semi-quantitative evaluation of the TGF-beta1 signal was performed on a sagittal plane from each kidney, and in each section, three areas corresponding to 75% of the cortex were analyzed (**Figure 5B**). In kidneys from vehicle-treated PHN rats, the TGF-beta1 signal was 53% greater than in kidneys from control rats, whereas no significant TGF-beta1 up-regulation was observed in kidneys from ouabain-treated PHN rats compared with kidneys from control rats (**Figure 5B,D**).

Damage of the glomerular basement membrane (GBM) was found in both vehicle- and ouabain-treated PHN rats. Jones silver staining showed a "spiked" appearance of the GBM, indicating the presence of sub-epithelial deposits (**Figure 4B**). Collagen IV accumulation, another sign of glomerular damage, was significantly increased to a greater extent in kidneys from vehicle-treated PHN rats than in kidneys from ouabain-treated PHN rats (**Figure 5C,D**).

Glomerular-tubular disconnection and loss of podocytes are indicators of permanent renal damage[33,36]. The extent of ongoing and existing glomerular-tubular disconnections was evaluated with morphometric analysis. Atubular glomeruli and glomeruli connected to atrophic tubuli were both significantly more common in vehicle-treated PHN rats than in ouabain-treated PHN rats.

Podocytes are readily identifiable in the glomeruli by nuclear staining for the cell-specific transcriptional factor WT-1 (**Figure 6C**). There was a 53% reduction of WT-1-positive cells/glomerulus in vehicle-treated PHN rats compared with control rats. Significantly more podocytes were preserved in the ouabain-treated group. Serum creatinine levels, another end-point in this study, were significantly lower in ouabain-treated PHN rats than in vehicle-treated PHN rats (**Figure 6D**).

Discussion

This study demonstrates that the primary event in albumin-induced injury to renal epithelial cells is the down-regulation of Bcl-xL accompanied by mitochondrial accumulation of Bax and the activation of the intrinsic mitochondrial apoptotic pathway. Ouabain-induced up-regulation of Bcl-xL counteracts the interaction between Bax and mitochondria and protects cells from albumin-triggered apoptosis. The in vivo studies provide proof that albumin toxicity is driven by apoptosis and show that ouabain provides long-term protection of renal tissue in proteinuria CKD.

The relationship between the two cardinal pro- and anti-apoptotic members of the Bcl2

family of proteins, Bax and Bcl-xL, plays a crucial role in determining the balance between cell life and death. Bcl-xL is reported to block the apoptotic effects of Bax by preventing its translocation to the mitochondria[29,37,38]. We demonstrated that excessive cellular uptake of albumin almost immediately alters the relationship between Bcl-xL and Bax. Cellular uptake of albumin causes rapid down-regulation of Bcl-xL[20] and accumulation of Bax around the mitochondria, resulting in the disabling of the mitochondrial membrane and initiation of the apoptotic process[20,37]. Ouabain protects cells from apoptosis by up-regulating Bcl-xL and preventing mitochondrial accumulation of Bax. There is little evidence that up-regulation of Bax exerts a negative feedback effect on Bcl-xL. Down-regulation of Bcl-xL is therefore most likely the initial cellular response to excessive albumin uptake. The ouabain signaling pathway includes the activation of the NF-kB subunit p65, a transcriptional activator of Bcl-xL. In the current study, p65 inhibition abolished the anti-apoptotic effect of ouabain.

The in vivo results are compatible with the notion that the pathological processes in chronic kidney disease associated with proteinuria are initiated and driven by apoptosis. An increased apoptotic index was found in both proximal tubule cells and podocytes and is likely the main cause of the loss of podocytes and of glomerular tubular disconnection observed at the end of the follow-up time. The occurrence of Ki-67-labeled and PCNA-labeled cells confirmed that there is an ongoing regeneration of tubular cells paralleling but not sufficiently substituting for the apoptotic process. This finding is consistent with what has been described after renal ischemic injury[34,35] and in response to proteinuria following diphtheria toxin-mediated podocyte ablation[39].

The apoptotic process is accompanied by fibrosis[25,41,42]. High levels of apoptosis are often observed in all types of fibrosis, including kidney, liver and lung fibrosis. The interrelationship between apoptosis and fibrosis remains to be clarified, but there is now evidence from studies performed on impaired lung and liver tissue that apoptotic cells may promote fibrotic outcomes either by direct stimulation of pro-fibrotic factors or by secretion of pro-fibrotic factors from macrophages following the engulfment of apoptotic cells[40-42]. Conversely, the pro-fibrotic factor TGF-beta 1 may activate apoptosis, either via intrinsic mitochondrial pathways or via extrinsic pathways[42]. In kidneys from PHN rats treated with ouabain, both apoptosis and fibrosis were less pronounced. This observation supports the idea that albumin toxicity in chronic kidney disease is driven by apoptosis because in in vitro studies, ouabain does not primarily protect from inflammatory reactions.

The results from this study have identified a potential new avenue by which the progression of chronic kidney disease might be halted. Ouabain belongs to the same family of cardiotonic

steroids as the plant-derived digitalis, which has been used extensively to treat cardiac insufficiency. Treatment of cardiac insufficiency with the plant-derived cardiotonic steroid digoxin has been associated with relatively few side effects, except in patients with hypercalcaemia[43]. Other cardiotonic steroids, such as digoxin, trigger a calcium signal with similar characteristics as ouabain[44] and might be as efficient as ouabain in protecting cells from apoptosis in CKD. There is a great need for safe and efficient anti-apoptotic drugs for use in the treatment of many common and devastating conditions, including neurodegenerative diseases. Despite an intensive search for such drugs, to date, no anti-apoptotic drugs have reached the market. Many attempts have been made to target caspases, but since their activation occurs late in the chain of events leading to apoptosis, they can only act to delay cell death, not prevent it. The many side effects of caspase inhibitors observed in early trials have also precluded the clinical use of these drugs. In contrast to caspase inhibitors, ouabain interferes with the onset of the apoptotic process, and there is presently no evidence for an effect of ouabain in cells where anti-apoptotic and apoptotic factors are in balance.

Concise materials and methods

Animals

Forty-day-old Male Sprague-Dawley rats with initial body weights of 100 to 120 g were used in this study. The animal care and treatment were conducted in accordance with the institutional guidelines that are in compliance with national and international laws and policies (EEC Council Directive 86/609, OJL358-1, December 1987; Guide for the Care and Use of Laboratory Animals, U.S. National Research Council, 1996).

Experimental Design

All of the animals were housed at a constant temperature with a 12-hour dark/12-hour light cycle and allowed free access to standard diet containing 20% protein by weight and tap water. The animals were divided into three groups: a control group (n =8), untreated PHN rats followed for 4 months after PHN induction (n=8), and rats treated with ouabain (15 μg/mL) or vehicle (PBS) delivered by subcutaneous mini-pumps from day 0 after PHN induction (n =7). PHN was induced in non-anesthetized rats by a single intravenous injection of 0.66 mg/100 g body wt of rabbit anti-Fx1A antibody. Albuminuria was measured every second week. At sacrifice, the kidneys were removed from anesthetized animals for histological and morphological studies and serum creatinine levels were measured.

Cells

RPTC were prepared from kidneys of 20-day-old male Sprague-Dawley rats as described previously[45]. The studies performed in Sweden followed the Karolinska Institutet regulations concerning care and use of laboratory animals and were approved by the Stockholm North ethical evaluation board for animal research. The kidneys were removed and placed in 0.9% NaCl at room temperature. The cortical layers were dissected and placed in Hank's balanced salt (Invitrogen, Grand Island, USA) solution at 37°C and gently mixed using a fire-polished Pasteur pipette. The reaction was stopped by washing the cells twice in a solution containing 1% trypsin inhibitor. After washing, equal volumes of cell suspension were plated on 12-mm glass coverslips in 24-well Petri dishes. The cells were cultured for 3 days in supplemented DMEM (20 mM HEPES, 24 mM $NaHCO_3$, 10 µg/ml penicillin, 10 µg/ml streptomycin, and 10% FBS) on glass coverslips in 5% CO_2 at 37°C. On day two in vitro, when the cells have been shown to maintain most of their proximal tubule characteristics,[45,46] the cells were exposed to the 0, 5, 10, or 20 mg/mL of fatty acid and endotoxin-free bovine albumin alone (Sigma-Aldrich, St.Louis, USA), with ouabain (Sigma-Aldrich, St.Louis, USA) or with vehicle (PBS) for 8 or 18 h.

Glomeruli Isolation

The rats were anesthetized by intraperitoneal injection of pentobarbital and perfused with $8x10^7$ Dynabeads M-450 (Dynal Biotech ASA, Oslo, Norway) diluted in 20 ml of Hank's balanced salt solution (Invitrogen, Grand Island, USA) through the left ventricle. After perfusion, the kidneys were removed, cut into 1 mm^3 pieces and digested in collagenase A and DNAse at 37°C for 30 min with gentle shaking. After digestion, the tissue was pressed gently through a 100-µm cell strainer (BD Falcon, Bedford, MA). Glomeruli that contained Dynabeads then were collected using a magnetic particle concentrator. The isolated glomeruli were washed three times with cold Hank's balanced salt solution and used for subsequent studies.

Analyticals

The urine albumin concentrations were determined using a commercially available kit specific for rat urine albumin (Nephrat; Exocell, Philadelphia). and an automated spectrophotometer. The urine samples were collected in the morning at the same time intervals after induction of PHN throughout the experiment. Blood was collected from the left ventricle of anesthetized animals. Serum was obtained after whole blood clotting. Serum creatinine

concentrations were determined using a quantitative colorimetric creatinine determination assay and an automated spectrophotometer.

Bax translocation assessment

RPTC were cultured as described previously. On day two in vitro, when they have been shown to maintain most of their proximal tubule characteristics[44,45], the cells were exposed to the mitochondria-targeted green fluorescent protein CellLight® Mitochondria-GFP BacMam (Life Technologies, Grand Island, USA) overnight in the incubator. On day three in vitro, RPTC were incubated with 0, 2.5 or 10 mg/mL of albumin with or without ouabain (5 nM) or vehicle (PBS) for 0-8 h. In another set of experiments, the cells were treated with 10 mg/mL albumin for 0, 15, 30 or 45 min. For Bax immunostaining, the cells were fixed in 4% PFA, washed once with cold PBS and treated with Triton X-100 (Sigma-Aldrich NV/SA, Bornem, Belgium). The mouse monoclonal anti-Bax [6A7] Ab primary antibodies (Abcam, Cambridge, UK) were applied overnight at 4 ºC. The controls were subjected to the same treatment, but the primary antibody was omitted. The secondary Alexa Fluor 546 goat anti-mouse IgG IgG (Invitrogen, Grand Island, NY, USA) was applied for 1 h at room temperature. The cells were mounted and observed using a Zeiss LSM 510 laser scanning confocal microscope and a 63X/1.4NA oil objective. Analysis of the Bax translocation to the mitochondria was performed with the Matlab image processing toolbox.

For Bcl-xL immunostaining, the cells were labeled with rabbit anti-human polyclonal Bcl-xL antibody (Cell Signaling Technology, Inc. Danvers, USA) and anti-rabbit IgG-Alexa 546 secondary antibody. The immune-labeled cells were observed with a Zeiss LSM 510 laser scanning confocal microscope and a 63X/1.4NA oil-immersion objective. Alexa Fluor 546 stain was detected using 561 nm excitation and a 575 nm long pass filter. The analysis of the Bcl-xL translocation to the mitochondria was performed with the Matlab image processing toolbox.

Mitochondrial Membrane Potential Determination

RPTC were exposed to 0, 2.5, or 10 mg/mL of albumin alone, with ouabain (5 nM) or with vehicle (PBS) for 0-8 h. In another set of experiments, RPTC were treated with 10 mg/mL albumin for 0, 15, 30, and 45 min. The integrity of the mitochondrial membrane potential was measured by JC-1 dye (5,5',6,6'-tetrachloro-1,1',3,3'-tetraethylbenzimidazolylcarbocyanine iodide) (Life Technologies, Grand Island, USA), a cationic dye that exhibits potential-dependent accumulation in mitochondria as demonstrated by a fluorescence emission shift from green (527nm) to red (590 nm). After incubation with albumin, the cells were washed and incubated with 2.5 μg/ml JC-1 dye

in cultured medium for 15 min at 37°C. The cells were then subjected to live cell imaging. The mitochondrial membrane potential change was quantified by calculating the ratio of red (polarized) to green (depolarized) pixels using ImageJ software (NIH Image, Baltimore, USA).

Detection of apoptotic cells: Terminal Deoxynucleotidyl (TdT)-Mediated dUTP Nick-End Labeling (TUNEL) assay

An ApopTag Red In Situ Apoptosis Detection kit (Chemicon International, USA) was used to determine the AI, according to the manufacturer's instructions. The nuclei were counterstained with 4',6-diamidino-2-phenylindole (DAPI) (Santa Cruz Biotechnology, Inc., California, USA). The cells were mounted in Immu-Mount (Thermo Shandon, Midland, Canada), and the images were recorded with a Zeiss LSM 510 laser scanning confocal microscope using a 25X/0.8NA oil-immersion objective. TUNEL stain was detected using 488 nm excitation and a 510-550 nm band-pass filter. ApopTag was detected using 561nm excitation and a 575 nm long pass filter, and DAPI was detected using 405 nm excitation and a 420-480 nm band-pass filter. Cells were considered apoptotic when they exhibited ApopTag Red staining and characteristic apoptotic morphology. The AI was calculated as the percentage of TUNEL-positive cells. The total number of cells was determined by DAPI stain. In each preparation, eight to ten randomly selected areas were examined, and in each area, between 100 and 200 DAPI-stained cells were counted.

In vitro Albumin Overload Protocol

RPTC and podocytes in primary culture were plated on 12-mm glass coverslips in 24-well cell culture plates and incubated in medium with delipidated, endotoxin-free albumin at concentrations of 0, 1, 5 or 10 mg/ml for 0-18 h.

Albumin internalization Protocol in vitro

Briefly, RPTC were incubated in medium with 2.5 mg/ml delipidated, endotoxin-free albumin with trace of Alexa-555-labeled albumin (Life Technologies, Grand Island, USA) for 0-8 h. In another set of experiments, cells were treated with 10 mg/mL albumin for 0, 15, 30 or 45 min. The cells were subjected to live cell imaging.

Renal Histology

The removed kidneys were fixed for 6 hours in Dubosq-Brazil, dehydrated in alcohol and embedded in paraffin. Sections of renal tissue (3 μm) were stained with periodic acid-Schiff

reagent. Sections including superficial and juxtamedullar glomeruli were evaluated. Tubulo-interstitial changes (fibrosis and inflammation) were evaluated. At least 10 randomly selected areas were examined for each slice.

Immunohistochemical Staining

For WT1 immunostaining, RPTC and podocytes in primary culture were fixed in 4% PFA, washed once with cold PBS and treated with Triton X-100 (Sigma-Aldrich NV/SA, Bornem, Belgium). After three washes with PBS, the sections were incubated with blocking buffer for 1 hour. The rabbit polyclonal anti-WT1 primary antibodies (Santa Cruz, USA) were applied overnight at 4 ^{o}C. The controls were subjected to the same treatment, but the primary antibody was omitted. The sections were incubated with a secondary Alexa Fluor 488 goat anti-rabbit IgG (Invitrogen, Grand Island, USA) for 1 h at room temperature. The nuclei were counterstained with DAPI (Santa Cruz Biotechnology, Inc., California, USA). The cells were mounted and observed with a Zeiss LSM 510 laser scanning confocal microscope using a 25X/0.8NA oil-immersion and 40 X/1.2NA water objectives. Alexa Fluor 488 stain was detected using 488 nm excitation and a 510-550 nm band-pass filter.

NF-κB p65 subunit translocation to the nucleus was used as an index of NF-κB p65 subunit activation. NF-κB immunostaining was performed as described previously. Briefly, the cells were labeled with rabbit anti-human polyclonal NF-κB p65 antibody (Santa Cruz Biotechnology, Santa Cruz, USA) and subsequently with anti-rabbit IgG-Alexa 546 secondary antibody. The nuclei were counterstained with DAPI (Santa Cruz Biotechnology, Inc., California, USA). The immune-labeled cells were observed with a Zeiss LSM 510 laser scanning confocal microscope using a 40X/1.2NA water-immersion objective. The Alexa Fluor 546 stain was detected using 561 nm excitation and a 575 nm long pass filter. The immunosignals in the nucleus and the cytosol were measured using ImageJ software (NIH Image, Baltimore, USA)., and the ratio was determined. An area corresponding to 90% of nucleus and an identically sized area of the cytoplasm were used to measure the intensity of the immunosignal.

For Bcl-xL immunostaining, the cells were labeled with rabbit anti-human polyclonal Bcl-xL antibody (Cell Signaling Technology, Inc. Danvers, USA) and subsequently labeled with anti-rabbit IgG-Alexa 546 secondary antibody. The immune-labeled cells were observed using a Zeiss LSM 510 laser scanning confocal microscope and a 63X/1.4NA oil-immersion objective. The Alexa Fluor 546 stain was detected using 561 nm excitation and a 575 nm long pass filter. The intensity of the immunosignal was measured using ImageJ software (NIH Image, Baltimore, MD, USA).

The 3-μm thick kidney sections were prepared using a routine procedure. The renal tissue was deparaffinized and rehydrated prior to processing. Antigen retrieval was performed by boiling in citrate buffer for 20 min. The sections were then treated with Triton X-100 (Sigma-Aldrich NV/SA, Bornem, Belgium). After three washes with PBS, the sections were incubated with blocking buffer for 1 hour. The rabbit polyclonal and mouse monoclonal anti-WT1 (Santa Cruz, USA), mouse monoclonal anti-PCNA Ab primary antibodies (Santa Cruz, USA), goat polyclonal anti-Ki-67 Ab primary antibodies (Santa Cruz, USA), and rabbit polyclonal anti-TGF-beta1 Ab (Novus Biologicals, USA) were applied overnight at 4 ºC. The controls were subjected to the same treatments, but the primary antibody was omitted. Following three PBS washes, the sections were incubated with a secondary Alexa Fluor 488 goat anti-rabbit IgG (Invitrogen, Grand Island, USA), Alexa Fluor 546 goat anti-mouse IgG (Invitrogen, Grand Island, USA), or Alexa Fluor 546 rabbit anti-goat IgG (Invitrogen, Grand Island, USA), for 1 h at room temperature. The nuclei were counterstained with DAPI (Santa Cruz Biotechnology, Inc., California, USA). All of the samples were stained for the same length of time under identical conditions, and the staining was assessed on a single day using identical gain settings. The immune-labeled WT1 cells were observed with a Zeiss LSM 510 laser scanning confocal microscope and a 40X/1.2NA water-immersion objective. For the podocytes, WT-1–positive cells were counted in at least 10 randomly chosen glomeruli for each rat. For quantitative determination of PCNA, Ki-67 and TGF-beta1, three areas in each section were analyzed.

To further assess matrix alterations, collagen IV immunostaining was performed. Three-micron thick sections were microwaved in 0.01 mol/L sodium citrate (pH 6.0) 4 × 5 min, incubated with rabbit anti-mouse collagen IV (Chemicon, Billerica, USA) overnight at 4°C and subjected to immunoperoxidase staining using a Vectastain ABC kit (Vector Laboratories, Burlingame, USA). DAB was used as a chromagen. The results of the collagen IV staining were quantified by ImageJ software, assessing area of positive staining in 20 consecutive glomeruli from each rat, deriving a collagen IV staining percent for each rat and then averaging these percentages to derive an average score for each group.

Detection of apoptotic podocytes

Renal tissue (3-μm sections) was deparaffinized and rehydrated prior to processing. Antigen retrieval was performed by boiling in citrate buffer for 20 min. After three PBS washes, the sections were incubated with blocking buffer for 1 hour. The mouse monoclonal anti-WT1 primary antibody (Santa Cruz, USA) was applied overnight at 4 ºC. The sections were then incubated with a

secondary Alexa Fluor 488 goat anti-mouse IgG (Invitrogen, Grand Island, USA)for 1 h at room temperature. The nuclei were counterstained with DAPI (Santa Cruz Biotechnology, Inc., California, USA). The apoptotic podocytes were identified using an ApopTag Red In Situ Apoptosis Detection kit (Chemicon International, USA). All of the samples were stained for the same length of time under identical conditions. The staining was assessed on the same day using identical gain settings. The immune-labeled cells were observed using a Zeiss LSM 510 laser scanning confocal microscope and a 40X/1.2NA water-immersion objective.

Morphometric Analysis

The kidney samples fixed in Dubosq-Brazil and embedded in paraffin were serially sectioned at 3-µm intervals and stained with periodic acid-Schiff reagent. An average of 75 sections for each rat was examined. The images of serially sectioned kidneys were obtained using a LSM-780 confocal microscope in tile-scanning mode. Only glomeruli contained entirely within the serially sectioned tissue were examined. For each animal group, 300-320 glomeruli were examined. A single section was selected as a map section for the morphometric analysis. The glomeruli were classified as connected to a normal proximal tubule, connected to an atrophic proximal tubule, or without a tubular connection. The proximal tubule segments connected to glomeruli were considered atrophic when there was thinning of the tubular cells accompanied by loss of brush border and narrowing of the tubular lumen. The findings were expressed as percentage of the three categories of glomeruli over the total number of glomeruli examined.

TUNEL assay on kidney tissue

A TUNEL assay for the detection of apoptosis was performed on Dubosq-Brazil-fixed and paraffin-embedded renal sections. Apoptosis was evaluated in two sections for all of the PHN animals at 4 months. Briefly, 3-µm sections were deparaffinized and treated with 20 µg/ml of proteinase K for 20 minutes at 37°C. To identify the apoptotic cells, we used a Peroxidase In Situ Apoptosis Detection kit (Chemicon International, USA). The TUNEL assay was conducted according to the manufacturer's instructions. The sections were then counterstained with Harris hematoxylin (Richard Allan Scientific, USA). For the negative control, terminal deoxynucleotidyl transferase was omitted in TUNEL reaction mixture, and for the positive control, DNase was added for 15 minutes at 37°C. The cells were observed using a 20X/1.4 oil objective, and the number of apoptotic cells per glomerular-tubular junction was determined. In each slice, 25 to 30 randomly selected glomeruli were examined.

Detection of Bax, Bcl-x, caspase-3, TGF-beta 1, IL-1 beta, and IL-6 by Western blotting

Proteins solubilized in Laemmli sample buffer were resolved in polyacrylamide gels by SDS-PAGE and transferred to a polyvinylidene difluoride membrane. The membranes were then blocked in 5% non-fat milk in TBS-T and immunoblotted using the Bax and Bcl-xL, caspase-3 Rabbit Ab (Cell Signaling Technology, Danvers, USA), TGF-beta Rabbit Ab (Cell Signaling Technology, Danvers, USA), IL-1 beta goat Ab, IL-6 goat Ab (R&D Systems, Inc. McKinley Place NE, Minneapolis, USA) and actin mouse mAb (BD, Lexington, USA). The actin mouse mAb was used as a loading control. After three washes with TBS-T, the membranes were incubated with secondary anti-rabbit, anti-goat or anti-mouse antibodies labeled with horseradish peroxidase for 1 h at room temperature. The membranes were washed three times with TBS-T, and the protein bands were visualized by chemiluminescent substrate ECL. The protein content was quantified by densitometric analysis.

Statistical Analysis

The data were expressed as the mean±SEM. To determine whether the differences among the groups were significant, two-way ANOVA followed by Fisher-LSD post-hoc test was used. If the distribution of the variables was not parametric, the data were analyzed using the non-parametric Mann-Whitney test. The comparisons between groups were made using Kruskal-Wallis one-way ANOVA on ranks with pair-wise multiple comparisons made by Dunn's method. The statistical significance level was defined as $P<0.05$.

References

1. United States Renal Data System. USRDS 2013 Annual Data Report: Atlas of Chronic Kidney Disease and End-Stage Renal Disease in the United States. National Institutes of Health. National Institute of Diabetes and Digestive and Kidney Diseases. Bethesda, MD (2013).
2. Anderson S, Halter JB, Hazzard WR, Himmelfarb J, Horne FMc, Kaysen JA, Kusek JW, Nayfield SJ, Schmader K, Tian Y, Ashworth JR, Clayton CP, Parker RP, Tarver ED, Woolard NF, High KP and for the workshop participants. Prediction, Progression, and Outcomes of Chronic Kidney Disease in Older Adults J Am Soc Nephrol 20 (6): 1199-1209 (2009).
3. Haraldsson B, Nyström J, Deen WM: Properties of the glomerular barrier and mechanisms of proteinuria. Physiol Rev 88(2): 451-487 (2008).
4. Remuzzi G, Perico N, Macia M, Ruggenenti P: The role of renin-angiotensin-aldosterone system in the progression of chronic kidney disease. Kidney Int Suppl 99: 57-65 (2005).
5. Chevalier RL, Forbes MS: Generation and Evolution of Atubular Glomeruli in the Progression of Renal Disorders. J Am Soc Nephrol 19(2): 197-206 (2008).
6. Tojo A, Kinugasa S: Mechanisms of Glomerular Albumin Filtration and Tubular Reabsorption. International Journal of Nephrology. Volume 2012, Article ID 481520, 9 pp.
7. Perkins BA, Ficociello LH, Ostrander BE, Silva KH, Weinberg J, Warram JH, Krolewski AS: Microalbuminuria and the Risk for Early Progressive Renal Function Decline in Type 1 Diabetes. J Am Soc Nephrol 18(4): 1353-1361 (2007).
8. Brezniceanu M-L, Liu F, Wei C-C, Che´nier I, Godin N, Zhang S-L, Filep LG, Ingelfinger JR, Chan JSD: Attenuation of Interstitial Fibrosis and Tubular Apoptosis in db/db Transgenic Mice Overexpressing Catalase in Renal Proximal Tubular Cells. Diabetes 57: 451–459 (2008).
9. Eddy AA: Molecular basis of renal fibrosis. Pediatr Nephrol 15: 290–301 (2000).
10. Jafar TH, Stark PC, Schmid CH, Landa M, Maschio G, de Jong PE, de Zeeuw D, Shahinfar S, Toto R, Levey AS: Progression of chronic kidney disease: the role of blood pressure control, proteinuria, and angiotensin-converting enzyme inhibition: a patient-level meta-analysis. Ann Intern Med 39: 244-252 (2003).
11. Jafar TH, Stark PC, Schmid CH, Strandgaard S, Kamper AL, Maschio G, Becker G, Perrone RD, Levey AS: The effect of angiotensin-converting-enzyme inhibitors on progression of advanced polycystic kidney disease. Kidney Int 67: 265–271 (2005).

12. Essien E, Goel N, Melamed ML: Role of vitamin D receptor activation in racial disparities in kidney disease outcomes. Semin Nephrol 33 (5): 416–424 (2013).
13. Akhurst RJ, Hata A: Targeting the TGFβ signalling pathway in disease. Nat Rev Drug Discov 11(10): 790–811 (2012).
14. de Zeeuw D, Agarwal R, Amdahl M, Audhya P, Coyne D, Garimella T, Parving HH, Pritchett Y, Remuzzi G, Ritz E, Andress D. Selective vitamin D receptor activation with paricalcitol for reduction of albuminuria in patients with type 2 diabetes (VITAL study): a randomised controlled trial. Lancet 376 (9752): 1543-1551 (2010).
15. Miyakawa-Naito A, Uhlen P, Lal M, Aizman O, Mikoshiba K, Brismar H, Zelenin S, and Aperia A: Cell signaling microdomain with Na,K-ATPase and inositol 1,4,5-trisphosphate receptor generates calcium oscillations. J Biol Chem 27: 50355-50361 (2003).
16. Aizman O, Uhlen P, Lal M, Brismar H, Aperia A: Ouabain, a steroid hormone that signals with slow calcium oscillations. Proc Natl Acad Sci USA 98: 13420–13424 (2001).
17. Li J, Zelenin S, Aperia A, Aizman O: Low doses of ouabain protect from serum deprivation–triggered apoptosis and stimulate kidney cell proliferation via activation of NF-κB. J Am Soc Nephrol 17: 1848-1857 (2006).
18. Li J, Khodus GR, Markus Kruusmägi M, Kamali-Zare P , Liu X, Eklöf A-Ch , Zelenin S, Brismar H, Aperia A: Ouabain protects against adverse developmental programming of the kidney. Nature Communications 27 (2010).
19. Burlaka Ie, Liu XL, Rebetz J, Arvidsson I, Yang L, Brismar H, Karpman D, Aperia A: Ouabain protects from Shiga toxin-triggered apoptosis by reversing the imbalance between Bax and Bcl-xL. J Am Soc Nephrol 24: 1413–1423 (2013).
20. Martinou J-C, Youle RJ: Mitochondria in Apoptosis: Bcl-2 family Members and Mitochondrial Dynamics. Dev Cell 21(1): 92–101 (2011).
21. Jefferson JA, Pippin JW, Shankland SJ: Experimental Models of Membranous Nephropathy. Drug Discov Today Dis Models 7(1-2): 27–33 (2010).
22. Amsellem S, Gburek J, Hamard G, Nielsen R, Willnow TE, Devuyst O, Nexo E, Verroust PJ, Christensen EI, Kozyraki R: Cubilin is essential for albumin reabsorption in the renal proximal tubule. J Am Soc Nephrol 21(11): 1859-1867 (2010).
23. Khan S, Abu Jawdeh BG, Goel M, Schilling WP, Parker MD, Puchowicz MA, Yadav SP, Harris RC, El-Meanawy A, Hoshi M, Shinlapawittayatorn K, Deschênes I, Ficker E, Schelling JR: Lipotoxic disruption of NHE1 interaction with PI(4,5)P2 expedites proximal tubule apoptosis. J Clin Invest 124(3): 1057-1068 (2014).

24. Dizin E, Hasler U, Nlandu-Khodo S, Fila M, Roth I, Ernandez T, Doucet A, Martin P-Y, Feraille E, de Seigneux S: Albuminuria induces a proinflammatory and profibrotic response in cortical collecting ducts via the 24p3 receptor. Am J Physiol Renal Physiol 305: 1053-1063 (2013).
25. Gentle ME, Shi S, Daehn I, Zhang T, Qi H, Yu L, D'Agati VD, Schlondorff DO, Bottinger EP: Epithelial cell TGFβ signaling induces acute tubular injury and interstitial inflammation. J Am Soc Nephrol 24(5): 787-799 (2013).
26. Zhang S, Malmersjo S, Li J, Ando, H., Aizman, O., Uhlen, P., Mikoshiba, K., and Aperia A: Distinct role of the N-terminal tail of the Na,K-ATPase catalytic subunit as a signal transducer. J Biol Chem. 281: 21954-21962 (2006).
27. Miyakawa-Naito A, Uhlen P, Lal M, Aizman O, Mikoshiba K, Brismar H, Zelenin S, and Aperia A: Cell signaling microdomain with Na,K-ATPase and inositol 1,4,5-trisphosphate receptor generates calcium oscillations. J Biol Chem 27: 50355-50361 (2003).
28. Okamura K, Dummer P, Kopp J, Qiu L, Levi M, Faubel S, Blaine J: Endocytosis of Albumin by Podocytes Elicits an Inflammatory Response and Induces Apoptotic Cell Death. Plos one 8(1): e54817 (2013).
29. Elmore S: Apoptosis: A Review of Programmed Cell Death Apoptosis: A Review of Programmed Cell Death. Toxicol Pathol 35(4): 495-516 (2007).
30. Nicholls D, Ward M: Mitochondrial membrane potential and neuronal glutamate excitotoxicity: mortality and millivolts. Trends Neurosci. 23: 166 -174 (2000).
31. Zanetti M and Druet P. Passive Heymann's nephritis as a model of immune glomerulonephritis mediated by antibodies to immunoglobulins. Clin Exp Immunol 41(2): 189–195 (1980).
32. Chang AM, Ohse T, Krofft RD, Wu JS, Eddy AA, Pippin JW and Shankland SJ: Albumin-induced apoptosis of glomerular parietal epithelial cells is modulated by extracellular signal-regulated kinase 1/2. Nephrol Dial Transplant 0: 1–13 (2011).
33. Chevalier RL, Forbes MS: Generation and Evolution of Atubular Glomeruli in the Progression of Renal Disorders. JASN 19(2): 197-206 (2008).
34. Kale S, Karihaloo A, Clark P, Kashgarian M, Krause D, Cantley L: Bone marrow stem cells contribute to repair of the ischemically injured renal tubule. J Clin Invest 112 : 42 –49 (2003).

35. Duffield JS, Park KM, Hsiao L-L, Kelley VR, Scadden DT, Ichimura T, Bonventre JV. Restoration of tubular epithelial cells during repair of the postischemic kidney occurs independently of bone marrow-derived stem cells. J Clin Invest 115 (7): 1743–1755 (2005).
36. Matsusaka T, Kobayashi K, Kon V, Pastan I, Fogo AB, Ichikawa I: Glomerular sclerosis is prevented during urinary tract obstruction due to podocyte protection. Am J Physiol Renal Physiol 300(3): 792–800 (2011).
37. Edlich F, Banerjee S, Suzuki M, Cleland MM, Arnoult D, Wang C, Neutzner A, Tjandra N, Youle RJ: Bcl-xL retrotranslocates Bax from the mitochondria into the cytosol. Cell 1; 145(1): 104–116 (2011).
38. Khoshnan A, Tindell C, Laux I, Bae D, Bennett B, Nel AE: The NF-kB Cascade Is Important in Bcl-xL Expression and for the Anti-Apoptotic Effects of the CD28 Receptor in Primary Human CD41 Lymphocytes. J. Immunol 165: 1743-1754 (2000).
39. Guo J-K, Arnaud Marlier A, Shi H, Shan A, Ardito TA, Du Z-P, Kashgarian M, Krause DS, Biemesderfer D, Cantley LD: Increased Tubular Proliferation as an Adaptive Response to Glomerular Albuminuria. J Am Soc Nephrol 23: 429–437 (2012).
40. Johnson A, Di Pietro LA: Apoptosis and angiogenesis: an evolving mechanism for fibrosis FASEB J. 27: 3893-3901 (2013).
41. Wang K, Lin B, Brems JJ, Gamelli R: Hepatic apoptosis can modulate liver fibrosis through TIMP1 pathway. Apoptosis 18(5): 566-577 (2013).
42. Spender LC, Carter MJ, O'Brien DI, Clark LJ, Yu J, Michalak EM, Happo L, Cragg MS, Inman GJ: Transforming Growth Factor-β Directly Induces p53-upregulated Modulator of Apoptosis (PUMA) during the Rapid Induction of Apoptosis in Myc-driven B-cell Lymphomas. The Journal of Biological Chemistry 288(7): 5198–5209 (2013).
43. Vellaa A, Gerberb TC, Hayesb DL, Reederb GS: Digoxin, hypercalcaemia, and cardiac conduction. Postgrad Med J 75: 554-556 (1999).
44. Fontana JM, Burlaka Ie, Khodus G, Brismar H, and Aperia A: Calcium oscillations triggered by cardiotonic steroids. FEBS Journal 280: 5450–5455 (2013).
45. Larsson SH, Aperia A, Lechene C: Studies on terminal differentiation of rat renal proximal tubular cells in culture: ouabain-sensitive K and NA transport. Acta Physiologica Scandinavica 132(2): 129-134 (1988).
46. Larsson SH: Short-term primary cultures in studies of growth regulation in rat proximal tubule cells. Pediatr Nephrol (6):798-801 (1993).

Acknowledgments

This study has been supported by the Swedish Research Council, the Family Erling-Persson Foundation, the Märta and Gunnar V Philipson foundation and the Karolinska Institute KIRT fellowship. We thank Kristoffer Bernhem for assistance with data analysis.

Figure 1. Excessive uptake of albumin triggers apoptosis and a subsequence increase in TGF-beta 1 expression levels in primary proximal tubule cells; ouabain rescues the cells from albumin-triggered apoptosis. (**A,B**). Time dependence of albumin-induced apoptosis and albumin-induced TGF-beta 1 expression in RPTC cells. RPTC cells were incubated with 10 mg/ml albumin in serum-free medium for 0, 2, 4 or 8 hours. RPTC were TUNEL-stained (red) to detect apoptotic cells and counterstained with DAPI (blue) (**A**). TGF-beta 1 expression was detected by Western blot analysis (**B**). Experiments were repeated four times. (**C**). Time dependence of Alexa Fluor 555-coupled albumin internalization by RPTC. Cells were subjected to live cell imaging. All images represent a single section through the focal plane. (**D**). Quantification of time-dependent albumin-induced apoptosis and TGF-beta 1 expression in RPTC cells. For TGF-beta 1 expression, densitometric quantification of bands was performed. The density of the band from control cells was set to 100%. The histograms show the means ± SEM as a % of change compared to control group. Experiments were repeated four times. One-way ANOVA was used to determine if differences were statistically significant. **$p<0.001$, *$p<0.01$. (**E**). Dose dependence of albumin-induced apoptosis in RPTC cells. RPTC cells were incubated for 18 hours with 0, 5, 10 or 20 mg/ml albumin with or without 5 nM ouabain in serum-free medium. RPTC were TUNEL-stained (red) to detect apoptotic cells and counterstained with DAPI (blue). (**F,G**). TGF-β1 expression in untreated RPTC and RPTC treated with 5 nM ouabain with or without 10 mg/ml albumin for 8 hours (**F**) or 18 hours (**G**). Densitometric quantification of bands was performed for the respective blots (J and K). The density of the band from control cells was set to 100%. Histograms represent means ± SEM. Experiments were repeated five times. The Mann-Whitney U test was used to determine if differences were statistically significant. **$p<0.001$, *$p<0.01$. (**H,I**). Dose dependence of albumin-induced apoptosis in RPTC cells. RPTC cells were incubated with 0, 5, 10 or 20 mg/ml albumin with or without 5 nM ouabain in serum-free medium for 8 (**H**) or 18 (**I**) hours. The AI was determined by analyzing five to seven randomly selected areas with 100 to 200 cells in each area. Histograms represent means ± SEM. Experiments were repeated four times. One-way ANOVA was used to determine if differences were statistically significant. **$p<0.001$, *$p<0.01$.

Figure 2. The rescuing effect of ouabain: time-dependent decrease in expression of the anti-apoptotic factor Bcl-xL, recruitment of Bax to mitochondria and mitochondrial depolarization in albumin-exposed cells. (**A**). Representative confocal images of Bcl-xL immunofluorescence signal (red) in RPTC. Cells were transfected with mitochondrial marker BacMam 2.0 (green) and incubated for 0, 1, 2, 3, or 8 hours with 2.5 mg/mL (**B**) or 10 mg/ml

albumin (**C**) with or without ouabain (5 nM) in serum-free medium. Thirty cells were analyzed in each experiment. Histograms show the means ± SEM. The experiments were repeated three times. One-way ANOVA Was used to determine if the differences were statistically significant. (**D**). Immunofluorescence staining of proapoptotic factor Bax (red) in RPTC incubated with 2.5 mg/ml albumin. Cells were transfected with mitochondrial marker BacMam 2.0 (green) and incubated for 0, 1, 2, 4, or 8 hours with 2.5 mg/mL (**E**) or 10 mg/ml albumin (**F**) with or without ouabain (5 nM) in serum-free medium. The number of co-localized Bax/mitochondrial peaks was counted. Histograms show the means ± SEM. The experiments were repeated four times. The Mann-Whitney U test was used to determine if differences were statistically significant. (**G,H**). Line scans show the fluorescence intensities of Bax signals (green) and mitochondria labeled with BacMam 2.0 (blue) along the selected line in vehicle-treated RPTC (**G**) and RPTC treated with 10 mg/mL albumin for 8 hours (**H**). (**I**). Demonstration of the time course of the mitochondrial membrane potential changes in RPTC incubated with 2.5 mg/ml (**J**) and 10 mg/ml albumin (**K**). Histograms show the means ± SEM. The experiments were repeated three times, and the Mann-Whitney U test was used to determine whether differences were statistically significant. (**L**). Time-dependence of Bax translocation to mitochondrial membrane and Bcl-xL expression in RPTC treated for 0, 1, 2, 4 and 8 hours with 10 mg/ml albumin. Histograms show the means ± SEM. (**M**). Effect of ouabain on albumin-induced Bax translocation to mitochondrial membrane, Bcl-xL expression and mitochondrial membrane potential changes in RPTC treated for 0-8 hours with 10 mg/ml albumin. Histograms show means ± SEM. For all analyses, $^{**}p<0.01$. (**N**). Immunofluorescence staining of proapoptotic factor Bcl-xL (red) in RPTC incubated with 10 mg/ml albumin. The number of co-localized Bcl-xL/mitochondrial peaks was counted. Histograms show the means ± SEM. The experiments were repeated four times. The Mann-Whitney U test was used to determine if differences were statistically significant.

Figure 3. Ouabain counteracts albumin-dependent increased expression of Bax and decreased expression of Bcl-xL. (A). Cartoon illustration of the ouabain/Na,K-ATPase/IP3R signaling pathway. Ouabain triggers the interaction between the N-terminus tail of the catalytic α subunit of Na, K-ATPase and the N-terminus of IP3R. This activates the IP3 receptor and triggers slow intracellular calcium oscillations, which subsequently activate the NF-κB p65 subunit and lead to protection from apoptosis. (**B**). Expression of the Bax, Bcl-xL and caspase-3 after incubation with 10 mg/mL albumin and 5 nM ouabain for 8 hours. Densitometric quantification of the Bax (**D**), Bcl-xL (**E**) and caspase-3 (**F**) bands was performed. The density of the band from the control cells was

set to 100%. Histograms show the means ± SEM. The experiments were repeated five times. The Mann-Whitney U test was used to determine if the differences were statistically significant. **p<0.001, *p<0.01. (**C**). Expression of the inflammatory cytokines (IL-1beta and IL-6) after incubation with 5 nM ouabain and LPS for 0, 1, 2, 4 or 8 hours. Densitometric quantification of the IL-1beta (**G**) and IL-6 (**H**) bands was performed. The density of the band from control cells was set to 100%. Histograms show the means ± SEM. The experiments were repeated three times, and the Mann-Whitney U test was used to determine if differences were statically significant. **p<0.001, *p<0.01.

Figure 4. Characteristics of PHN rats followed for 16 weeks. Ongoing apoptosis of podocytes and proximal tubule cells in the glomerular-tubular junction is much more pronounced in kidneys from vehicle-treated PHN rats than from ouabain-treated PHN rats, whereas proliferating cells are more common in kidneys from vehicle-treated rats than ouabain-treated rats. (**A**). Concentration of albumin in urine from control rats, rats with accelerated PHN and ouabain-treated PHN rats. Data are presented as the means ± SEM. Statistical analysis was performed using the two-way ANOVA. (**B**). Glomerular basement membrane detected by Jones' silver staining in control rats, rats with accelerated PHN and ouabain-treated rats. G – glomerular basement membrane, S – "spiked" glomerular basement membrane. (**C**). Representative TUNEL staining of proximal tubules normally connected to an atrophic tubule of PHN rats and ouabain-treated PHN rats at four months. Quantitative determination of apoptotic proximal tubule cells (**G**). Histograms show the means ± SEM. Statistical analysis was performed using the Mann-Whitney U test. *p<0.01. Original magnifications, x400. (**D**). Representative micrographs demonstrate apoptotic podocytes in control rats, rats with accelerated PHN and ouabain-treated PHN rats. Kidney sections were subjected to terminal deoxynucleotidyl transferase–mediated dUTP nick-end labeling (TUNEL) staining to identify apoptotic cells and WT-1 staining to recognize podocytes. The TUNEL and WT-1 staining images are superimposed. Arrow indicates an apoptotic podocytes. Quantitative determination of apoptotic podocytes (**H**). Histograms show the means ± SEM. The Mann-Whitney U test was used to determine if the differences were statistically significant. **p<0.01, *p<0.05. (**E,F**). Representative micrographs demonstrate Ki-67 staining (**E**) and PCNA staining (**F**) from PHN rats with and without continuous ouabain treatment. Ki-67 and PCNA were used to identify proliferating cells. Histograms show the means ± SEM (**I**,**J**). Statistical analysis was performed using the Mann-Whitney U test. ***P*<0.001.

Figure 5. Extent of glomerulosclerosis and expression of TGF-beta 1 are more pronounced in kidneys from vehicle-treated PHN rats than in kidneys from ouabain-treated PHN rats. (**A**). PAS staining of kidney sections (×200), showing segmental glomerulosclerosis and tubulointerstitial damage (fibrosis, infiltration with inflammatory cells) in control rats, rats with accelerated PHN and ouabain-treated PHN rats. The depicted pictures are representative. (**B**). Representative confocal images of kidney sections from PHN rats with and without continuous treatment with ouabain. Sections were immunohistochemically stained for TGF-β1 (red), nuclei were counterstained with 4′,6-diamidino-2-phenylindole (DAPI, blue) and the images were merged. Immunoreactivity for TGF-β1 is expressed as % deviation from control. Histograms show means ± SEM (E)**.** Statistical analysis was performed using the Mann-Whitney U test. **p<0.001**.** (**C**). Collage IV immunostaining in glomeruli of control rats, rats with accelerated PHN and ouabain-treated PHN rats. The images are representative. (**D**). Histograms show the means ± SEM. Statistical analysis was performed using the Mann-Whitney U test. *P<0.05.

Figure 6. Kidneys from ouabain-treated PHN rats have more preserved podocytes and fewer disconnected proximal tubules than kidneys from vehicle-treated PHN rats; serum creatinine is significantly lower in ouabain-treated PHN rats than in vehicle-treated PHN rats. (**A**). Schematic representation of the procedures for evaluating the glomerular-tubular connections in individual glomeruli. On the right side of the figure, the pictures show the pattern of glomerular-tubular connections. (**B**). Summary of morphometric studies. Quantitative determination of glomeruli. Histograms represent means ± SEM. **p<0.001, *p<0.01. (**C**). Representative micrographs demonstrate podocytes in control rats, rats with accelerated PHN and ouabain-treated PHN rats. WT-1 staining was used to identify podocytes, and the results were quantified (**D**). Histograms show the means ± SEM. The Mann-Whitney U test was used to determine if differences were statistically significant. **p<0.01, *p<0.05. (**E**). Blood creatinine levels in control rats, rats with accelerated PHN and ouabain-treated PHN rats. Histograms show the mean ± SEM. The Mann-Whitney U test was used to determine if differences were statistically significant. *p<0.001 (control vs. PHN, PHN vs. PHN+ouabain).

Figure 1.

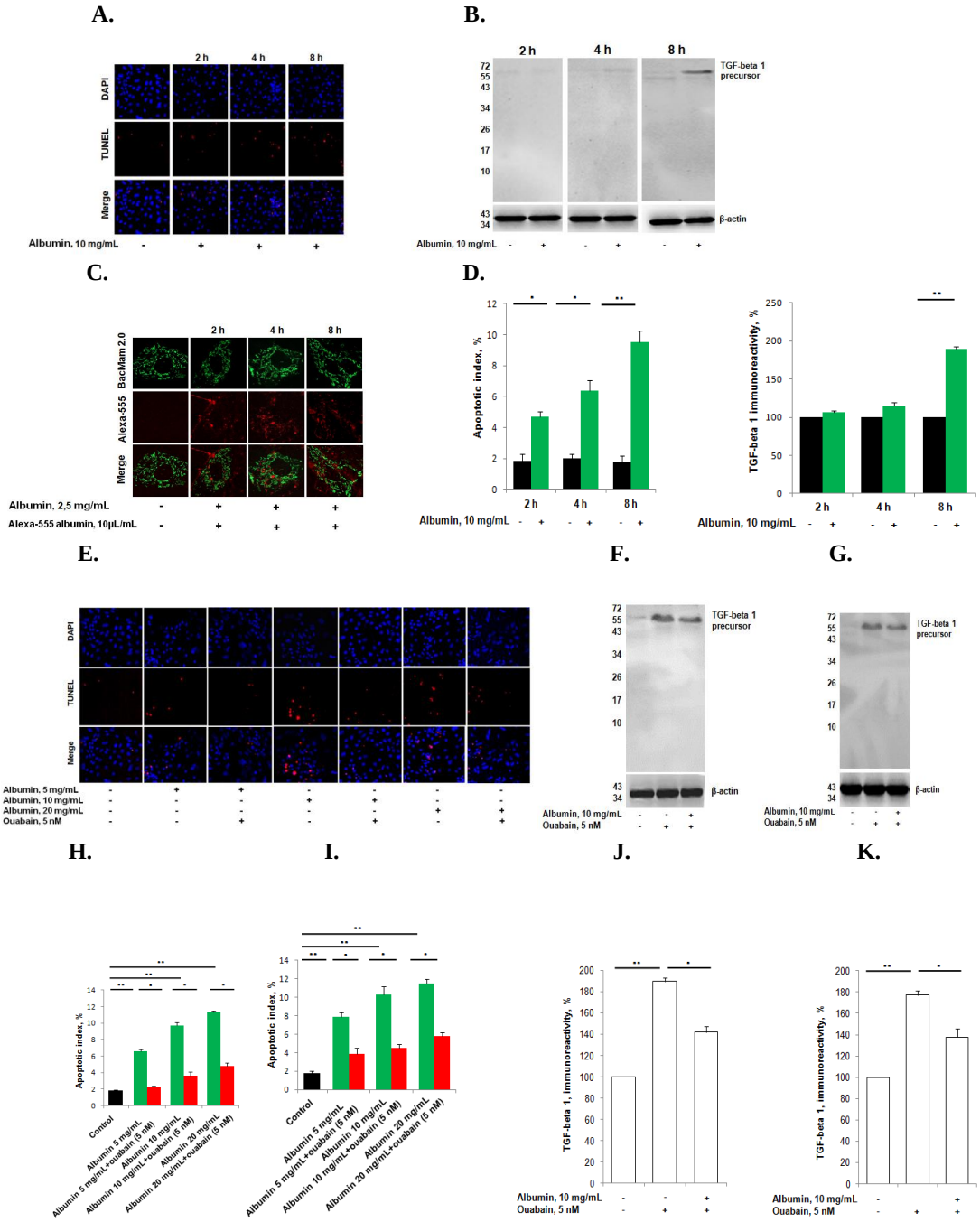
A.
B.
2 h
4 h
8 h
DAPI
TUNEL
Merge
Albumin, 10 mg/mL
TGF-beta 1 precursor
β-actin
C.
D.
BacMam 2.0
Alexa-555
Albumin, 2,5 mg/mL
Alexa-555 albumin, 10μL/mL
Apoptotic index, %
TGF-beta 1 immunoreactivity, %
E.
F.
G.
Albumin, 5 mg/mL
Albumin, 10 mg/mL
Albumin, 20 mg/mL
Ouabain, 5 nM
H.
I.
J.
K.
Control
Albumin 5 mg/mL
Albumin 5 mg/mL+ouabain (5 nM)
Albumin 10 mg/mL
Albumin 10 mg/mL+ouabain (5 nM)
Albumin 20 mg/mL
Albumin 20 mg/mL+ouabain (5 nM)
TGF-beta 1, immunoreactivity, %

Figure 2.

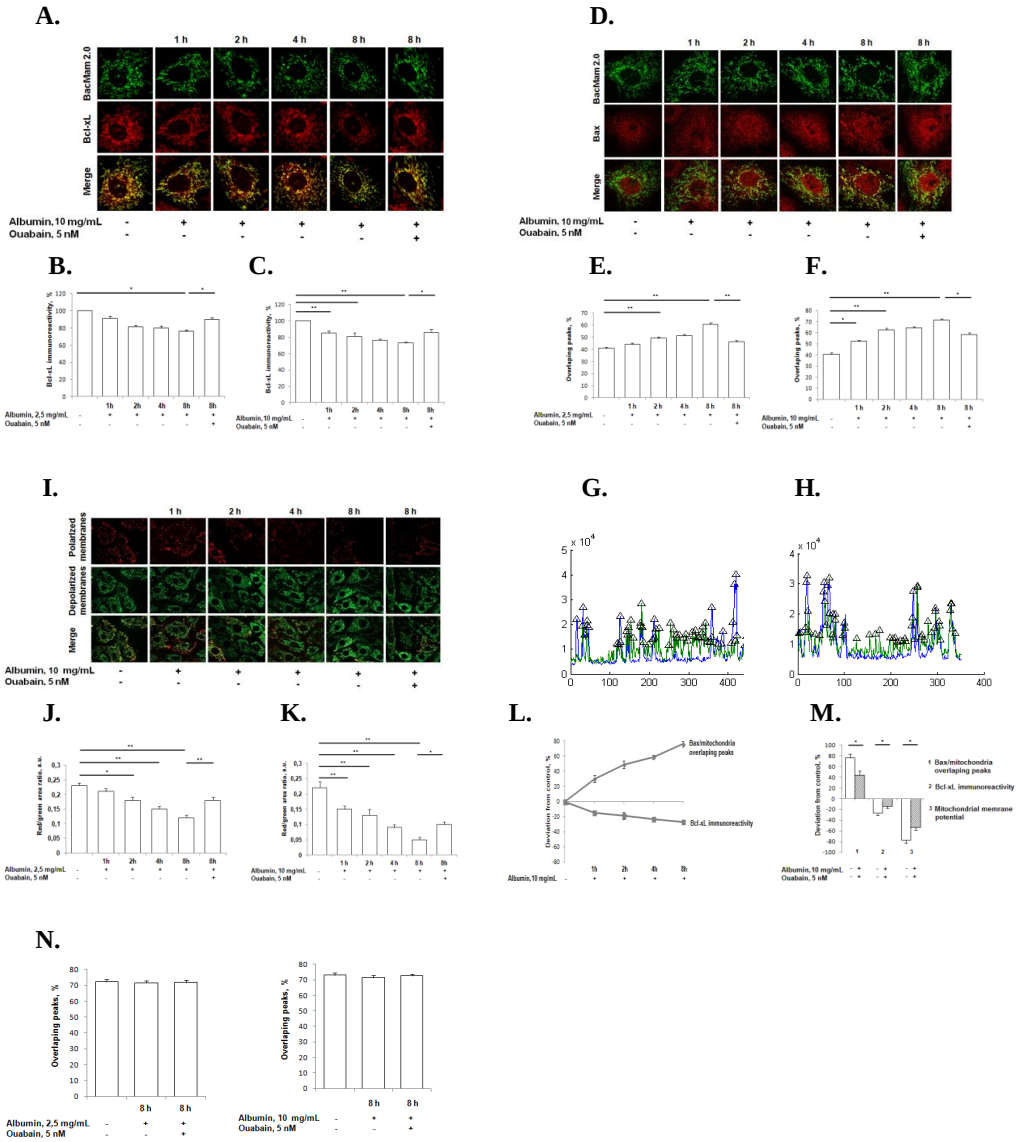
A.
1 h
2 h
4 h
8 h
8 h
BacMam 2.0
Bcl-xL
Merge
Albumin, 10 mg/mL
Ouabain, 5 nM
D.
BacMam 2.0
Bax
Merge
B.
C.
E.
F.
Bcl-xL immunoreactivity, %
Overlaping peaks, %
Albumin, 2,5 mg/mL
Albumin, 10 mg/mL
I.
Polarized membranes
Depolarized membranes
G.
H.
J.
K.
L.
M.
Bax/mitochondria overlaping peaks
Bcl-xL immunoreactivity
Mitochondrial memrane potential
N.

Figure 3.

A.

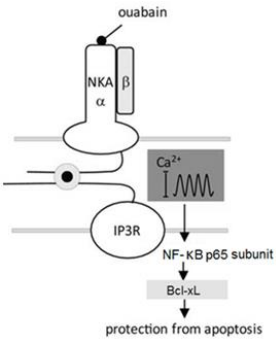

B.

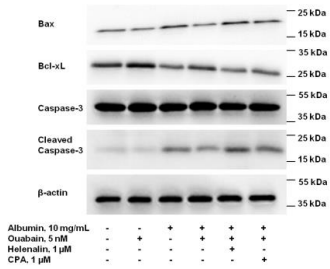

C.

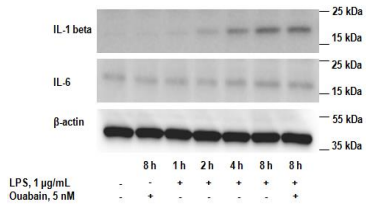

D.

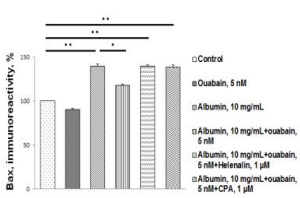

E.

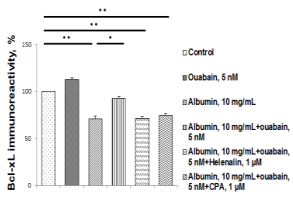

F.

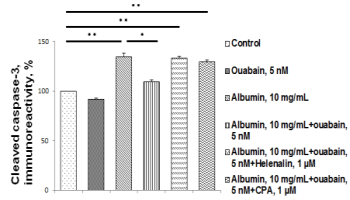

G.

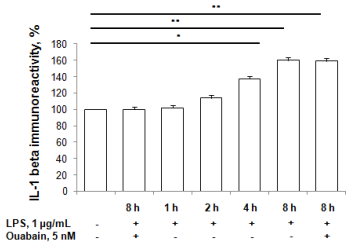

H.

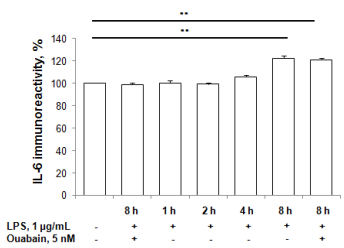

Figure 4.

A.

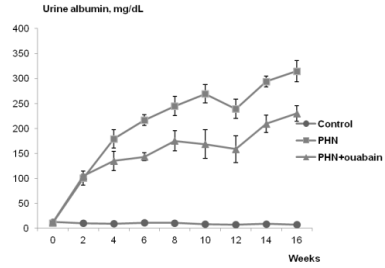

B.

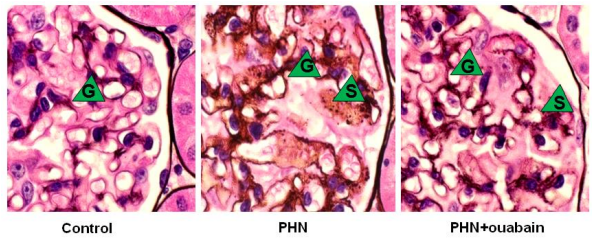

C.

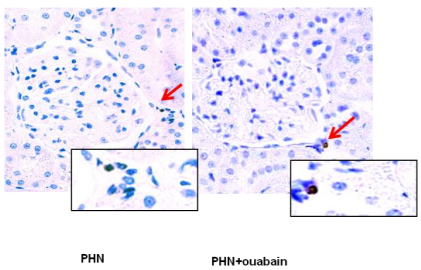

D.

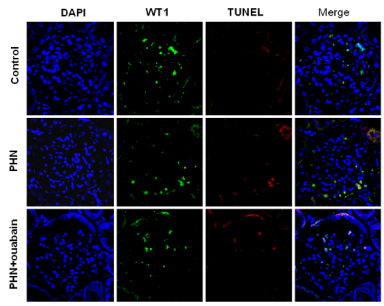

E.

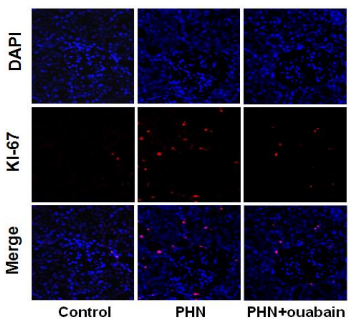

F.

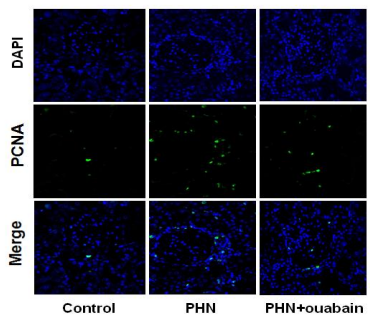

G.

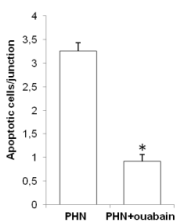

H.

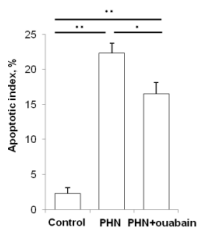

I.

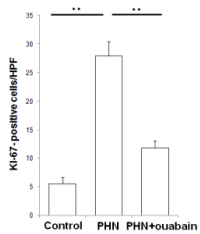

J.

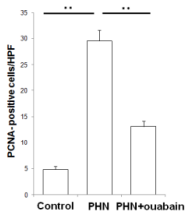

Figure 5.

A.

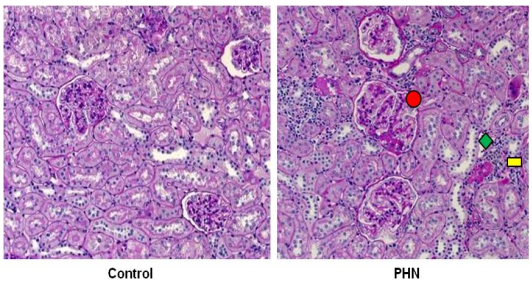

B.

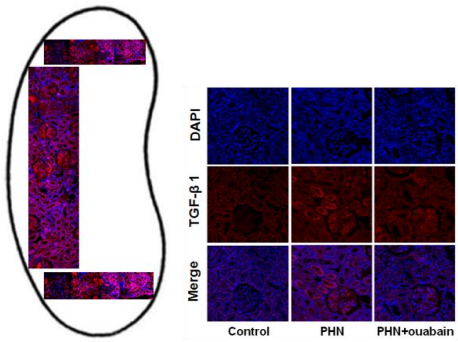

C.

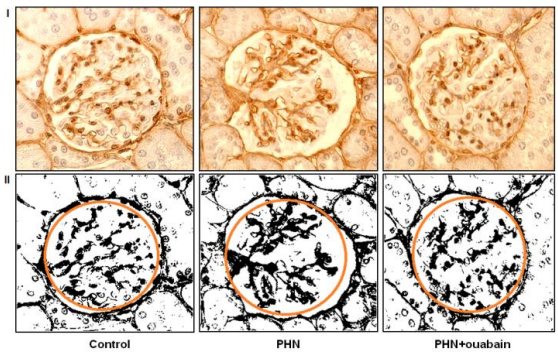

D.

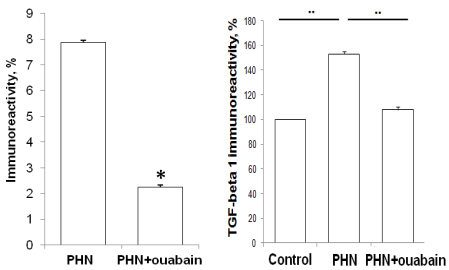

Figure 6.

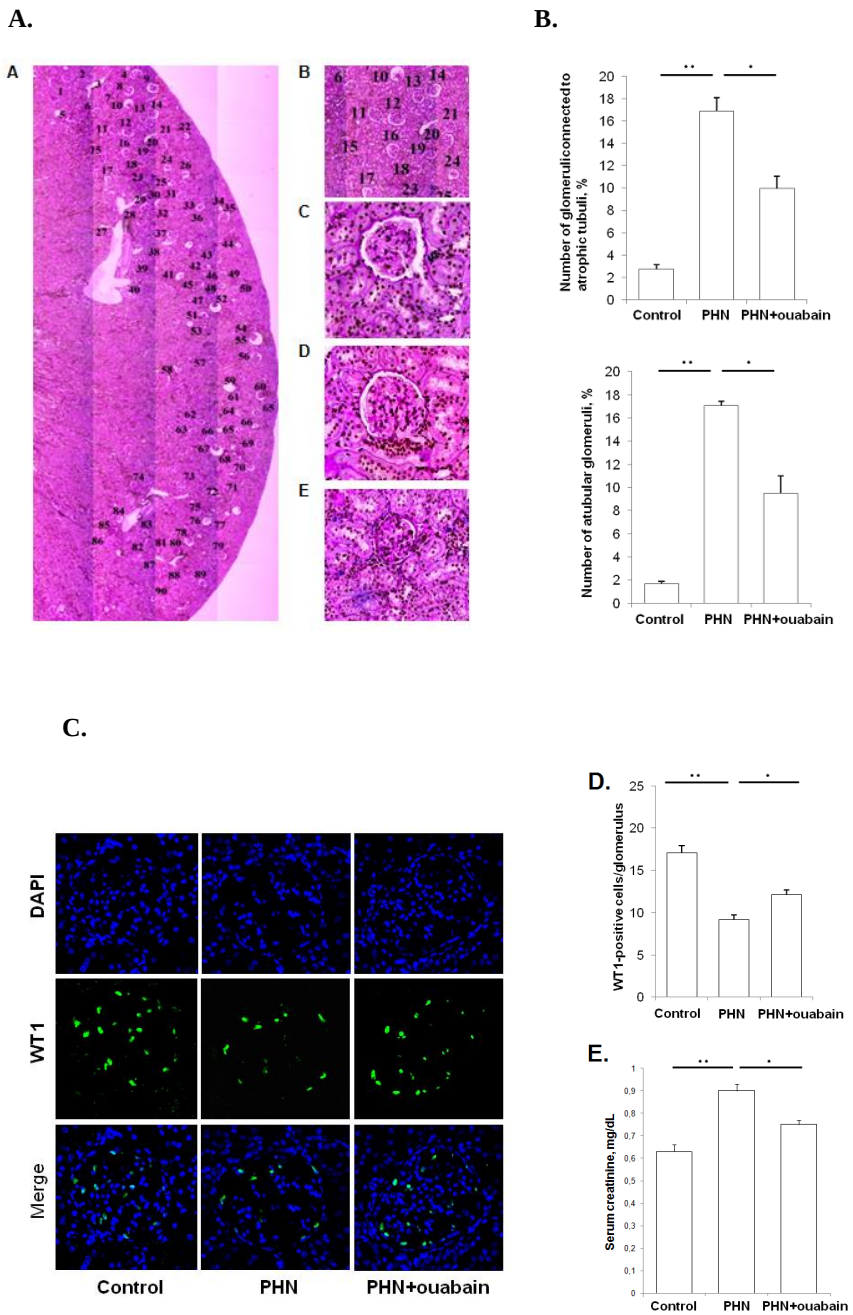
A.
B.
A
B
C
D
E
Number of glomeruliconnectedtro atrophic tubuli, %
Number of atubular glomeruli, %
Control
PHN
PHN+ouabain
C.
DAPI
WT1
Merge
Control
PHN
PHN+ouabain
D.
WT1-positive cells/glomerulus
E.
Serum creatinine, mg/dL

Supplementary figure 1. Albumin-triggered apoptosis in primary podocytes. Rescue by ouabain.

A. Representative confocal image of podocytes in primary culture. Isolated glomeruli with migrated podocytes were subjected to WT-1 staining to recognize podocytes (green). Cells were counterstained with DAPI (blue).

B. Dose dependence of albumin-induced apoptosis in primary podocytes. Podocytes were incubated for 18 hours with 0 to 10 mg/ml albumin with or without ouabain (5 nM) in serum-free medium. Podocytes were TUNEL-stained (red) to detect apoptotic cells and counterstained with DAPI (blue). WT-1 staining has been used to recognize podocytes (green).

C. AI of podocytes was determined by analyzing five to seven randomly selected areas with 20 to 30 cells in each area. Histograms represent means ± SEM. ** - $p<0,001$, * - $p<0.01$. Statistical analysis was performed using one-way ANOVA (B). Experiments were repeated four times.

D. Dose-dependent effect of albumin in presence or absence of ouabain (5 nM) on RPTC and podocytes in primary culture. Histograms represent means ± SEM. Experiments were repeated four times.

Supplementary figure 2.

A. Representative confocal images of NF-κB p65 subunit immunofluorescence signal in RPTC. Bars show mean nuclear/cytosol NF-κB p65 subunit signal. 50 – 100 cells were analyzed in each experiment. Histograms represent means ± SEM. * $p<0.001$ - control vs. ouabain, alnumin vs. albumin+ouabain. Experiments were repeated four times.

B. RPTC cells were incubated for 8 hours with 10 mg/ml albumin with or without ouabain (5 nM), helenalin (1μM) and CPA (1μM) in serum-free medium. RPTC were TUNEL-stained (red) to detect apoptotic cells and counterstained with DAPI (blue). AI was determined by analyzing five to seven randomly selected areas with 100 to 200 cells in each area. Histograms represent means ± SEM. ** - $p<0.001$, * - $p<0.01$. Statistical analysis was performed using one-way ANOVA. Experiments were repeated four times.

Supplementary figure 3.

Podocytes were incubated for 18 hours with 10 mg/ml albumin with or without ouabain (5 nM), helenalin (1μM) and CPA (1μM) in serum-free medium in serum-free medium. Podocytes were TUNEL-stained (red) to detect apoptotic cells and counterstained with DAPI (blue). WT-1 staining has been used to recognize podocytes (green). AI was determined by analyzing five to seven randomly selected areas with 20 to 30 cells in each area. Histograms represent means ± SEM.

** - p<0,001, * - p<0.01. Statistical analysis was performed using the Mann-Whitney U test. Experiments were repeated four times.

Supplementary figure 4.

Representative confocal images of NF-κB p65 subunit immunofluorescense signal in podocytes. Bars show mean nuclear/cytosol NF-κB p65 subunit signal. 30 – 60 cells were analyzed in each experiment. Histograms represent means ± SEM. * p<0.001 - control vs. ouabain, albumin vs. albumin+ouabain. Statistical analysis was performed using the Mann-Whitney U test. Experiments were repeated four times.

Supplementary figure 5.

A. Time dependence of Alexa Fluor 555-coupled albumin internalization by RPTC. Cells were subjected to live cell imaging. All images represent a single section through the focal plane.

B. Immunofluorescence staining of proapoptotic factor Bax (red) in RPTC incubated with 10 mg/ml albumin. Cells were transfected with mitochondrial marker BacMam 2.0 (green). Number of co-localized Bax/mitochondrial peaks was counted. . **p<0.01; *p<0.05. Statistical analysis was performed using the Mann-Whitney U test. Experiments were repeated three times.

C. Demonstration of the time course of the mitochondrial membrane potential changes in RPTC incubated with 10 mg/ml albumin. **p<0.01. Statistical analysis was performed using the Mann-Whitney U test. Experiments were repeated three times.

Supplementary figure 6.

A. Mean blood pressure in control rat and rats under treatment with ouabain. Data presented as means ± SEM. Statistical analysis was performed using the two-way ANOVA.

B. Heart rate in control rat and rats under treatment with ouabain. Data presented as means ± SEM. Statistical analysis was performed using the two-way ANOVA.

Supplementary figure 1.

A.

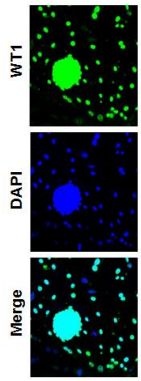

B.

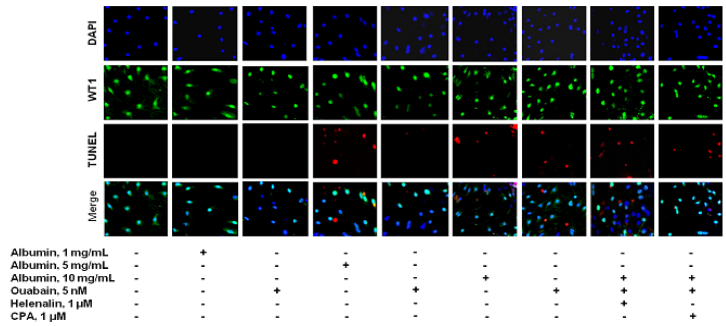

C.

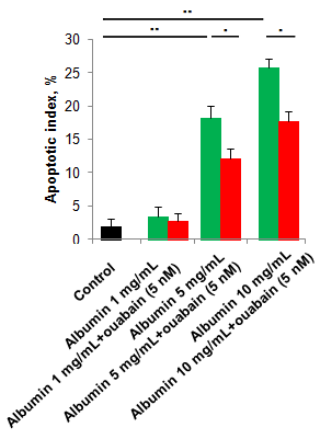

D.

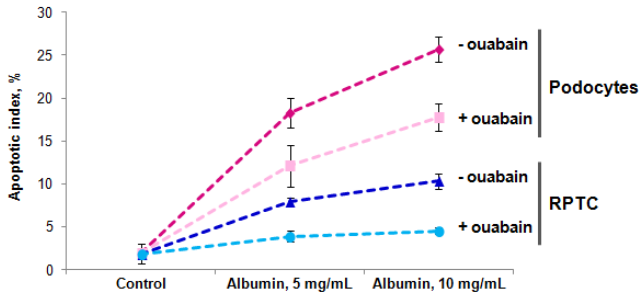

Supplementary figure 2.

A.

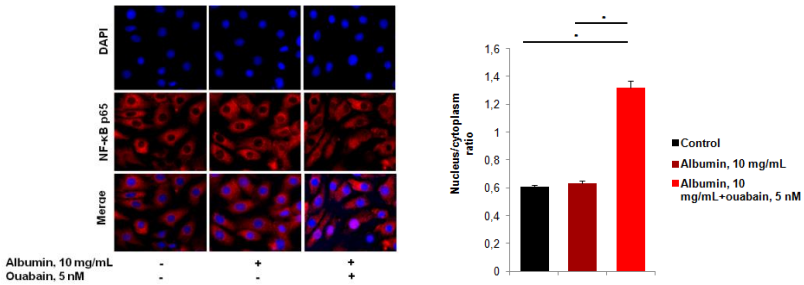

B.

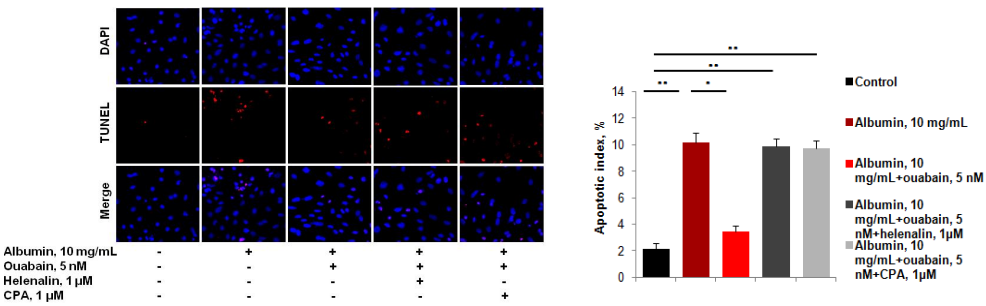

Supplementary figure 3.

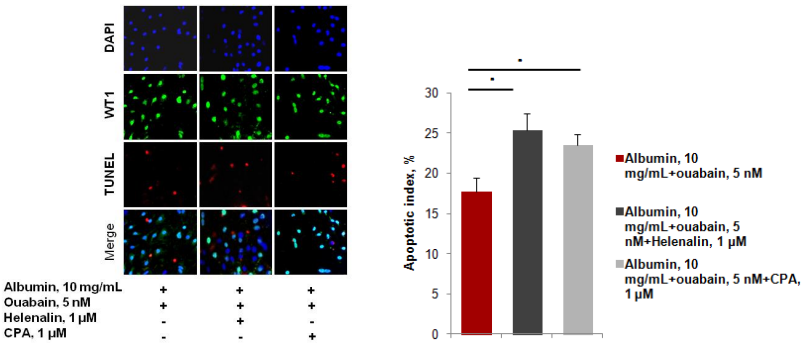

Supplementary figure 4.

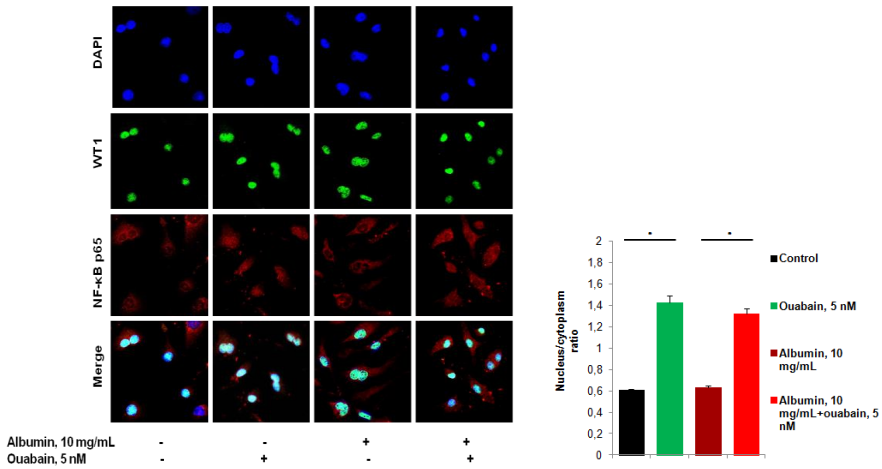

Supplementary figure 5.

A.

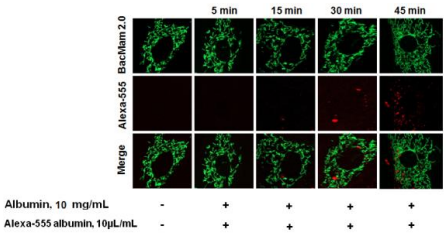

B.

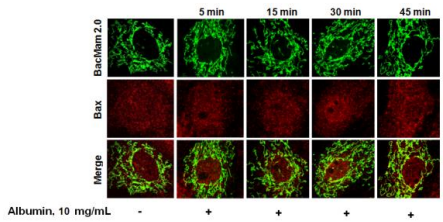

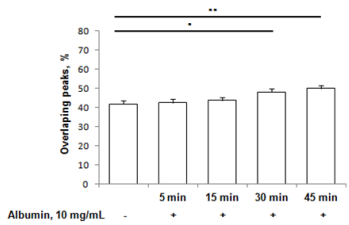

C.

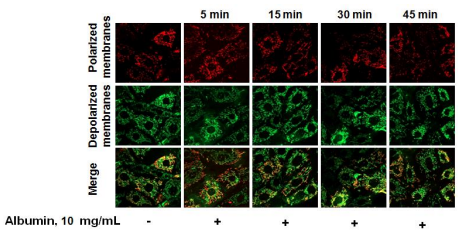

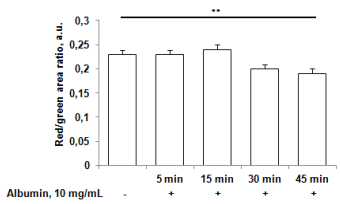

Supplementary figure 6.

A.

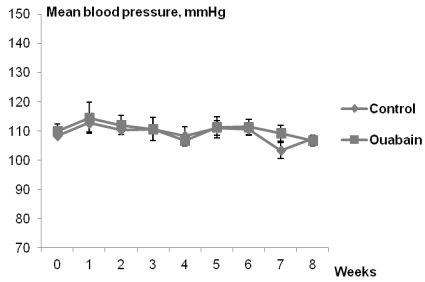

B.